PHYSICO - CHEMICAL STUDIES OF INTERMOLECULAR INTERACTIONS

ABSTRACT

THESIS

SUBMITTED FOR THE AWARD OF THE DEGREE OF

Doctor of Philosophy

IN

CHEMISTRY

BY

SAEEDA NAQVI

DEPARTMENT OF CHEMISTRY
ALIGARH MUSLIM UNIVERSITY
ALIGARH (INDIA)
1994

A B S T R A C T

The densities, viscosities and ultrasonic velocities of several compositions of $[x\ NaNO_3 + (1-x)KNO_3] + RH_2O$ (R = 6,10,14 and 15) systems were studied at different temperatures. The data were least-squares fitted to appropriate models and the relevant parameters thus obtained were employed for understanding the intermolecular interactions. The thermodynamic functions viz., free energy of activation, enthalpy and entropy of viscous flow were also evaluated for (I) benzyl alcohol + iso-amyl alcohol (II) benzyl alcohol + iso-propyl alcohol systems, lending further support to the presence of intermolecular interactions in these systems.

Similarly, an attempt was made to predict the energies of transitions in mixed halide complexes of Nickel (II) ions in different intraionic as well as interionic interactions in some controlled reactions expected to yield $[NiI_3Cl]^{2-}$, $[NiI_2Cl_2]^{2-}$, $[NiICl_3]^{2-}$, $[NiBr_3Cl]^{2-}$, $[NiBr_2Cl_2]^{2-}$, $[NiBrCl_3]^{2-}$, $[NiI_3Br]^{2-}$, $[NiI_2Br_2]^{2-}$, $[NiIBr_3]^{2-}$ species out of which the presence of $[NiI_2Cl_2]^{2-}$, $[NiBr_2Cl_2]^{2-}$ and $[NiI_2Br_2]^{2-}$ types of ions have already been established.

PHYSICO - CHEMICAL STUDIES OF INTERMOLECULAR INTERACTIONS

THESIS

SUBMITTED FOR THE AWARD OF THE DEGREE OF

Doctor of Philosophy

IN

CHEMISTRY

BY

SAEEDA NAQVI

DEPARTMENT OF CHEMISTRY
ALIGARH MUSLIM UNIVERSITY
ALIGARH (INDIA)
1994

DEDICATED TO

MY BABBA MUMMY

Whose love and affection has been a constant source of inspiration.

How do I love thee? Let me count the ways

I love thee to the depth and breadth and height

My soul can reach.....

PHONE (0571) -[illegible]

DEPARTMENT OF CHEMISTRY
ALIGARH MUSLIM UNIVERSITY
ALIGARH 202002

Dated 26.05.1994

CERTIFICATE

This is to certify that the work presented in this thesis entitled 'Physico-Chemical Studies of Intermolecular Interactions' is original, carried out by **Ms. Saeeda Naqvi** under my supervision and is suitable for submission for the award of Ph.D. degree in Chemistry of this University.

June 3, 19[illegible]

(PROF. NURUL ISLAM)
Ph.D. (New York)

A C K N O W L E D G E M E N T

The most important acknowledgement by far, is to my respected teacher and supervisor, Prof. Nurul Islam, who guided me with whole hearted attention and unswerving devotion. His intellectual vigour and generously given support have been invaluable to me and have been responsible for improving the content of the subject matter. But for his unremitting attention to my work, the same could not have been brought to fruition.

I extend my sincere thanks to Prof. S.A.A.Zaidi and Prof. M.A. Beg, former Chairman and Prof. A.A. Khan, the Chairman, Department of Chemistry for providing all the necessary facilities during the course of this work.

For provision of computer programm and support service, I express my gratitude to Mr. M.Afzal and Prof. Akhtar of Computer Centre.

I owe a special debt to my colleagues Riyazuddin and Razaque for their continued help and cooperation.

My friends Dr. (Ms) Subuhi Khan, Dr. (Ms) Naseem, Ms. Faran Yasmeen, Ms. Tahseen and Ms. Preethy Francis deserve my special commendation for their affection and support.

I am extremely thankful to my husband Mr. S.Zamir Abbas for the moral support, encouragement and help.

Words fail me to mention the motivation of my parents, brothers Mr. Hasan Zia and Hasan Shuja, and my Auntie Ms. K. Naqvi who always inspired me.

Thanks are due to Mr. Zakiur Rahman for taking pains to finish the typing of thesis in time.

(SAEEDA NAQVI)

C O N T E N T S

-o-o-o-o-

GENERAL INTRODUCTION

The structural studies of liquid mixtures are based on ultrasonic velocity and viscosity data. The velocities of sound, compressibilities and viscosities are useful tools in styding the nature and degree of association or dissociation, complex formation and dispersion forces in liquids and liquid mixtures.

Ultrasonic parameters are being extensively used to study the molecular interactions in pure liquids[1], their binary and ternary mixtures[2-6] and the ionic interactions in single and mixed salt solutions[7,8]. A departure from linearity in the velocity versus composition behaviour in liquid mixtures is taken as an indication of the existence of interaction between the different species[5-8]. However, a representation in terms of observed properties/behaviour such as the velocity of ultrasonic waves and the viscosity have a limited utility. On the other hand, a number of theoretical[9] and experimental investigations[10,11] have shown that an insight into the nature and the relative strengths of the various intermolecular interactions is provided by a representation in terms of the derived parameters, e.g., adiabatic compressibility (β_s), Wada's constant (β), specific acoustic impedence (Z), etc.

Nomoto[12] and Bhimsenachar et al[13] evaluated the ultrasonic velocity in binary liquid mixtures by using the Nomoto's relation. Van Dael and Vangeel[14] have applied the ideal mixing relation for evaluating the ultrasonic velocities in liquids. The free length theory of Jacobson[15] has been applied to evaluate the ultrasonic velocity in binary liquid mixtures[16-21] as well as in molten salt mixtures[22,23].

Schaaff's[24] collision factor theory has also been successfully employed to evaluate the ultrasonic velocity in binary liquid mixtures[16,19-21] and in molten salt mixtures[22].

Theoretical evaluation of sound velocity has also been done using the various liquid state theories for various molten electrolytes[25,26], their binary mixtures[27] as well as for ternary liquid mixtures[28,29].

The ultrasonic velocity data have been employed to evaluate the thermodynamic properties including the compressibilities of molten salts[30], their binary and ternary mixtures[22,27,31] and also of aqueous solutions of single and mixed molten electrolytes[23,22,32-34].

The viscosities of aqueous solutions of electrolytes have been studied in detail since Arrhenius began his investigations of the properties of electrolyte solutions in 1880's and many empirical relations have been explored for single and mixed electrolyte solutions. Einstein[36] in 1906, deduced an equation from the classical principles of hydrodynamics of aqueous solutions, which contain spherically incompressible uncharged particles of solute which are larger in comparison to water molecules.

Later, Falkenhagen and Dole[36] considered the problem of viscosity of electrolyte solutions in terms of the interionic interactions in the adjacent layers of an electrolyte solution. They proposed that the electrical forces between the ions in a solution tend to establish and maintain a preferred rearrangement and thus to stiffen the solution, i.e., to increase its viscosity. Falkenhagen introduced an empirical parameter, B, which represents the ion-solvent interaction. The B coefficient is found to be highly specific for the electrolyte and temperature. Negative values for this coefficient are found for ions which exert a 'structure-breaking' effect on the solution,

while the coefficient has positive values for the ions which are strongly hydrated, i.e., structure makers.

There are two semi empirical theories for explaining the behaviour of liquid viscosities. The first one is the absolute reaction rate theory of Eyring and coworkers[37], which relates the viscosity to the free-energy needed for a molecule to overcome the attractive force field of its neighbours while the second one is the free-volume theory,[38-40] which relates the viscosity to the probability of occurrence of an empty neighbouring site into which a molecule can jump. Macedo and Litovitz[41] suggested that for pure liquids, better results are obtained by combining the two theories. Bloomfield and Dewan[42] developed the thermodynamic intrinsic viscosity theory and compared it with that of the continuum hydrodynamic treatment of the intrinsic viscosity of chain molecules.

Pandey et al[43] employed the significant structure theory of Eyring to calculate theoretically the viscosity of binary molten electrolytes on the basis of rigid sphere model. Pandey and coworkers[44] determined the viscosities as well as the excess viscosities of binary molten electrolyte mixtures and compared

these values with those obtained from the Flory's statistical theory[45,46] and observed a satisfactory agreement.

The viscous behaviour and the intermolecular interactions in ternary liquid mixtures were studied[44] in terms of the excess free-energy of mixing, the strength of interaction parameter and the interaction energy. Such a study provided a good means for the estimation of interaction in ternary liquid mixtures qualitatively as well as quantitatively.

Pandey and coworkers[47] evaluated the viscosities of binary mixtures of organic compounds using the theories of Bloomfield and Dewan[48] as well as the Flory's statistical theory[45,46].

An equation for the viscous flow of binary liquid mixtures has been deduced by Sharma and Bhatnagar[49] taking into account the contributions made by configurational partition function and the energy of fluctuation due to a localized order in the liquid state.

Internal pressure has also been found to be a very important parameter in the theory of liquid state. Dunlop et al[50] determined the internal pressure of different liquid

mixtures and compared it with their cohesive energy density values. The interaction in liquid mixtures was predicted by Stavely et al[51] by comparing the internal pressure of individual components. Several workers[52] attempted to evaluate the excess internal pressure for the liquid mixtures and correlated it with those of the intermolecular interactions.

Gruneisen parameter, a dimensionless constant governed by the molecular order and structure had been a subject of study for solids[53,54], was later extended by Knopoff et al[55] for liquids. The original Gruneisen parameter is related with the thermal expansion coefficient and the specific heat at constant volume. Later, the utility of this parameter[56] was extended to the structural study of liquids, by defining its Pseudo counterpart, which is related to the velocity of ultrasound in the liquid.

Among the various physical properties which have been investigated to elucidate ionic interactions in binary mixtures of electrolytes, surface tension is one of those which has been treated theoretically. Guggenheim[57] derived equations for the surface tension for ideal and regular solutions using the quasi-

crystalline model. The thermodynamic method of Guggenheim was used by Heymann[58] to test the formation of complexes in certain molten salts. Bertozzi and G. Sternheim[59,60] calculated the surface tension of alkali nitrates and binary halide systems and obtained good agreement with the exprimental results by introducing a parameter in the derivations called the 'Tobolsky parameter', which is a function of interionic distances of the respective pure salts. Nissen and Domelen[61,62] proposed that an equation based on the regular solution theory, assuming the quasi-lattice model and the random distributions of species both in the bulk phase and in the surface phase, can be used to calculate the surface tension of binary salt mixtures.

Various thermodynamic properties of aqueous mixtures of two electrolytes having a common ion were reported by Owen and Cooke[63] in 1937 at 25°C. Rush and coworkers[64] determined the osmotic coefficient , for various aqueous solutions of electrolytes and examined their experimental results in the light of equations suggested by Scatchard[65] . Friedman[66] dealt with the free-energies of mixed electrolyte solutions and pointed out the existence of a limiting slope for the interaction parameters

at infinite dilution. Thermodynamic properties, e.g., enthalpy changes on mixing[67] have been found to suggest the importance of the cation-cation pair interaction and the cation-anion-cation triplet interaction. The free-energy of mixing for solutions of electrolytes having common anions has been determined by W.Y. Wen and coworkers[68].

Few workers[69,70] have calculated the various thermodynamic parameters of activation of viscous flow by least-squares fitting the densities and the viscosities data to empirical equations stating their dependence on temperature and composition of the mixtures. These parameters suggest the type and strength of interaction between the components of mixture. Palepu et al[69] calculated such thermodynamic parameters for the binary acid-base mixtures while Corradini and coworkers[70] obtained these for the binary mixtures of alcohols and amides.

The structure of water as suggested by Samoilov[71] and supported by Danford and Levy[72] is believed to be a bulky network structure having spaces within the framework of molecules in the tetrahedral coordination, these cavities are occupied by interstitial molecules, which interact with the framework. As

suggested by Debye, the electrostatic field of ions exert electrostatic pressure which has the same effect as that of an external pressure and thus decreases the compressibility of water molecules.

Flory's statistical theory[45,46] has been employed to evaluate the reduced and the characteristic thermodynamic parameters which, in turn, can be used to calculate the viscosity, the surface tension, the interaction parameter, the ultrasonic velocity and the excess thermodynamic properties.

In addition to anion-cation, cation-anion-cation, anion-cation-anion, ion-solvent, dipole-dipole etc. intermolecular/interionic interactions, transition metal complex ionic species may also have variations in their interactions depending upon the type of ligands surrounding the central metal ions, the composition/concentration ratio of metal ion-ligand, as well as the temperature of study. For instance, $NiCl_4^{2-}$, $NiBr_4^{2-}$ and NiI_4^{2-} are expected to have different ionic interactions in the three cases. Similarly, if it is possible to stabilize the species of mixed ligands of these complex ions in some sort of a controlled reaction, then starting from NiI_4^{2-} one may obtain

NiI_3Br^{2-}, $NiI_2Br_2^{2-}$, $NiIBr_3^{2-}$, $NiBr_4^{2-}$ $NiBr_3Cl^{2-}$, $NiBr_2Cl_2^{2-}$, $NiBrCl_3^{2-}$, $NiCl_4^{2-}$, NiI_3Cl^{2-}, $NiI_2Cl_2^{2-}$, $NiICl_3^{2-}$ ions. Such a consideration has prompted to undertake the construction of energy-level diagrams for these species using the ligand-field strength, the spin-orbit coupling and the two electron-electron repulsion parameters for solving the five Liehr-Ballhausen[140] matrices which yield twenty energy states for the possible intraconfigurational transitions.

Consequently, with a view to understanding the inter-molecular/interionic interactions, the densities, the viscosities and the ultrasonic velocities were measured for several compositions of systems under investigation: $[xNaNO_3 + (1-x)\ KNO_3]$ + RH_2O (where R = 6, 10, 14 or 15) at different temperatures. In addition, the energies of possible transitions for the mixed ligand-nickel (II) ions have also been computed.

EXPERIMENTAL

MATERIALS:

Recrystallized sodium and potassium nitrates and double distilled water were used in preparing binary mixtures of these salts in aqueous medium while pure and distilled toluene and quinoline were used to calibrate the pyknometer and the viscometer. The ultrasonic interferometer was calibrated using triply distilled water.

TEMPERATURE CONTROL:

A thermostated paraffin bath was used to maintain a uniform temperature during the measurements of density and viscosity. The paraffin bath of about 10 litres' capacity consisted of an immersion heater (1.0 KW), a stirrer, a check thermometer, a contact thermometer and a relay [Jumo type NT 15.0, 220 V$\simeq$15 (Germany)]. Thermal stability was found to be within $\pm$ 0.1^{o}.

PURIFICATION OF TOLUENE[73]:

Commercial toluene contains methyl thiophene, b.p.112-113^{o}C, which can not be removed by distillation. Toluene was purified

by shaking repeatedly with about 15 percent of its volume of concentrated sulphuric acid in a stoppered separating funnel until the acid layer becomes colourless or pale yellow on standing or until the thiophene test is negative. After each shaking lasting a few minutes, the mixture was allowed to settle and the lower layer of acid was drawn off. The toluene was then shaked twice with water in order to remove most of the acid, once with 10 per cent sodium carbonate solution, again with water and finally dried with anhydrous calcium chloride. After filteration the toluene was distilled through an efficient column and the fraction, b.p. 80-81°C, was collected. Sodium wire was introduced into the distilled toluene.

PURIFICATION OF QUINOLINE[73] :

Quinoline was distilled under reduced pressure, b.p. 118-120°C/20 mm.

SAMPLE PREPARATION:

Recrystallized sodium and potassium nitrates and triple distilled water were used for the sample preparation. All the

solutions were prepared by weight (molal solutions).

Concentration of solution is given in terms of R, which is equal to water/salt ratio. This concentration unit was first introduced by Angell and Gruen and is useful for the composition region in which there are insufficient water molecules to fill more than one or two hydration shells per cation or anion.

DENSITY MEASUREMENT:

Pyknometer[74,75] is a flat bottom flask of nearly 7 ml capacity, fitted with a stem which is graduated in 0.01 ml divisions. The pyknometer was calibrated with purified toluene used as a reference liquid. The pyknometer was weighed and filled with pure and distilled toluene and again weighed. The weight of toluene taken was determined by the difference in these two weights. The pyknometer was immersed in the paraffin bath maintained at the required temperature, and volume changes were recorded as a function of temperature, and thus each mark of the stem was calibrated. The density of toluene at different temperatures required for calibration was given by the standard equation,

$$\rho = 0.88412 - 0.92248 \times 10^{-3}\, t + 0.0152 \times 10^{-6}\, t^{2} - 4.223 \times 10^{-9}\, t^{3}.$$

where t is the temperature in ^{o}C. The ratio of the amount of toluene to the above calculated densities at different temperatures gave the volume of pyknometer at the corresponding marks on the stem. Reproducibility of calibration was checked by repeating the above procedure with different weights of toluene. Using the known volume of calibrated pyknometer at each mark and mass of toluene, the densities at the required temperature were calculated. The experimental densities thus obtained were found to be within $\pm$ 0.01% accuracy.

The test solution was introduced into the calibrated pyknometer, weighed and then it was immersed in the paraffin bath. By recording the volume changes as a function of temperature, the densities were determined at required temperatures.

VISCOSITY MEASUREMENT:

Cannon-Ubbelohde[76] viscometer was used for the viscosity measurement of aqueous solutions of sodium and potassium nitrates.

The viscometer consists of three parallel arms, viz., receiving, measuring and auxiliary, for forming the suspended level arrangement in a triangular fashion. The receiving arm forms a 'U' with the measuring arm through a bulb D. The measuring arm has two bulbs A and B. The two fudicial marks a and b were used on the two sides of the bulb B for recording the time of fall of the test solution. The auxiliary arm was sealed to the receiving arm through a bulb C. In between the bulbs B and C there lies a capillary of appropriate dimensions. It has been designed in such a way that the centre of gravity of the three bulbs A,B and C was aligned vertically to reduce the acceleration due to gravity, so that the experimental errors could be minimized.

Special feature of the suspended level viscometer was that the capillary effects of the two liquid surfaces were neutralized by each other so that the surface tension correction for the apparatus was negligible and the transport of momentum was carried out freely under the weight of the total volume of the test liquid.

The calibration of viscometer was done by using the distilled toluene. The viscometer was then filled with the test liquid whose amount should be sufficient to avoid any air bubble being introduced into the capillary arm while fudicial bulb was filled. The open ends of the three arms of viscometer were fitted with the calcium chloride tubes through the rubber tubes to avoid the absorption of moisture. The viscometer was clamped in the vertical position in the thermostated paraffin bath for about half an hour before recording the time of fall, so that the thermal fluctuation in the viscometer was minimized. Then the sample was sucked into the bulb A with the vacuum pump and was allowed to stand there for about 15 minutes by closing the calcium chloride tubes with the rubber corks. The corks were then removed from the tubes and the time of fall of the sample from the upper fudicial mark 'a' to the lower mark 'b' was recorded several times and the mean of very close readings was determined at each required temperature. The time of fall of liquid was measured with a stop watch (accuracy: 0.1 second). Poiseuille's equation was employed to calculate the viscosities using the density and the time of fall,

$$\eta = \rho \beta t$$

in which β is a constant and has been calculated by making use of the reported values[77] of viscosities of toluene at several temperatures. The accuracy of the calibrated viscometer was checked by measuring the viscosities of toluene at test temperatures and then comparing the experimental values with the reported ones[77]. Reproducibility was found to be within $\pm$0.2%.

MEASUREMENT OF ULTRASONIC VELOCITY:

WORKING PRINCIPLE:

A multifrequency ultrasonic interferometer (Mittal's M-83) was used to determine the ultrasonic velocity in the test solutions.

The ultrasonic waves of known frequency (ν = 4 MHz) are produced by a quartz plate fixed at the bottom of the cell. These waves were reflected by a movable metallic plate kept parallel to the quartz plate. If the separation between these two plates is exactly a whole multiple of the sound wave-length, standing waves are formed in the medium. This acoustic resonance gives rise to an electrical reaction to the generator driving

the quartz plate and the anode current of the generator becomes maximum.

If the distance is now increased or decreased and the variation is exactly one half wavelength ($\lambda/2$) or multiple of it, the anode current becomes maximum. Knowing the value of wavelength, the ultrasonic velocity can be obtained from the equation

$$U = \lambda \times \nu$$

DESCRIPTION:

The ultrasonic interferometer consists of two parts, (1) high frequency generator and (2) the measuring cell.

(1) HIGH FREQUENCY GENERATOR:

It is designed to excite the quartz plate fixed at the bottom of the measuring cell at its resonant frequency to generate ultrasonic waves in the experimental liquid filled in the measuring cell. A micrometer which observes the change in current and two controls for the purpose of sensitivity regulation and initial adjustment of micrometer are provided on the panel of the high frequency generator.

(2) MEASURING CELL:

It is a double walled cell, which maintains the temperature of the test solution at a constant value during the experiment. A fine micrometer screw is provided at the top, which is used to raise or lower the reflector plate in the liquid in cell through a known distance. A quartz plate is fixed at the bottom of this cell.

ADJUSTMENT OF ULTRASONIC INTERFEROMETER:

Adjustment of the instrument is done in the following manner.

(1) The cell was inserted in the square base socket and was clamped there with the help of a screw provided on one side.

(2) The cap of the cell was unscrewed and removed from the cell, the test liquid was poured into the cell, and the cap was again screwed on it.

(3) Water was circulated through the two tubes in the double walled cell to maintain the desired temperature of the test liquid.

(4) The cell was, then connected with the high frequency generator by a co-axial cable provided with the instrument.

The two knobs are provided on a high frequency generator for the initial adjustment, one is marked with 'Adj' and the other with 'Gain'. The position of needle on the ammeter is adjusted with the knob marked 'Adj' and the knob marked 'Gain' is used to increase the sensitivity of the instrument for greater deflection. The ammeter was used to record the maximum deflections by adjusting the micrometer.

MEASUREMENTS:

The measuring cell was connected to the output terminal of high frequency generator through a co-axial cable. The cell was filled with the test liquid before switching on the generator. The ultrasonic waves of 4 MHz frequency produced by a gold plated quartz crystal fixed at the bottom of a cell are passed through the medium and are reflected by a movable plate and the standing waves are formed in the liquid in between the reflector plate and the quartz crystal. Acoustic resonance due to these standing waves gives rise to an electrical reaction to the generator driving the quartz plate and the anode current of

the generator becomes maximum. The micrometer screw was raised slowly to record the maximum anode current. The wavelength was determined with the help of total distance moved by the micrometer for twenty maxima of anode current. The total distance (d) travelled by the micrometer gives the value of wavelength with the help of the relation, $d = n \times \lambda/2$, where n is the number of maxima in anode current. Once, the wavelength is known, ultrasonic velocity can be calculated as described earlier. The accuracy in velocity measurement was found to be within $\pm 0.20\%$.

PART - I

CHAPTER-I

ULTRASONIC VELOCITIES AND IONIC INTERACTIONS IN MIXTURES OF SODIUM AND POTASSIUM NITRATES IN AQUEOUS MEDIUM

INTRODUCTION

Theoretical evaluation of ultrasonic velocity of molten electrolytes[25,26], their mixtures[27] and for organic mixtures[28,29] has been carried out by many workers. Measurement of ultrasonic velocities has been made by many investigators using organic liquids[81,82] and their mixtures[28,78-80] as well as aqueous solutions of several electrolytes[14,32,33]. Such data are employed to evaluate the thermodynamic properties of pure liquids[83-85], liquid mixtures[16,86-89], molten electrolytes[12,13] and their mixtures[27].

The importance of ultrasonic velocity data lies in the fact that either it directly or through its derived parameters, such as adiabatic compressibility (β_s), molar ultrasonic velocity (R^*), specific acoustic impedence (Z), and Wada's constant (B) provide a basis for understanding the type and the extent of intermolecular interactions such as weak or strong or no interaction at all, and may throw some light qualitatively on the mechanism of intermolecular processes.

Consequently, several workers have also evaluated the ultrasonic velocities theoretically using the Nomoto relation[12],

the ideal mixing relation of Van Dael and Vangeel[14], the collision factor theory of Schaaffs[24], the free-length theory of Jacobson[15], the Flory statistical theory[45,46] and other equations[28] for molten electrolytes[25,26] and their mixtures[27] as well as for organic systems[28,29], but few attempts[22,31] have been made to determine the ultrasonic velocity in aqueous solutions of electrolytes and their mixtures.

In addition, the behaviour of ultrasonic velocity in a solution is known to depend on temperature as well as on the composition of solution. Even though aqueous solutions of electrolytes generally show an increase in the value of ultrasonic velocity with increase in solute concentration, a less common trend of decrease [in the value of ultrasonic velocity with increase in solute concentration] has also been recorded in certain aqueous solutions of electrolytes having heavy metallic radicals[90,91]. The later trend is similar to that observed in respect of adiabatic compressibility.

Such a trend of variation in some of these properties of aqueous solutions of electrolytes may seem to stem from the peculiar structure of water. For example, one of the abnormal

properties of water is the variation of its ultrasonic velocity with temperature. The propagation velocity of ultrasound in normal liquids has been found to fall off with increase in temperature, while in the case of water, it attains a maximum value of 1557 ms^{-1} at $74^{o}C$ and then decreases with further increase in temperature. Furthermore, the adiabatic compressibility of water shows a minimum at $64^{o}C$, reinforcing the view that such unusual trends in the behaviour of these properties seem to have been caused by the peculiar liquid structure of water.

Depending upon the type of interaction among the solute ions and water, the ultrasonic velocity varies with concentration and temperature.

In the present work, attempt has been made to obtain the various derived parameters using the ultrasonic velocity recorded in aqueous solutions of mixed electrolytes : $[x\ NaNO_3 + (1-x)\ KNO_3] + RH_2O$. The ultrasonic velocities have also been evaluated theoretically using the Nomoto equation and the equation of Van Dael and Vangeel to examine their suitability in the case of the systems under investigation .

THEORETICAL

The following relations are employed to evaluate the derived parameters[14,92,93]:

$$\beta_s = u^{-2} \rho^{-1} \quad (1.1)$$

$$R^* = Mu^{2/3}/\rho = Vu^{2/3} \quad (1.2)$$

$$Z = u\rho \quad (1.3)$$

$$B = V\beta_s^{-1/7} \quad (1.4)$$

$$\beta_s^E = \beta_s - (x\beta s_1 + (1-x)\beta s_2] \quad (1.5)$$

where u denotes the ultrasonic velocity, ρ the density, M the molecular weight, V the molar volume of ternary solution, Z the specific acoustic impedence, B the Wada's constant and β_s^E the excess adiabatic compressibility of mixtures while x is the mole fraction of $NaNO_3$, and $(1-x)$ is that of KNO_3. βs_1 and βs_2 are the adiabatic compressibilities of aqueous solutions of sodium and potassium nitrates, respectively, while βs stands for the aqueous solution of their mixture.

The molar sound velocity, R^*, is given by the following equation by Nomoto,

$$R^* = x R_1^* + (1-x) R_2^* \qquad (1.6)$$

where R^* is considered as the linear function of molar concentrations of the two components, where x and $(1-x)$ are the mole fractions of $NaNO_3$ and KNO_3, respectively, as already stated above.

R^* may also be expressed as

$$R^* = \frac{Mu^{1/3}}{\rho} = V u^{1/3}. \qquad (1.7)$$

The molar volume being additive in nature is expressed as

$$V = x V_1 + (1-x) V_2. \qquad (1.8)$$

On substituting the values of R^* and V in eq. (1.7), we get,

$$U = \left(\frac{R^*}{V}\right)^3 = \left(\frac{x R_1^* + (1-x)R_2^*}{x V_1 + (1-x)V_2}\right)^3. \qquad (1.9)$$

These equations are found to be quite satisfactory when applied to molecular liquids. Higgs and Litovitz and Subramanyam and Bhimsenachar[92] proposed an expression for the molar sound velocity in molten salts,

$$R^* = \frac{Mu^{2/3}}{\rho} = V\, u^{2/3} . \qquad (1.10)$$

Eq. (1.10) has also been applied to binary mixtures of molten salts in the following form,

$$U = \left(\frac{R^*}{V}\right)^{3/2} = \left(\frac{xR_1^* + (1-x)\, R_2^*}{x\, V_1 + (1-x)\, V_2}\right)^{3/2} . \qquad (1.11)$$

Another equation for the evaluation of ultrasonic velocity in mixtures as suggested by Van Dael and Vangeel is given as

$$\frac{1}{xM_1 + (1-x)M_2}\ \frac{1}{u^2(\mathrm{im})} = \frac{x}{M_1 u_1^2} + \frac{(1-x)}{M_2\, u_2^2} \qquad (1.12)$$

where M_1 and M_2 are the molecular weights of the two components while $U(\mathrm{im})$ stands for the ultrasonic velocity for ideal mixing in solutions.

Eq. (1.12) for the ultrasonic velocity is derived from the definition of adiabatic compressibility, β_s, proposed by Van Dael and Vangeel for a binary mixture as,

$$\beta_s(\text{im}) = \theta_1 \frac{\gamma_1}{\gamma(\text{im})} \beta_{s1} + \theta_2 \frac{\gamma_2}{\gamma(\text{im})} \beta_{s2} \qquad (1.13)$$

where θ and γ refer, respectively, to the volume fraction and the principal specific heat ratio and im refers to the ideal mixing. Eq. (1.13) is applicable to ideal mixtures, if it satisfies the condition $\gamma_1 = \gamma_2 = \gamma(\text{im})$, then it takes on the form,

$$\beta_s(\text{im}) = \theta_1 \beta_{s1} + \theta_2 \beta_{s2}. \qquad (1.14)$$

Eq. (1.14) can be simplified further and β_s can be expressed as a linear combination of mole fractions assuming that $V_1 = V_2$,

$$\beta_s(\text{im}) = x \beta_{s1} + (1-x)\beta_{s2}. \qquad (1.15)$$

Jacobson's free-length theory, originally designed to explain the behaviour of molecular liquids having weak intermolecular forces, fails to account for the behaviour of ionic liquids[22]. According to this theory,

$$u = \frac{K}{L_{f(mix)}\, \rho^{1/2}} \qquad (1.16)$$

where K is a temperature dependent parameter and L_f is the intermolecular free-length, defined as,

$$L_{f(mix)} = \frac{2[V_m - (x\, V_{01} + (1-x)\, V_{02})]}{x\, y_1 + (1-x)\, y_2} \qquad (1.17)$$

where '0' refers to the solvent and y, to the surface area per mole.

According to Auerbach[94], the surface tension, σ, is evaluated using the experimental values of the ultrasonic velocity, u, and the density of the liquid, ρ, as follows:

$$u = \left(\frac{\sigma}{6.3 \times 10^{-4}\, \rho}\right)^{2/3} . \qquad (1.18)$$

RESULTS AND DISCUSSION

A computer program in pascal language has been used (given in the appendix) to calculate the various parameters using the density, the viscosity and the ultrasonic velocity data.

The density data of aqueous solutions of electrolytes, $[x\ NaNO_3 + (1-x)\ KNO_3] + RH_2O$ (where R = 6, 10, 14 or 15) have been least-squares fitted to a linear equation of the form, $\rho = a - bT$, where ρ is the density at temperature T, while a and b are the constants (Table 1.1.).

The measured values of ultrasonic velocities are listed in Table 1.2 at several temperatures (313.15 K to 328.15 K) for each of the compositions studied. The values of u are found to decrease linearly with increase in temperature, and are also affected by change in concentration. The variation in the values of u with x at different temperatures is shown in Fig. 1.1. The values of ultrasonic velocities computed using Nomoto's equation in good agreement with those obtained experimentally.

TABLE 1.1: BEST FIT PARAMETERS OF THE DENSITY EQUATION, $\rho = a - bT$ FOR $[x\ NaNO_3 + (1-x)KNO_3] + RH_2O$ SYSTEMS (where R = 6, 10, 14 or 15).

x	a/gm.cm^{-3}	b x 10^{4} / gm.cm^{-3}.K^{-1}	- (Corr. Coeff.)
	R = 6		
0.0	1.5188	6.2390	1.0000
0.6	1.6012	7.6460	1.0000
0.7	1.6660	7.9671	1.0000
0.8	1.7003	8.3080	0.9999
0.9	1.5747	7.3891	0.9999
1.0	1.5997	7.9080	1.0000
	R = 10		
0.0	1.4038	6.4936	0.9999
0.4	1.4617	6.9277	1.0000
0.5	1.4616	6.9620	1.0000
0.7	1.2806	7.1565	0.9998
1.0	1.4231	7.2199	0.9999

Contd...

x	a/g.cm^{-3}	b x 10^{4}/ g.cm^{-3}.K^{-1}	- (corr.coeff.)
	R = 14		
0.0	1.3403	5.9552	1.0000
0.3	1.3893	6.4302	0.9998
0.6	1.3652	6.2650	1.0000
1.0	1.3357	6.5430	0.9998
	R = 15		
0.0	1.3737	6.2140	0.9999
0.4	1.3757	6.4190	0.9998
0.6	1.3175	6.1470	1.0000
1.0	1.4384	7.0210	1.0000

The adiabatic compressibility, βs (Table 1.3) obtained from the ultrasonic velocity and the density of solutions is useful for the purpose of studying the structural changes of liquid water induced by the solute molecules. The structure of water proposed by Samoilov and supported by Danford and Levy consists of a network in which each molecule is tetrahedrally co-ordinated. Such a structure is quite bulky, and has spaces within the framework of molecules, which are quite large and can accommodate additional water molecules which interact with the framework.

Water is regarded as an equilibrium mixture of two structures, an ice-like structure and a close-packed structure[35]. As temperature increases, the cluster part of water decreases, resulting in a decrease in the structural compressibility, at the same time, the molecular distance increases with temperature rise due to increase in thermal motion, which causes increase in compressibility due to compression of the free spaces between the non-associated water molecules. These opposite effects lead to a minimum of compressibility at 64°C and the sound velocity maximum at 74°C.

TBALE 1.2: EXPERIMENTAL AND THEORETICAL ULTRASONIC VELOCITIES, u(m/s), AS FUNCTIONS OF COMPOSITION AND TEMPERATURE FOR THE SYSTEM: $[x\ NaNO_3 + (1-x)KNO_3] + RH_2O$ (where R = 6,10,14 or 15).

T(K) / x	313.15	318.15	323.15	328.15
		R = 6		
0.0	1719.0	1716.6	1714.2	1711.8
0.6	1755.6	1752.2	1749.6	1746.2
	(1753.8)	(1751.0)	(1747.0)	(1741.1)
	$(1843.6)^+$	$(1840.1)^+$	$(1835.4)^+$	$(1828.8)^+$
0.7	1758.2	1756.0	1753.4	1750.6
	(1756.5)	(1754.6)	(1751.3)	(1748.0)
	$(2069.9)^+$	$(2066.1)^+$	$(2060.8)^+$	$(2053.2)^+$
0.8	1764.6	1758.6	1754.8	1751.6
	(1763.3)	(1756.5)	(1752.0)	(1750.1)
	$(2168.2)^+$	$(2164.1)^+$	$(2158.2)^+$	$(2149.4)^+$
0.9	1774.8	1770.0	1766.0	1761.6
	1773.1	1768.2	1764.5	1760.0
	$(2180.0)^+$	$(2174.6)^+$	$(2170.5)^+$	$(2166.3)^+$
1.0	1780.0	1777.3	1774.0	1772.5

Contd.....

T(K) x	313.15	318.15	323.15	328.15
		R = 10		
0.0	1649.4	1645.2	1643.0	1641.0
0.4	1672.0	1671.2	1670.2	1668.2
	(1670.0)	(1668.8)	(1668.5)	(1665.1)
	(1866.3)$^{+}$	(1863.6)$^{+}$	(1862.2)$^{+}$	(1860.6)$^{+}$
0.5	1676.6	1675.8	1674.8	1673.0
	(1672.9)	(1671.2)	(1670.3)	(1670.0)
	(1867.2)$^{+}$	(1866.5)$^{+}$	(1866.0)$^{+}$	(1865.3)$^{+}$
0.7	1693.2	1689.2	1686.4	1685.0
	(1689.3)	(1685.5)	(1683.6)	(1680.5)
	(1880.3)$^{+}$	(1878.5)$^{+}$	(1877.2)$^{+}$	(1875.7)$^{+}$
1.0	1710.5	1707.3	1705.0	1702.0

Contd....

T(K) x	313.15	318.15	323.15	328.15
		R = 14		
0.0	1621.6	1619.8	1618.0	1616.2
0.3	1634.0	1633.6	1632.4	1631.6
	(1631.7)	(1630.5)	(1630.3)	(1630.9)
	(1808.1)+	(1803.7)+	(1800.2)+	(1798.3)+
0.6	1644.8	1644.0	1643.1	1642.2
	(1641.9)	(1642.3)	(1640.4)	(1641.8)
	(1769.2)+	(1768.1)+	(1767.0)+	(1766.2)+
1.0	1658.0	1656.0	1654.8	1654.0
		R = 15		
0.0	1619.8	1618.0	1616.8	1615.0
0.4	1635.2	1634.2	1632.2	1630.2
	(1631.1)	(1629.6)	(1629.0)	(1628.2)
	(1713.8)+	(1710.7)+	(1708.2)+	(1700.5)+
0.6	1640.6	1639.4	1638.2	1637.3
	(1637.8)	(1635.1)	(1634.2)	(1634.0)
	(1739.9)+	(1736.8)+	(1733.0)+	(1731.3)+
1.0	1655.0	1654.2	1653.0	1651.0

VALUES OF u EVALUATED USING NOMOTO'S EQUATION ARE GIVEN IN PARENTHESES AND THOSE EVALUATED BY VAN DAEL EQUATION ARE GIVEN IN PARENTHESES MARKED WITH +.

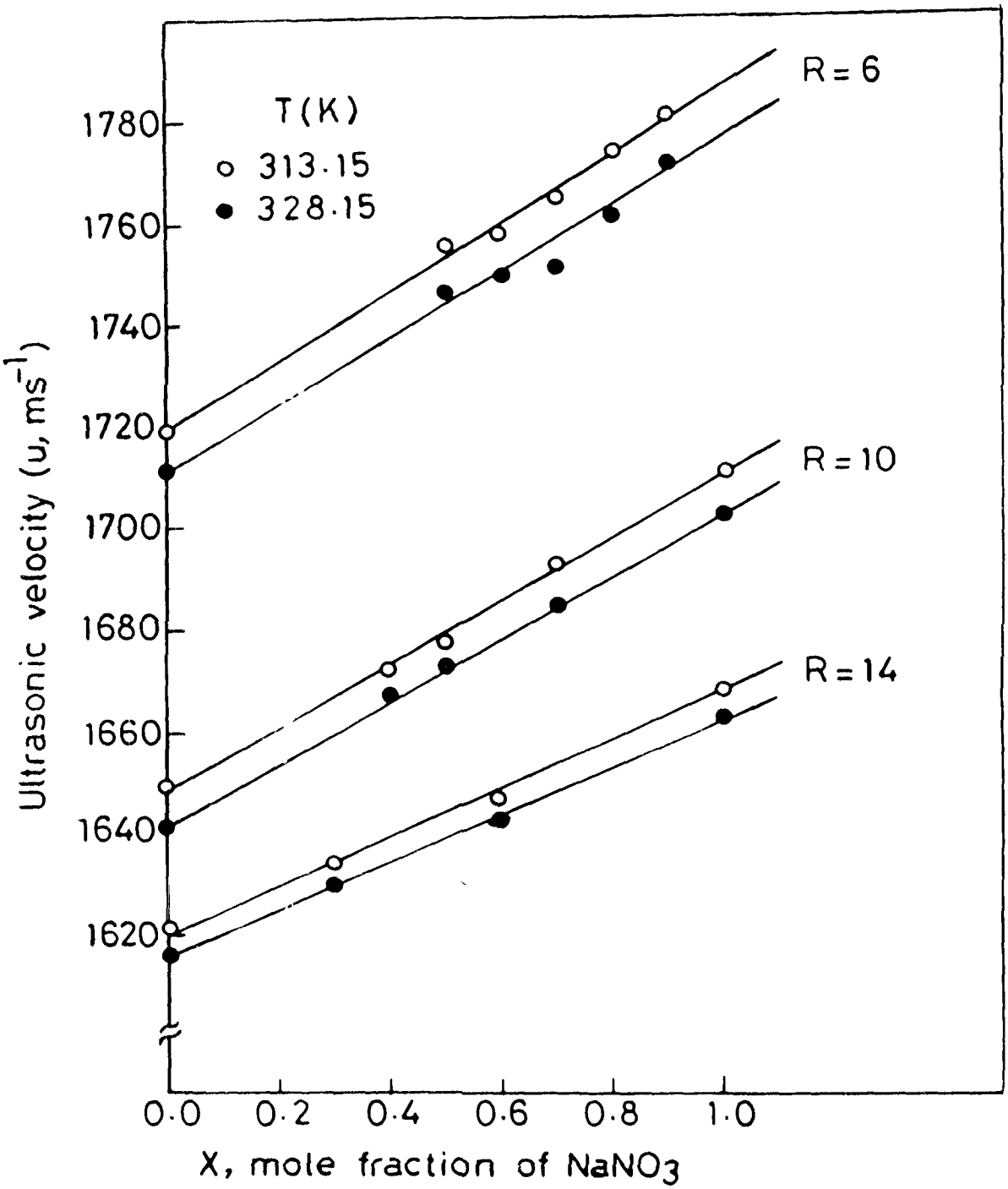

Fig. 1.1: Plots of u of $[x\ NaNO_3 + (1-x)KNO_3] + RH_2O$ (R = 6, 10 and 14) versus mole fraction of $NaNO_3$ at different temperatures.

Results indicate a lowering of compressibility in aqueous solutions of electrolytes below that of pure water. This decrease is attributed to two effects (1) introduction of incompressible ions causes decrease in the compressibility and (2) structure of water changes when ions are added.

Each alkali metal ion in water shows either of these two effects, since NO_3^- ion is common to both the electrolytes in the systems under investigation, the relative effects of cations may thus be studied.

An ion when added to water, affects the thermal motion of water molecules around it. The Na^+ ion is found to be a weak structure making ion[33] i.e. no disordered water molecules exist outside the reoriented water molecules around the Na^+ ion. According to Samiolov, the value of τ_i/τ_o for the Na^+ ion is 1.3 at room temperature, where τ_i and τ_o are the mean residence times of a water molecule in the immediate vicinity of the ion in the aqueous solution and in the immediate neighbourhood of a water molecule in pure state, respectively. The structure of water around the Na^+ ion is very much similar to that of the pure water because the coordination number of

TABLE 1.3: ADIABATIC COMPRESSIBILITIES $\beta s(10^{11}\ Cm^2\ dyne^{-1})$ AS FUNCTIONS OF TEMPERATURE FOR SOME COMPOSITIONS OF THE SYSTEMS: $[x\ NaNO_3 + (1-x)\ KNO_3) + RH_2O$ (where R = 6,10,14 or 15)

T(K) / x	313.15	318.15	323.15	328.15
		R = 6		
0.0	2.55	2.57	2.58	2.59
0.6	2.38	2.39	2.41	2.43
	(2.41)	(2.43)	(2.44)	(2.46)
0.7	2.33	2.35	2.37	2.38
	(2.38)	(2.39)	(2.40)	(2.42)
0.8	2.29	2.31	2.32	2.34
	(2.35)	(2.37)	(2.38)	(2.39)
0.9	2.26	2.28	2.29	2.31
	(2.30)	(2.31)	(2.33)	(2.34)
1.0	2.24	2.26	2.27	2.29

Contd...

T(K) x	313.15	318.15	323.15	328.15
		R = 10		
0.0	3.00	3.02	3.04	3.05
0.4	2.87	2.88	2.89	2.91
	(2.95)	(2.95)	(2.96)	(2.98)
0.5	2.86	2.87	2.88	2.89
	(2.90)	(2.92)	(2.95)	(2.95)
0.7	2.80	2.81	2.84	2.86
	(2.85)	(2.87)	(2.88)	(2.89)
1.0	2.75	2.77	2.78	2.80
		R = 14		
0.0	3.31	3.32	3.33	3.34
0.3	3.15	3.16	3.17	3.18
	(3.21)	(3.21)	(3.22)	(3.24)
0.6	3.05	3.06	3.07	3.09
	(3.10)	(3.10)	(3.12)	(3.14)
1.0	2.90	2.91	2.93	2.96

Contd....

T(K) x	313.15	318.15	323.15	328.15
		R = 15		
0.0	3.39	3.40	3.41	3.43
0.4	3.30	3.32	3.33	3.35
	(3.36)	(3.40)	(3.40)	(3.41)
0.6	3.24	3.26	3.27	3.29
	(3.27)	(3.30)	(3.35)	(3.35)
1.0	3.11	3.13	3.15	3.16

VALUES OF βs CALCULATED USING NOMOTO'S RELATION ARE GIVEN WITHIN PARENTHESES.

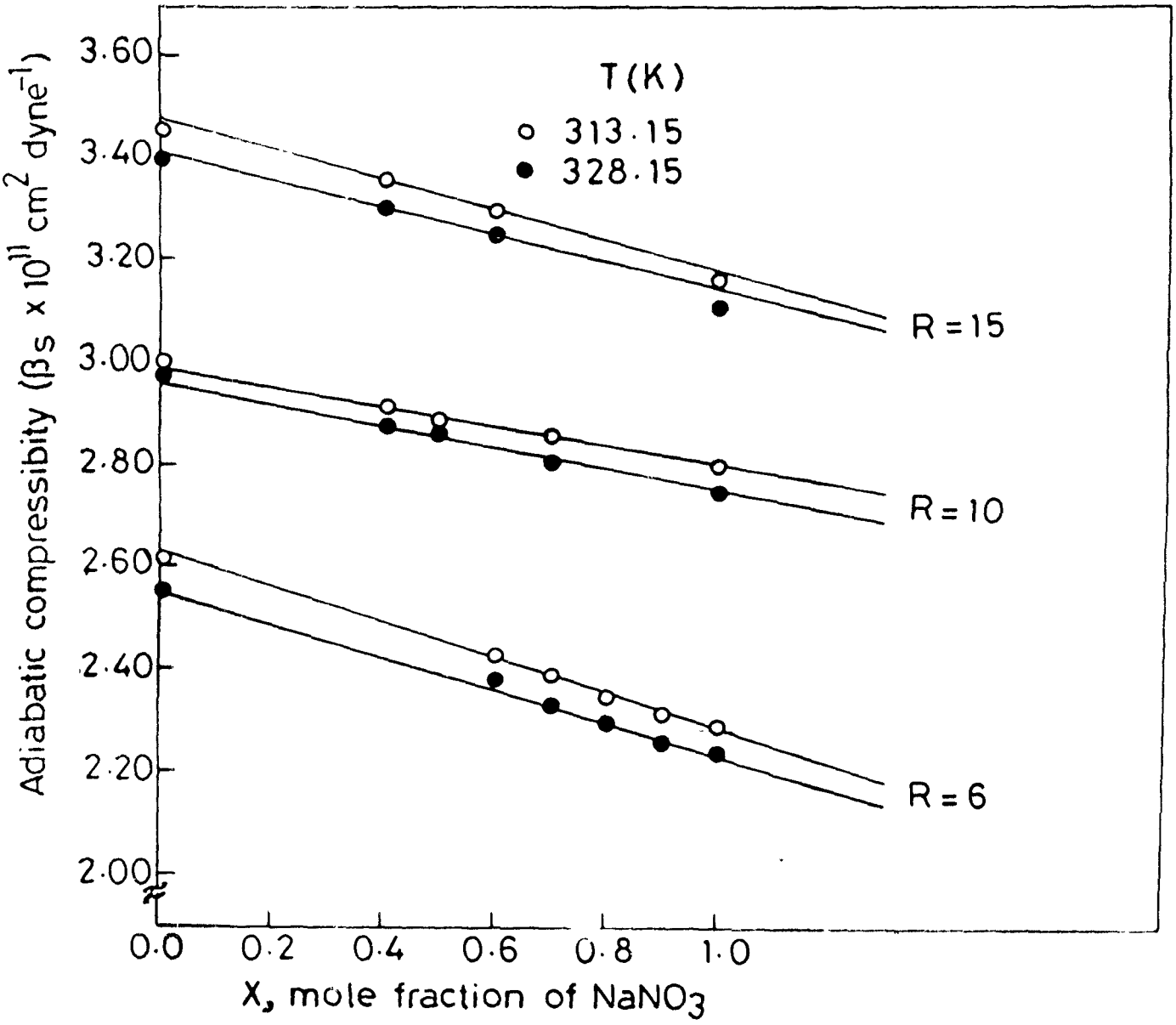

Fig. 1.2: Plots of β_s of $[x\ NaNO_3 + (1-x)KNO_3] + RH_2O$ (R = 6, 10 and 15) versus mole fraction of $NaNO_3$ at different temperatures.

TABLE 1.4: EXCESS ADIABATIC COMPRESSIBILITY, βs^E (10^{12},cm^2 $dyne^{-1}$) FOR SOME COMPOSITIONS AS A FUNCTION OF TEMPERATURE FOR THE SYSTEMS: [x $NaNO_3$ + (1-x)KNO_3]+ RH_2O (where R = 6,10,14 or 15)

T(K) / x	313.15	318.15	323.15	328.15
		R = 6		
0.6	-0.3343	-0.3154	-0.3503	-0.4125
0.7	-1.1033	-1.1238	-1.1731	-1.2708
0.8	-1.6766	-1.6365	-1.6578	-1.7334
0.9	+0.4196	-0.5042	-0.3707	0.2832
		R = 10		
0.4	-1.3715	-1.3483	-1.3195	-1.2058
0.5	-1.2934	-1.2896	-1.2826	-1.2043
0.7	0.3150	0.3639	0.3714	0.3766
		R = 14		
0.3	+1.3498	+1.3081	+1.2259	+1.3411
0.6	+0.9491	+0.9571	+1.0159	+1.0269
		R = 15		
0.4	+0.5007	+0.4962	+0.5212	+0.5100
0.6	+0.2228	+0.2257	+0.2331	+0.2355

the water molecule around Na^+ ion is 4. Thus, a decrease in the compressibility value of the aqueous solution of $NaNO_3$ below that of the pure water is attributed to the effect (1), also known as the dilution effect.

The K^+ ion, on the other hand, is a weak structure breaking ion. The structure breaking ions increase the thermal motion of water molecules[33]. According to Samiolov, surface density of the distribution of water molecules around the ion decreases as the ionic radius increases. Thus, K^+, a structure breaking ion causes the compressibility of the solution to increase in comparison to that of the $NaNO_3$ solution.

As Na^+ ions are added to the aqueous solution of K^+ ions, compressibility of solution decreases (Table 1.3). Addition of incompressible ions results in decrease in the compressibility of the solution. As the value of R decreases indicating an increase in the ionic concentration, the value of βs decreases [Aqueous solution with R = 6 has lower βs values in comparison to the solution with R = 10]. The variation of βs with x and temperature is shown in Fig. 1.2.

TABLE 1.5: MOLAR ULTRASONIC VELOCITIES AS FUNCTIONS OF COMPOSITION AND TEMPERATURE FOR THE SYSTEM: $[x\ NaNO_3 + (1-x)\ KNO_3] + RH_2O$ (where R = 6, 10, 14 or 15).

T(K) / x	313.15	318.15	323.15	328.15
		R = 6		
0.0	1255.0	1257.3	1259.7	1262.1
0.6	1170.9	1173.4	1176.1	1178.7
	(1180.1)	(1182.7)	(1185.1)	(1187.0)
0.7	1163.9	1166.3	1169.5	1171.5
	(1171.9)	(1172.5)	(1174.8)	(1174.7)
0.8	1158.8	1162.5	1165.8	1167.9
	(1165.9)	(1169.6)	(1170.8)	(1172.7)
0.9	1151.5	1154.5	1157.6	1160.4
	(1159.6)	(1161.9)	(1164.2)	(1166.0)
1.0	1140.8	1143.4	1146.0	1148.6

Contd....

T(K) / x	313.15	318.15	323.15	328.15
		R = 10		
0.0	1135.4	1139.1	1142.8	1147.0
0.4	1107.8	1109.9	1112.8	1116.0
	(1115.5)	(1119.7)	(1121.0)	(1122.6)
0.5	1100.2	1103.1	1106.0	1108.7
	(1110.4)	(1112.3)	(1113.7)	(1118.9)
0.7	1089.8	1092.5	1095.6	1098.9
	(1100.8)	(1104.8)	(1106.7)	(1107.9)
1.0	1075.3	1078.5	1081.5	1084.9
		R = 14		
0.0	1090.1	1093.3	1095.8	1098.3
0.3	1068.6	1071.4	1074.1	1077.9
	(1075.3)	(1078.7)	(1080.8)	(1084.5)
0.6	1052.6	1055.8	1057.9	1060.3
	(1058.2)	(1059.4)	(1062.5)	(1065.2)
1.0	1031.3	1034.1	1037.0	1040.0

Contd.....

T(K) / x	313.15	318.15	323.15	328.15
		R = 15		
0.0	1071.3	1074.5	1078.1	1081.3
0.4	1059.6	1062.9	1066.3	1069.5
	(1063.2)	(1066.9)	(1069.8)	(1073.7)
0.6	1035.8	1038.9	1042.3	1045.6
	(1039.3)	(1042.6)	(1046.0)	(1049.0)
1.0	998.3	1002.1	1005.3	1008.4

VALUES OF R^{*} OBTAINED USING NOMOTO'S EQUATION ARE GIVEN IN PARENTHESES.

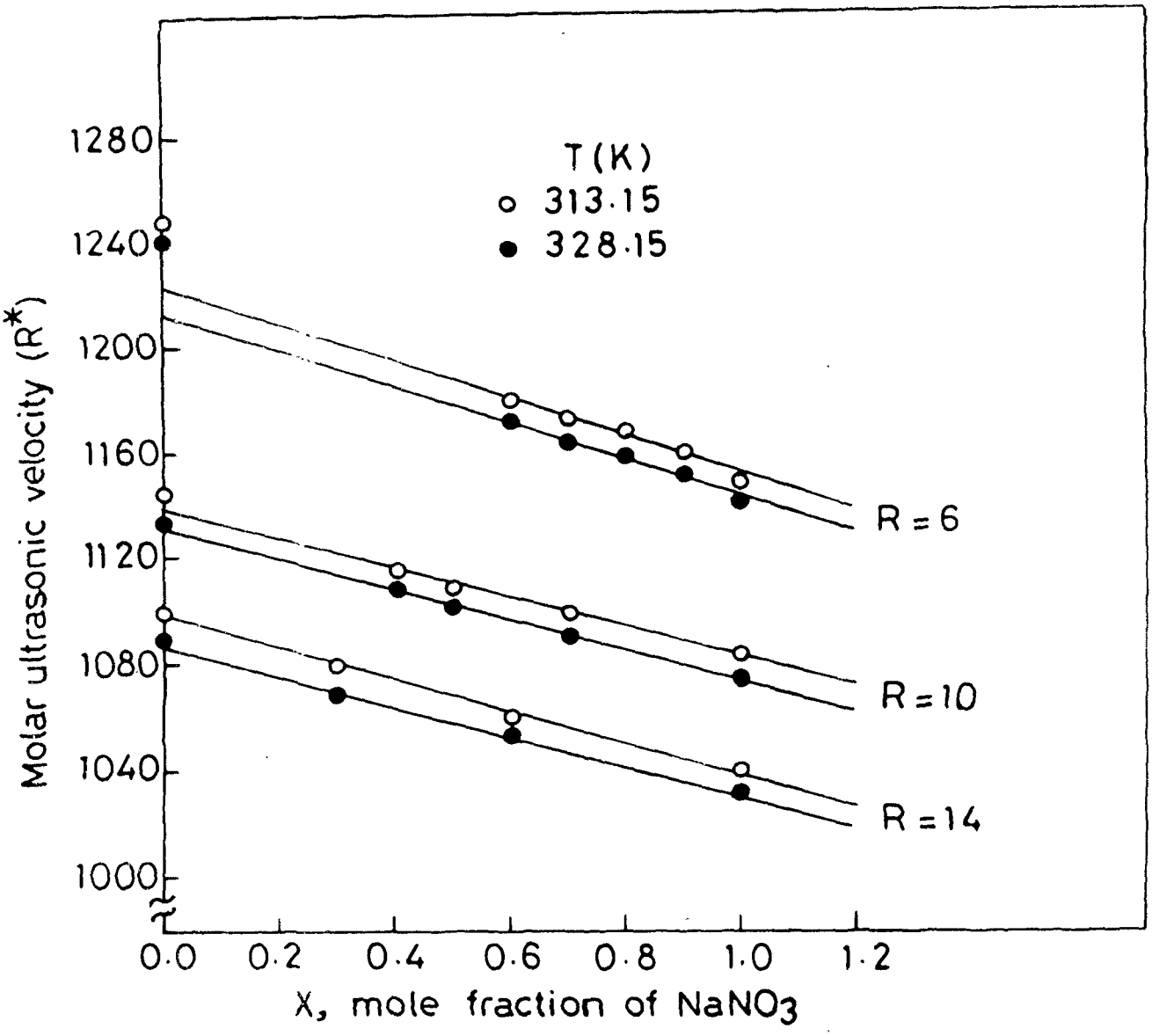

Fig. 1.3: Plots of Molar ultrasonic velocity (R^*) of $[x\ NaNO_3 + (1-x)KNO_3] + RH_2O$ (R = 6, 10 and 14) versus mole fraction of $NaNO_3$ of different temperatures.

TABLE 1.6: WADA's CONSTANT, B, AS A FUNCTION OF TEMPERATURE AND COMPOSITION FOR THE SYSTEMS: [x $NaNO_3$ + (1-x) KNO_3] + RH_2O (where R = 6,10,14 or 15)

T(K) / x	313.15	318.15	323.15	328.15
		R = 6		
0.0	735.75	736.94	738.15	739.35
0.6	688.57	689.85	691.23	692.52
0.7	660.81	662.17	663.50	664.81
0.8	648.44	649.54	650.74	651.89
0.9	640.53	641.60	642.71	643.79
1.0	633.78	635.12	636.30	637.41
		R = 10		
0.0	675.31	677.12	678.95	681.04
0.4	652.94	654.39	655.83	657.15
0.5	647.07	648.52	649.56	650.63
0.7	630.82	631.90	632.91	633.95
1.0	615.35	616.43	617.50	618.61

Contd....

T(K) x	313.15	318.15	323.15	328.15
		R = 14		
0.0	640.74	642.36	644.00	645.64
0.3	618.41	619.81	621.12	623.01
0.6	610.52	611.76	612.95	614.06
1.0	600.35	601.56	602.81	604.12
		R = 15		
0.0	629.61	631.21	633.00	634.57
0.4	612.27	613.92	615.58	617.18
0.6	601.53	602.85	604.33	605.92
1.0	579.81	581.45	583.03	584.56

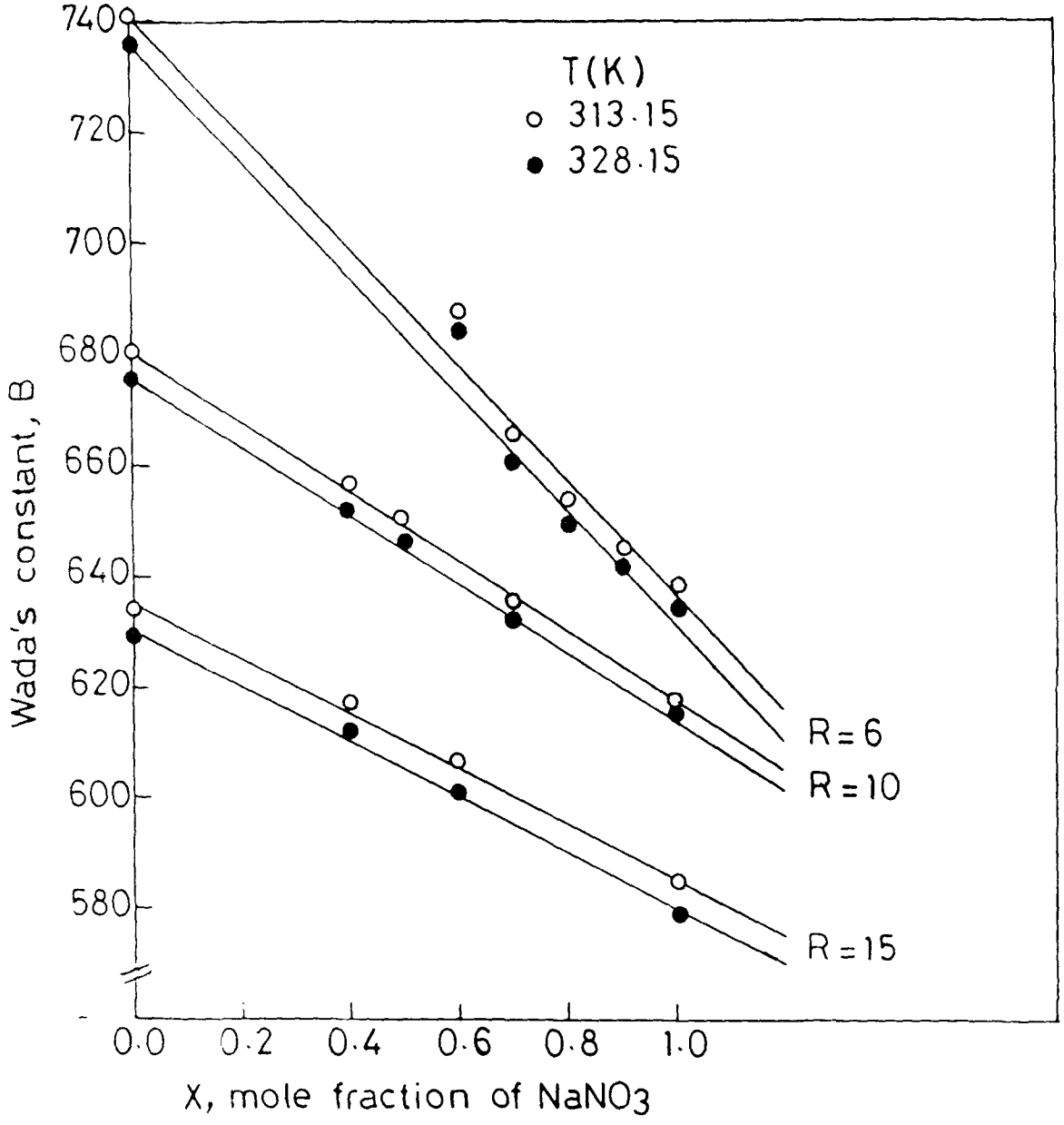

Fig. 1.4: Plots of Wada's constant, B of $[x\ NaNO_3 + (1-x)\ KNO_3] + RH_2O$ (R = 6, 10 and 15) versus mole fraction of $NaNO_3$ at different temperature.

The excess adiabatic compressibility, βs^E, which is a measure of the ionic interactions, shows positive values for the higher values of R, indicating weak ion-ion interaction, while negative values of βs^E for the lower R values indicate strong ionic interactions (Table 1.4).

The molar sound velocities, R^*, are obtained (Table 1.5) using equations (1.10) and (1.6) proposed by Subramanyam and Bhimsenachar[92] and Nomoto, respectively, and the values are listed in Table 1.5. The molar ultrasonic velocity is found to decrease with an increase in the concentration of $NaNO_3$, and increases with increase in temperature (Fig. 1.3).

The Wada's constant, B, is found to increase with increase in temperature (Table 1.6) and varies also with composition (Fig. 1.4).

The specific acoustic impedence, Z, is found to decrease with increase in temperature (Table 1.7). This is in accordance with equation (1.3), in which Z is directly proportional to density, which decreases with an increase in temperature. An increase in the value of Z is also noted with an increase in the mole fraction of $NaNO_3$.

TABLE 1.7: SPECIFIC ACOUSTIC IMPEDENCE ($Z \times 10^{-5}$, $gm.cm^{-2}.s^{-1}$) AS FUNCTIONS OF COMPOSITION AND TEMPERATURE FOR THE SYSTEMS: $[x\ NaNO_3 + (1-x)\ KNO_3] + RH_2O$ (where R = 6, 10,14 and 15)

T(K) / x	313.15	318.15	323.15	328.15
		R = 6		
0.0	2.2749	2.2664	2.2579	2.2494
0.6	2.3907	2.3794	2.3692	2.3579
0.7	2.4807	2.4708	2.4601	2.4492
0.8	2.5560	2.5417	2.5286	2.5150
0.9	2.6061	2.5942	2.5812	2.5683
1.0	2.6463	2.6312	2.6201	2.6084
		R = 10		
0.0	1.9699	1.9632	1.9530	1.9500
0.4	2.0812	2.0744	2.0674	2.0591
0.5	2.0852	2.0782	2.0711	2.0630
0.7	2.1132	2.1021	2.0922	2.0830
1.0	2.2147	2.2053	2.1960	2.1883

Contd....

T(K) x	313.15	318.15	323.15	328.15
		R = 14		
0.0	1.8647	1.8620	1.8592	1.8565
0.3	1.9410	1.9353	1.9286	1.9281
0.6	2.0251	2.0192	2.0030	1.9973
1.0	2.1273	2.1183	2.1135	2.1083
		R = 15		
0.0	1.8351	1.8301	1.8261	1.8202
0.4	1.9151	1.9035	1.9002	1.8957
0.6	1.9437	1.9388	1.9312	1.9273
1.0	2.0051	2.0008	1.9943	1.9895

TABLE 1.8: COMPUTED VALUES OF SURFACE TENSION (σ, dyne cm^{-1}) AS FUNCTIONS OF TEMPERATURE AND COMPOSITION FOR THE SYSTEMS: [x $NaNO_3$ + (1-x) KNO_3] + RH_2O (where R = 6,10,14 or 15)

T(K) / x	313.15	318.15	323.15	328.15
		R = 6		
0.0	59.42	59.15	58.89	58.63
0.6	62.10	62.74	62.43	62.07
0.7	64.80	64.49	64.16	63.82
0.8	66.83	66.36	65.94	65.50
0.9	67.75	67.20	66.73	66.25
1.0	68.63	68.12	67.68	67.20
		R = 10		
0.0	50.27	50.22	50.19	50.07
0.4	52.61	53.42	53.22	52.98
0.5	53.78	53.59	53.39	53.16
7	54.09	53.90	53.67	53.48
1.0	56.58	56.31	56.08	55.95

T(K) x	313.15	318.15	323.15	328.15
		R = 14		
0.0	47.22	47.18	47.10	47.07
0.3	49.43	49.27	49.09	48.98
0.6	51.98	51.78	51.59	51.37
1.0	54.07	53.96	53.78	53.60
		R = 15		
0.0	45.15	45.09	45.01	44.92
0.4	47.57	47.39	47.18	47.01
0.6	49.72	49.53	49.30	49.12
1.0	52.46	52.30	52.15	52.02

Addition of an electrolyte to water causes an increase in the value of its surface tension, which probably corresponds to desorption of salt from the surface region.[96] Several workers[97] have considered that the surface layer on electrolyte solutions consists of a salt-free zone ca 10^{-10} m thick and its thickness varies depending on the extent of desorption. The values of surface tension obtained using Eq. (1.18) for the systems under investigation show a decrease with an increase in temperature (Table 1.8). Such a behaviour may be attributed to a decrease in the ion-ion interaction. A decrease in the R value shows an increase in the surface tension, indicating an increase in the attractive forces among ions as expected on increasing the concentration.

INTRODUCTION

The measurement of ultrasonic velocity helps in understanding the nature of intermolecular interactions in liquids through a number of thermodynamic properties derived from it. Among these properties, the internal pressure is one of the important properties of liquids[98-100]. The thermodynamic and ultrasonic measurements are used to determine the internal pressure of liquids[101]. Internal pressure data for liquids was used by Stavely *et al*[51] to predict the intermolecular interactions in liquid mixtures. The relation proposed by Buchler *et al*[102] for obtaining the internal pressure has been used for the determination of internal pressure of molten salts and liquid metals[103]. Dunlop *et al*[50] also determined the internal pressure of different liquid mixtures and compared them with their cohesive energy density .alues.

The Pseudo-Gruneisen parameter, Γ, is a useful parameter for the study of thermodynamics of any system and has been calculated by several workers[55,56,88,104].

A number of fluid equations of state for the hard-spheres

have been proposed recently[105-113]. Chaturvedi *et al*[114] used the equation of Carnahan and Starling[105] and Thiele[106] to obtain the isothermal compressibility and the related properties of several liquids.

In the present work, an attempt has been made to calculate the internal pressure, p_i, the isothermal compressibility, β_T, and the Pseudo-Gruneisen parameter, Γ, using the ultrasonic velocity data.

THEORETICAL

Following are the rigid-sphere equations of state used for the calculation of isothermal compressibility:

$$\frac{PV}{NkT} = \frac{1+y+y^2}{(1-y)^3} \qquad (2.1)$$

$$\frac{PV}{NkT} = \frac{1+2y+3y^2}{(1-y)^2} \qquad (2.2)$$

$$\frac{PV}{NkT} = \frac{1+y+y^2-y^3}{(1-y)^3} \qquad (2.3)$$

$$\frac{PV}{NkT} = \frac{1}{(1-y)^4} \qquad (2.4)$$

and

$$\frac{PV}{NkT} = \frac{1}{(1-y)^2} \qquad (2.5)$$

where P, V, T, N and k are the pressure, the volume, the absolute temperature, the Avogadro's number and the Boltzmann constant, respectively. Here, y is the packing fraction, which is expressed as

$$y = \frac{\pi d^3 N}{6V} \qquad (2.6)$$

where d is the rigid sphere diameter of the molecules comprising the pure liquids.

For the calculation of 'd', the following equation[118] is used:

$$d^{5/2} = \frac{V}{7.21 \times 10^{19}} \left(\frac{\sigma}{T_c}\right)^{1/4} \qquad (2.7)$$

where σ, T_c and V are the surface tension, the critical temperature and the molar volume, respectively. The critical temperature, T_c, is calculated using the equation,

$$V_o = V_T \left(1 - \frac{T}{T_c}\right)^{0.3} \tag{2.8}$$

where V_o and V_T are the molar volumes at the zero degree absolute and the absolute temperature, T, respectively.

The values of surface tension, σ, have been obtained by employing eq. (1.18).

Using equations (2.1) to (2.5), the isothermal compressibilities, β_T, are calculated from the following expressions:

$$\beta_T = \frac{V}{R'T} \cdot \frac{(1-y)^4}{(1+2y)^2} \tag{2.9}$$

$$\beta_T = \frac{V}{R'T} \cdot \frac{(1-y)^3}{1+5y+9y^2-3y^3} \tag{2.10}$$

$$\beta_T = \frac{V}{R'T} \cdot \frac{(1-y)^4}{1+4y+4y^2-4y^3+y^4} \tag{2.11}$$

$$\beta_T = \frac{V}{R'T} \cdot \frac{(1-y)^5}{1+3y} \tag{2.12}$$

$$\beta_T = \frac{V}{R'T} \cdot \frac{(1-y)^3}{1+y} \cdot \tag{2.13}$$

CHAPTER II

ISOTHERMAL COMPRESSIBILITY AND INTERNAL PRESSURE OF SODIUM AND POTASSIUM NITRATES IN AQUEOUS MEDIUM

The internal pressure can be obtained using the relation ,

$$P_i V \left(1 - \frac{d}{b}\right) = R'T \qquad (2.14)$$

where P_i, V, d, b, R' and T stand for the internal pressure, the molar volume, the molecular diameter, the shortest distance between the nearest neighbours, the gas constant and the absolute temperature, respectively. The molecular volume, $v \left(= \frac{V}{N} \right)$ is related to b, the distance between the nearest neighbours as follows:

$$v = \frac{b^3}{2^{1/2} V^2} \cdot \qquad (2.15)$$

This expression is then rearranged to give the value of b, as follows:

$$b = \frac{2^{1/6} V^{1/3}}{N^{1/3}} \cdot \qquad (2.16)$$

Substituting the value of b in the equation for internal pressure, P_i, [eq. (2.14)], we obtain,

$$P_i = \frac{2^{1/6} R' T}{(2^{1/6} V - d N^{1/3} V^{2/3})} \quad . \qquad (2.17)$$

The molecular diameter is obtained by using eq. (2.7).

The Pseudo-Gruneisen parameter, Γ, is calculated using the expression,

$$\Gamma = \frac{\gamma - 1}{T\alpha} \qquad (2.18)$$

where γ and α stand for the specific heat ratio and the thermal expansion coefficient, respectively.

For the calculation of γ, the following relation is used:

$$\beta_T = \beta_S \gamma \qquad (2.19)$$

where β_S is the adiabatic compressibility.

For obtaining α, the density equation[119] is used,

$$\alpha = \frac{1}{\rho} \left(\frac{\delta \rho}{\delta T}\right) \qquad (2.20)$$

where, ρ stands for the density of the system.

RESULTS AND DISCUSSION

The isothermal compressibility values, β_T, of binary and ternary solutions of sodium and potassium nitrates in aqueous medium have been obtained using equations (2.9) to (2.13). An examination of Table 2.1 reveals that the calculated values of β_T at 313.15 K increase with increase in the R value (i.e., with decrease in the ionic concentration). This increase in β_T is attributed to a decrease in the concentration of incompressible ions. The values of β_T, on the other hand, show a decreasing trend with increase in the mole fraction, x.

The calculated values of internal pressure, P_i (Table 2.2), based on eq. (2.17) are found to increase with increase in the mole fraction of $NaNO_3$. These values also increase with increase in temperature. This trend in their behaviour may be attributed to the low compressibility of these solutions due to which an increase in temperature causes an increase in the internal pressure. P_i also increases with an increase in the value of R.

TABLE 2.1: ISOTHERMAL COMPRESSIBILITY, β_T (10^{11}, cm^2 $dyne^{-1}$) FOR [x $NaNO_3$ + (1-x) KNO_3] + RH_2O (where R = 6, 10, 14 or 15) SYSTEMS AT 313.15 K.

x	EQNS: 2.9	2.10	2.11	2.12	2.13
			R = 6		
0.0	3.69	4.65	3.96	8.91	13.93
0.6	2.96	3.81	3.20	7.44	11.77
0.7	2.79	3.60	3.01	7.03	11.13
0.8	2.63	3.41	2.84	6.69	10.62
0.9	2.46	3.23	2.66	6.28	9.97
1.0	2.31	3.02	2.43	5.86	9.48
			R = 10		
0.0	3.88	4.81	4.15	9.08	14.09
0.4	3.50	4.36	3.75	8.28	12.90
0.5	3.47	4.33	3.71	8.22	12.80
0.7	3.39	4.10	3.43	8.01	12.73
1.0	3.08	3.74	3.05	7.69	12.58

Contd...

EQS: x	2.9	2.10	2.11	2.12	2.13
		R = 14			
0.0	4.20	5.11	4.47	9.49	14.58
0.3	3.83	4.70	4.08	8.78	13.54
0.6	3.78	4.58	3.93	8.53	13.38
1.0	3.62	4.39	3.78	8.37	13.13
		R = 15			
0.0	4.29	5.20	4.55	9.57	14.65
0.4	4.13	4.71	4.10	8.79	13.55
0.6	3.98	4.57	3.97	8.67	13.42
1.0	3.70	4.36	3.75	8.45	13.23

TABLE 2.2: INTERNAL PRESSURE, P_i (10^{-10} dyne cm^{-2}) AS FUNCTIONS OF MOLE-FRACTION AND TEMPERATURE FOR THE SYSTEMS: $[x\ NaNO_3 + (1-x)KNO_3] + RH_2O$ (where R = 6,10,14 or 15)

T(K) / x	313.15	318.15	323.15	328.15
		R = 6		
0.0	0.595	0.599	0.605	0.611
0.6	0.621	0.626	0.630	0.637
0.7	0.624	0.628	0.631	0.636
0.8	0.630	0.635	0.640	0.646
0.9	0.637	0.642	0.647	0.651
1.0	0.650	0.654	0.659	0.666
		R = 10		
0.0	0.613	0.621	0.629	0.634
0.4	0.642	0.645	0.649	0.653
0.5	0.648	0.654	0.658	0.662
0.7	0.657	0.660	0.664	0.669
1.0	0.668	0.672	0.676	0.718

Contd...

T(K) / x	313.15	318.15	323.15	328.15
		R = 14		
0.0	0.625	0.629	0.634	0.639
0.3	0.639	0.643	0.649	0.651
0.6	0.658	0.661	0.663	0.667
1.0	0.679	0.682	0.686	0.689
		R =15		
0.0	0.635	0.643	0.651	0.659
0.4	0.651	0.659	0.667	0.675
0.6	0.667	0.675	0.681	0.687
1.0	0.689	0.693	0.699	0.708

TABLE 2.3: PSEUDO-GRUNEISEN PARAMETER, Γ, FOR THE SYSTEMS: $[x\ NaNO_3 + (1-x)KNO_3] + RH_2O$ (where R = 6, 10, 14 or 15) AS A FUNCTION OF COMPOSITION AND TEMPERATURE.

T(K) / x	313.15	318.15	323.15	328.15
		R = 6		
0.0	5.890	5.693	5.480	5.275
0.6	4.628	4.403	4.191	3.987
0.7	4.434	4.219	4.013	3.816
0.8	4.130	3.917	3.717	3.526
0.9	3.808	3.620	3.418	3.220
1.0	3.512	3.314	3.120	2.890
		R = 10		
0.0	4.402	4.199	4.007	3.836
0.4	4.022	3.819	3.624	3.435
0.5	3.959	3.758	3.566	3.380
0.7	3.700	3.518	3.331	3.138
1.0	3.318	3.133	2.955	2.787

Contd.....

T(K) x	313.15	318.15	323.15	328.15
		R = 14		
0.0	4.100	3.905	3.732	3.557
0.3	3.884	3.681	3.484	3.324
0.6	3.605	3.345	3.200	3.035
1.0	3.379	3.189	3.013	2.848
		R = 15		
0.0	4.065	3.866	3.687	3.505
0.4	3.710	3.525	3.350	3.181
0.6	3.532	3.317	3.205	3.112
1.0	3.015	2.976	2.813	2.705

The calculated values of Pseudo-Gruneisen parameter, Γ, (Table 2.3) obtained using eq. (2.18) for the aqueous solutions of mixed electrolytes show dependence on temperature as well as on composition.

It may, therefore, be concluded from the above results that the solute-solute and the solute-solvent interactions increase in magnitude with increase in the concentration of electrolytes.

CHAPTER-III

APPLICATION OF FLORY THEORY TO MIXTURES OF SODIUM AND POTASSIUM NITRATES IN AQUEOUS MEDIUM.

INTRODUCTION

P.J. Flory[45] proposed a simple theory representing the liquid state properties on the basis of a simple partition function to explain the properties of liquid mixtures of non-polar molecules. Properties of mixtures were analysed by Flory using the parameters characterizing the pure components, e.g., density, thermal expansion coefficient and thermal pressure coefficient; theoretical expressions for free-energy, entropy, enthalpy and excess volumes were derived. Since this theory is mathematically simple, it has been used extensively for predicting the various properties of liquids. Flory theory has been employed to calculate the reduced and the characteristic parameters of liquids which, in turn, have been used to calculate the interaction parameter, X_{12}, the surface tension, σ, the free-energy, G, the entropy, S, the viscosity of pure liquids, η_i as well as of their binary mixtures, η. In addition, the excess free-energy, ΔG^E, the excess entropy of mixing, ΔS^E, the excess viscosity, η^E, the excess molar volume, ΔV^E and the ultrasonic velocity, u have also been evaluated. The values of σ and those of u have

been obtained for the ternary systems[4,5].

Applicability of this theory has also been tested[97,117-123] over a wide range of room temperature liquids and their binary mixtures. Some workers have also made attempts to apply it to molten salts[124] and their binary mixtures[22,125]. Results of the theoretical evaluation were found to be in agreement with those of the experimental values.

An attempt has, therefore, been made to apply the Flory's statistical theory to the aqueous solutions of sodium and potassium nitrates and their mixtures.

THEORETICAL

TREATMENT OF DATA OF PURE COMPONENTS:

The thermal coefficient, α, is derived from the density equation[116],

$$\alpha = \frac{1}{\rho}\left(\frac{\delta\rho}{\delta T}\right) \qquad (3.1)$$

where ρ is the density of the system.

The reduced equation of state given by Flory[45,46],

$$\tilde{P}\tilde{V}/\tilde{T} = [\tilde{V}^{1/3}/(\tilde{V}^{1/3}-1)] - 1/\tilde{V}\tilde{T} \qquad (3.2)$$

is of the same form as given by Eyring and Hirschfelder[126,127].

The reduced quantities viz., the reduced volume, $\tilde{V}$, the reduced temperature, $\tilde{T}$, and the reduced pressure, $\tilde{P}$, are expressed as

$$\tilde{V} = V/V^* \qquad (3.3)$$

$$\tilde{P} = P/P^* \qquad (3.4)$$

$$\tilde{T} = T/T^* \qquad (3.5)$$

where V, P and T represent the molar volume, the atmospheric pressure and the absolute temperature, respectively, while V^*, P^* and T^* represent the characteristic quantities of the pure components.

The reduced volume, $\tilde{V}$, is also given by

$$\tilde{V}^{1/3} - 1 = \alpha T/3(1+\alpha T) \qquad (3.6)$$

where α is the coefficient of thermal expansion at temperat

T; here pressure is assumed to be zero. Eq. (3.6) has been found to be applicable to systems not only in the low pressure range but also at atmospheric pressure with insignificant error. The reduced temperature is obtained by using the value of reduced volume obtained from eq.(3.6),

$$\tilde{T} = \frac{\tilde{V}^{1/3} - 1}{\tilde{V}^{4/3}} \quad . \tag{3.7}$$

The characteristic pressure, P^*, is obtained from the reduced equation of state as,

$$P^* = \gamma \, T \, \tilde{V}^2 \tag{3.8}$$

where γ, the thermal pressure coefficient, is given as

$$\gamma = \left(\frac{\delta P}{\delta T}\right)_V = \frac{\alpha}{\beta_T} \tag{3.9}$$

where β_T is the isothermal compressibility and α is the thermal expansion coefficient.

In order to evaluate the various reduced and the characteristic parameters using the Flory theory, the aqueous solutions of $NaNO_3$ and KNO_3 have been treated as the two pure

TREATMENT OF DATA OF BINARY MIXTURES:

The reduced volume of mixtures is obtained by the extension of Flory's statistical theory to binary systems and is given as,

$$\tilde{V} = \frac{V}{x V_1^* + (1-x) V_2^*} \qquad (3.10)$$

The reduced temperature, $\tilde{T}$, is given as

$$\tilde{T} = (\psi_1 P_1^* \tilde{T}_1 + \psi_2 P_2^* \tilde{T}_2)/(\psi_1 P_1^* + \psi_2 P_2^* - \psi_1 \theta_2 X_{12}) \qquad (3.11)$$

where θ, ψ and X_{12} represent the site fraction, the segment fraction and the interaction parameter, respectively. Subscripts 1 and 2 refer to the two components.

Following expressions are employed to evaluate the characteristic parameters of binary mixtures:

$$V^* = x V_1^* + (1-x) V_2^* ; \qquad (3.12)$$

$$P^* = \psi_1 P_1^* + \psi_2 P_2^* - \psi_1 \theta_2 X_{12} \qquad (3.13)$$

$$T^* = \left(\frac{\psi_1 P_1^*}{T_1^*} + \frac{\psi_2 P_2^*}{T_2^*}\right)^{-1} (\psi_1 P_1^* + \psi_2 P_2^* - \psi_1 \theta_2 X_{12}) \qquad (3.14)$$

where x and (1-x) represent the mole fractions of components 1 and 2 respectively, in the binary mixture.

To obtain the segment fractions ψ_1 and ψ_2, the site fractions θ_1 and θ_2, and the interaction parameter, X_{12}, for the components, the following expressions are used:

$$\psi_2 = 1 - \psi_1 = \frac{(1-x)}{(1-x)+x\left(\frac{V_1^*}{V_2^*}\right)} ; \tag{3.15}$$

$$\theta_2 = 1 - \theta_1 = \frac{\psi_2}{\psi_2 + \psi_1 \left(\frac{V_1^*}{V_2^*}\right)^{-1/3}} ; \text{ and} \tag{3.16}$$

$$X_{12} = P_1^* \left[1 - \left(\frac{V_2^*}{V_1^*}\right)^{-1/6} \left(\frac{P_2^*}{P_1^*}\right)^{1/2}\right]^2 . \tag{3.17}$$

The reduced volume of mixtures is also obtained by an alternative method. The ideal reduced volume, $\tilde{V}_o$, is given as,

$$\tilde{V}_o = \psi_1 \tilde{V}_1 + \psi_2 \tilde{V}_2 . \tag{3.18}$$

The ideal reduced temperature, $\tilde{T}_o$, is expressed as,

$$\tilde{T}_o = (\tilde{V}_o^{1/3} - 1)/\tilde{V}_o^{4/3} . \qquad (3.19)$$

The excess reduced volume is given by

$$\tilde{V}^E = (\partial\tilde{V}/\partial\tilde{T})(\tilde{T} - \tilde{T}_o)$$

$$= \tilde{V}_o^{7/3} \left(\frac{4}{3} - \tilde{V}_o^{1/3}\right)^{-1} (\tilde{T} - \tilde{T}_o); \qquad (3.20)$$

and the $\tilde{V}_{calcd}$ as,

$$\tilde{V}_{calcd} = \tilde{V}_o - \tilde{V}^E . \qquad (3.21)$$

EXCESS VOLUME: The observed reduced volume, $\tilde{V}_{obsd}$, obtained from eq. (3.10) and the excess reduced volume, $\tilde{V}^E$, are related to each other by the expression,

$$\tilde{V}_{obsd} - \tilde{V}_o = \tilde{V}^E = V^E/(xV_1^* + (1-x)V_2^*) \qquad (3.22)$$

where $\tilde{V}_o$ is given by eq. (3.18). From equations (3.22) and (3.18), we obtain,

$$V^E = [xV_1^* + (1-x)V_2^*]\ [\tilde{V} - (\psi_1\tilde{V}_1 + \psi_2\tilde{V}_2)]. \qquad (3.23)$$

VISCOSITY: The thermodynamic functions of mixing can be expressed in terms of the solution activation energy, ΔG^*, the pure liquid activation energies, ΔG_1^* and ΔG_2^*, and the excess free energy of mixing, ΔG_M, as follows:

$$\Delta G^* = X \Delta G_1^* + (1-x)\ \Delta G_2^* - \Delta G_M \ . \qquad (3.24)$$

The viscosity of the pure component i, is related to the solution activation energy, ΔG_i^*, through the expression,

$$\eta_i = A \exp \left[\Delta G_i^* / R' T + (\tilde{V}_i - 1)^{-1} \right] \qquad (3.25)$$

where R' is the gas constant.

Taking logarithm of eq. (3.25), we obtain,

$$\ell n\ \eta_i = \ell n\ A + \frac{\Delta G_i^*}{R'T} + (\tilde{V}_i - 1)^{-1} . \qquad (3.26)$$

An expression for the excess viscosity is obtained by applying eq. (3.26) to the mixture and its pure components as follows:

$$\Delta \ell n\ \eta = \ell n\ \eta_{mix} - (x\ \ell n\ \eta_1 + (1-x)\ \ell n\ \eta_2) \qquad (3.27)$$

where η_1 and η_2 stand for the viscosities of pure components of binary mixtures. Substituting the values of η_i from eq. (3.25) and that of ΔG from eq. (3.24); eq. (3.27) takes on the form,

$$\Delta \ell n \ \eta = -\Delta G_M/R'T + \frac{1}{\tilde{V} - 1} - \frac{x}{\tilde{V}_1 - 1} - \frac{(1 - x)}{\tilde{V}_2 - 1} . \qquad (3.28)$$

Equations (3.27) and (3.28) give,

$$\ell n \ \eta_{mix} = -\Delta G_M/R'T + \frac{1}{\tilde{V} - 1} - \frac{x}{\tilde{V}_1 - 1} - \frac{(1 - x)}{\tilde{V}_2 - 1} + x \ell n \ \eta_1 + (1-x) \ell n \ \eta_2 . \qquad (3.29)$$

The excess free energy of mixing is obtained as

$$\Delta G_M = x P_1^* V_1^* [(\frac{1}{\tilde{V}_1} - \frac{1}{\tilde{V}}) + 3 \tilde{T}_1 \ell n (\frac{\tilde{V}_1^{1/3} - 1}{\tilde{V}^{1/3} - 1})] + (1-x) P_2^* V_2^* [(\frac{1}{\tilde{V}_2} - \frac{1}{\tilde{V}}) + 3 \tilde{T}_2 \ell n (\frac{\tilde{V}_2^{1/3} - 1}{\tilde{V}^{1/3} - 1}) + x V_1^* \theta_2 \ X_{12} \ V \qquad (3.30)$$

where all the symbols have their usual meaning.

In the present work, an attempt has been made to evaluate the various reduced and the characteristic parameters and the measured values of viscosities have been compared with those calculated using the Flory's statistical theory. (The ternary mixtures of sodium and potassium nitrates in aqueous media have been treated as binary mixtures for the purpose of calculation without introducing much error.)

RESULTS AND DISCUSSION

The calculated values of thermal expansion coefficient, α, obtained (Table 3.1) using eq. (3.1) are found to decrease slightly with increase in temperature and increase with increase in the concentration of $NaNO_3$.

The reduced volumes, $\tilde{V}$, of binary solutions (obtained by using eq. (3.6) and of ternary solutions (obtained by using equations (3.10) and (3.21) listed in Table 3.2 show an increase in their values with increase in temperature. The values of $\tilde{V}_{obsd}$ are not found to be affected significantly by variations in the values of R. An agreement between the $\tilde{V}_{obsd}$ and $\tilde{V}_{calcd}$ values is found to be quite reasonable. The values of reduced temperature, $\tilde{T}$ (Table 3.3) obtained by using equations (3.7) and (3.11) for the binary and the ternary solutions, respectively, show an increase with increase in temperature and also increase with increase in the concentration of $NaNO_3$. $\tilde{T}$ unlike $\tilde{V}$ has been found to increase with increase in the R value.

The characteristic volumes, V^*, calculated by using equations (3.3) and (3.12) for the binary and the ternary

TABLE 3.1: THERMAL EXPANSION COEFFICIENT (α, 10^{3} K^{-1}) OF THE SYSTEMS: $[x\ NaNO_3 + (1-x)KNO_3] + RH_2O$ (where R = 6,10,14 or 15).

T(K) / x	313.15	318.15	323.15	328.15	333.15	338.15
			R = 6			
0.0	0.3639	0.3633	0.3626	0.3619	0.3613	0.3606
0.6	0.4153	0.4145	0.4136	0.4128	0.4119	0.4111
0.7	0.4159	0.4150	0.4142	0.4133	0.4125	0.4116
0.8	0.4237	0.4228	0.4229	0.421[illegible]	0.4202	0.4193
0.9	0.4211	0.4082	0.4204	0.4206	0.4187	0.4149
1.0	0.4280	0.4271	0.4262	0.4253	0.4244	0.4235
			R = 10			
0.0	0.3840	0.3832	0.3824	0.3816	0.3808	0.3800
0.4	0.4126	0.4118	0.4110	0.4101	0.4093	0.4084
0.5	0.4144	0.4136	0.4127	0.4114	0.4110	0.4012
0.7	0.4255	0.4244	0.4333	0.4722	0.4210	0.4199
1.0	0.4393	0.4383	0.4374	0.4364	0.4355	0.4345

Contd...

T(K) x	313.15	318.15	323.15	328.15	333.15	338.15
			R = 14			
0.0	0.3900	0.3892	0.3885	0.3877	0.3870	0.3862
0.3	0.4042	0.4034	0.4026	0.4018	0.4010	0.4002
0.6	0.4012	0.4004	0.3996	0.3988	0.3980	0.3972
1.0	0.4246	0.4237	0.4228	0.4220	0.4211	0.4202
			R = 15			
0.0	0.3962	0.3954	0.3946	0.3938	0.3930	0.3923
0.4	0.4070	0.4062	0.4054	0.4046	0.4038	0.4029
0.6	0.4070	0.4061	0.4055	0.4055	0.4049	0.4029
1.0	0.4233	0.4224	0.4215	0.4207	0.4198	0.4189

TABLE 3.2: REDUCED VOLUME ($\tilde{V}_{obsd.}$ and $\tilde{V}_{calcd.}$) OF THE SYSTEMS: $[x\ NaNO_3 + (1-x)KNO_3] + RH_2O$ (where R = 6,10,14 or 15).

T(K) / x	313.15	318.15	323.15	328.15	333.15	338.15
			R = 6			
0.0	1.105	1.107	1.108	1.109	1.111	1.112
0.6	1.097	1.099	0.101	1.102	1.104	1.105
	(1.108)	(1.110)	(1.112)	(1.113)	(1.114)	(1.116)
0.7	1.090	1.089	1.093	1.094	1.096	1.097
	(1.105)	(1.106)	(1.108)	(1.110)	(1.112)	(1.114)
0.8	1.091	1.092	1.092	1.095	1.097	1.098
	(1.103)	(1.104)	(1.106)	(1.108)	(1.109)	(1.110)
0.9	1.095	1.096	1.097	1.099	1.100	1.102
	(1.108)	(1.109)	(1.110)	(1.112)	(1.114)	(1.115)
1.0	1.102	1.103	1.105	1.106	1.107	1.108
			R = 10			
0.0	1.111	1.113	1.114	1.115	1.117	1.119
0.4	1.098	1.099	1.100	1.102	1.103	1.104
	(1.110)	(1.112)	(1.113)	(1.114)	(1.116)	(1.117)
0.5	1.095	1.096	1.093	1.099	1.101	1.103
	(1.112)	(1.113)	(1.114)	(1.115)	(1.116)	(1.117)
0.7	1.104	1.105	1.106	1.107	1.109	1.110
	(1.117)	(1.119)	(1.120)	(1.121)	(1.123)	(1.125)
1.0	1.107	1.108	1.109	1.110	1.112	1.113

T(K) / x	313.15	318.15	323.15	328.15	333.15	338.15
			R = 14			
0.0	1.112	1.113	1.115	1.117	1.119	1.120
0.3	1.099	1.099	1.102	1.105	1.108	1.110
	(1.107)	(1.109)	(1.110)	(1.111)	(1.112)	(1.114)
0.6	1.105	1.107	1.109	1.110	1.112	1.114
	(1.112)	(1.114)	(1.116)	(1.118)	(1.119)	(1.121)
1.0	1.115	1.116	1.117	1.118	1.119	1.120
			R = 15			
0.0	1.114	1.115	1.116	1.118	1.118	1.122
0.4	1.110	1.111	1.113	1.115	1.117	1.118
	(1.121)	(1.122)	(1.124)	(1.126)	(1.127)	(1.129)
0.6	1.115	1.116	1.118	1.119	1.121	1.123
	(1.124)	(1.126)	(1.127)	(1.129)	(1.131)	(1.133)
1.0	1.121	1.122	1.123	1.124	1.125	1.126

* $\tilde{V}_{calcd.}$ VALUES ARE GIVEN WITHIN PARENTHESES.

TABLE 3.3: REDUCED TEMPERATURE, $\tilde{T}$ OF THE SYSTEMS: $[x\ NaNO_3 + (1-x)KNO_3] + RH_2O$ (where R = 6,10, 14 or 15).

T(K) / x	313.15	318.15	323.15	328.15	333.15	338.15
			R = 6			
0.0	0.0205	0.0207	0.0209	0.0212	0.0215	0.0218
0.6	0.0208	0.0211	0.0214	0.0217	0.0220	0.0223
0.7	0.0212	0.0213	0.0216	0.0219	0.0221	0.0224
0.8	0.0218	0.0219	0.0223	0.0226	0.0229	0.0232
0.9	0.0219	0.0221	0.0225	0.0228	0.0231	0.0233
1.0	0.0223	0.0226	0.0227	0.0229	0.0232	0.0236
			R = 10			
0.0	0.0210	0.0213	0.0216	0.0217	0.0217	0.0220
0.4	0.0214	0.0216	0.0218	0.0221	0.0224	0.0227
0.5	0.0213	0.0215	0.0218	0.0222	0.0225	0.0228
0.7	0.0216	0.0220	0.0224	0.0226	0.0228	0.0230
1.0	0.0220	0.0224	0.0226	0.0228	0.0231	0.0234

Contd....

T(K) x	313.15	318.15	323.15	328.15	333.15	338.15
			R = 14			
0.0	0.0219	0.0221	0.0224	0.0227	0.0225	0.0225
0.3	0.0224	0.0227	0.0230	0.0232	0.0235	0.0238
0.6	0.0226	0.0230	0.0233	0.0236	0.0239	0.0241
1.0	0.0230	0.0230	0.0235	0.0238	0.0241	0.0243
			R = 15			
0.0	0.0221	0.0223	0.0223	0.0226	0.0228	0.0231
0.4	0.0227	0.0229	0.0232	0.0234	0.0237	0.0238
0.6	0.0223	0.0223	0.0226	0.0228	0.0231	0.0234
1.0	0.0229	0.0230	0.0233	0.0236	0.0240	0.0243

TABLE 3.4: CHARACTERISTIC VOLUME (V^*, cc mol^{-1}) OF THE SYSTEMS: [x $NaNO_3$ + (1-x) KNO_3] + RH_2O (where R = 6,10,14 or 15).

T(K) / x	313.15	318.15	323.15	328.15	333.15	338.15
			R = 6			
0.0	22.410	22.433	22.456	22.479	22.503	22.527
0.6	20.048	20.078	20.100	20.127	20.154	20.181
0.7	19.833	19.859	19.886	19.913	19.941	19.969
0.8	19.623	19.650	19.678	19.706	19.734	19.762
0.9	19.399	19.426	19.454	19.482	19.511	19.540
1.0	19.157	19.185	19.214	19.243	19.272	19.302
			R = 10			
0.0	20.065	20.091	19.118	19.145	19.172	19.200
0.4	19.590	19.618	19.646	19.674	19.702	19.731
0.5	19.470	19.498	19.526	19.554	19.583	19.613
0.7	19.241	19.270	19.298	19.327	19.357	19.387
1.0	18.888	18.917	18.947	18.977	19.008	19.039

Contd....

T(K) x	313.15	318.15	323.15	328.15	333.15	338.15
			R = 14			
0.0	18.332	18.356	18.380	18.404	18.428	18.453
0.3	18.146	18.170	18.195	18.220	18.246	18.272
0.6	17.953	17.958	17.979	18.005	18.031	18.058
1.0	17.705	17.732	17.759	17.787	17.815	17.844
			R = 15			
0.0	17.649	17.672	17.696	17.720	17.744	17.769
0.4	17.077	17.101	17.125	17.149	17.174	17.199
0.6	16.809	16.833	16.856	16.882	16.907	16.933
1.0	16.232	16.256	16.281	16.306	16.332	16.358

TABLE 3.5: CHARACTERISTIC PRESSURE ($P^* \times 10^{-10}$, dyne cm^{-2}) OF THE SYSTEMS: $[x\ NaNO_3 + (1-x)KNO_3] + RH_2O$ (where R = 6, 10, 14 or 15) AT 313.15 K

X ⟶ / R ↓	0.0	0.3	0.4	0.5	0.6	0.7	0.8	0.9	1.0
6	0.3394	-	-	-	0.3871	0.4055	0.4238	0.4440	0.4663
10	0.3275	-	0.3578	0.3671	-	0.3853	-	-	0.4144
14	0.3152	0.3413	-	-	0.3571	-	-	-	0.3927
15	0.2955	-	0.3121	-	0.3322	-	-	-	0.3590

TABLE 3.6: CHARACTERISTIC TEMPERATURE (T^*,K) OF THE SYSTEMS: $[x\ NaNO_3 + (1-x)KNO_3] + RH_2O$ (where R = 6,10,14 or 15).

T(K) / x	313.15	318.15	323.15	328.15
		R = 6		
0.0	10050.00	10055.19	11006.38	11035.58
0.6	9533.42	9586.37	9640.59	9696.63
0.7	9443.44	9496.27	9550.07	9605.59
0.8	9374.94	9427.61	9481.07	9535.65
0.9	9319.03	9371.47	9424.37	9477.88
1.0	9276.49	9328.65	9380.86	9433.08
		R = 10		
0.0	9741.10	9793.21	9845.34	9897.47
0.4	9449.75	9503.94	9558.62	9634.44
.5	9328.13	9385.17	9436.44	9491.22
0.7	9220.27	9273.97	9327.86	9382.15
1.0	9150.39	9202.65	9254.91	9307.20

Contd....

T(K) / x	313.15	318.15	323.15	328.15
		R = 14		
0.0	9553.22	9600.52	9605.72	9613.93
0.3	9428.84	9481.98	9536.92	9587.78
0.6	9324.38	9377.71	9430.83	9483.86
1.0	9231.40	9284.57	9335.75	9387.96
		R = 15		
0.0	9534.73	9586.79	9638.86	9690.95
0.4	9301.60	9353.68	9408.41	9434.83
0.6	9201.15	9253.28	9307.05	9358.51
1.0	9053.15	9081.32	9143.49	9187.69

TABLE 3.7: COMPARISON OF EXPERIMENTAL AND COMPUTED VALUES OF VISCOSITY ($\eta \times 10^{2}$, $Ns\ m^{-2}$) OF [x $NaNO_3$+ (1-x) KNO_3] + RH_2O (where R = 6,10,14 or 15).

T(K) / x	313.15	318.15	323.15	328.15	333.15	338.15
			R = 6			
0.0	0.836	0.803	0.770	0.739	0.704	0.680
6	1.361 (0.078)	1.245 (0.071)	1.162 (0.068)	1.074 (0.064)	0.999 (0.056)	0.947 (0.055)
0.7	1.504 (0.091)	1.373 (0.085)	1.273 (0.081)	1.185 (0.076)	1.096 (0.071)	1.052 (0.061)
0.8	1.552 (1.003)	1.421 (1.001)	1.303 (0.093)	1.209 (0.086)	1.119 (0.081)	1.065 (0.076)
0.9	1.604 (1.012)	1.468 (1.003)	1.362 (0.094)	1.255 (0.089)	1.162 (0.078)	1.097 (0.071)
1.0	1.678	1.530	1.405	1.291	1.189	1.126
			R = 10			
0.0	0.729	0.679	0.638	0.596	0.559	0.535
0.4	0.878 (0.583)	0.802 (0.580)	0.747 (0.551)	0.692 (0.526)	0.639 (0.510)	0.608 (0.430)
0.5	0.918 (0.536)	0.850 (0.518)	0.792 (0.503)	0.733 (0.493)	0.688 (0.487)	0.658 (0.430)
0.7	0.947 (0.618)	0.873 (0.601)	0.821 (0.587)	0.759 (0.531)	0.708 (0.528)	0.673 (0.513)
1.0	1.025	0.930	0.863	0.798	0.736	0.697

Contd

T(K) x	313.15	318.15	323.15	328.15	333.15	338.15
			R = 14			
0.0	0.715	0.670	0.627	0.586	0.549	0.527
0.3	0.710 (0.450)	0.703 (0.443)	0.683 (0.439)	0.658 (0.415)	0.655 (0.414)	0.603 (0.401)
0.6	0.796 (0.463)	0.732 (0.451)	0.683 (0.435)	0.649 (0.431)	0.592 (0.421)	0.561 (0.403)
1.0	0.942	0.867	0.766	0.715	0.665	0.630
			R = 15			
0.0	0.671	0.628	0.589	0.551	0.497	0.474
0.4	0.779 (0.458)	0.721 (0.450)	0.671 (0.442)	0.627 (0.431)	0.584 (0.412)	0.559 (0.398)
0.6	0.837 (0.450)	0.771 (0.444)	0.716 (0.431)	0.669 (0.421)	0.622 (0.410)	0.584 (0.408)
1.0	0.891	0.843	0.793	0.722	0.683	0.630

* COMPUTED VALUES OF VISCOSITY (USING FLORY THEORY) ARE GIVEN WITHIN PARENTHESES.

solutions, respectively, are reported in Table 3.4. The values of V^* are found to show an increase with increase in temperature and decrease with increase in the mole fraction, X, of $NaNO_3$.

The values of characteristic pressure, P^*, of binary and ternary solutions (calculated using equations (3.8) and (3.13), respectively.) listed in Table 3.5 are found to increase with increase in the mole fraction of $NaNO_3$ and decrease with increase in the R value. The characteristic temperature, T^*, calculated using equations (3.5) and (3.14) for the binary and the ternary mixtures, respectively, (Table 3.6) increases with increase in temperature for the samples under investigation and decreases with increase in the mole fraction of sodium nitrate.

The viscosities for the samples $[x\ NaNO_3 + (1-x)KNO_3]+RH_2O$ (where R = 6,10,14 or 15) listed in Table 3.7, show acceptable agreement between their calculated and measured values.

Thus, the Flory's statistical theory which was originally meant for the molecular liquids, is found to be equally applicable to ionic liquids as well.

PART - II

THERMODYNAMIC PROPERTIES OF MIXED ALCOHOLS

INTRODUCTION

A knowledge of the solution properties for mixed solvents of two or more components is required for understanding the transport behaviour as well as their industrial applications. Some of the common solution properties include the density, the viscosity, the surface tension, the refractive index and the ultrasonic velocity.

Alcohols are known to be strongly self-associated liquids[128] and it is further believed that for the binary solutions rich[129] in alcohols, a three-dimensional network of hydrogen bonded alcohol molecules exists.

When a second component is mixed with alcohol, there may be two possible contributions towards the excess properties of mixing due to the structural changes in alcohol:

(i) the breaking-up of alcohol structure into fragments due to addition of the second component an (ii) the geometrical adjustment of the second component into the remaining alcohol structure. The first factor contributes to the positive values while the second has a negative contribution towards the excess

properties.

An attempt has been made in the present work to evaluate the thermodynamic properties of viscous flow, using the density and the viscosity data reported earlier,[130] for the binary systems: (i) benzyl alcohol + iso-amyl alcohol and (ii) benzyl alcohol + iso-propyl alcohol.

CALCULATION OF THERMODYNAMIC PROPERTIES:

Densities at required temperatures are calculated using the least squares fitted parameters from the reported data with the help of the density equation, $\rho = a - bT$.

Molar volume, V_m, of the mixtures have been calculated from the corresponding mixture densities using the relation,

$$V_m = \frac{xM_1 + (1-x)M_2}{\rho} \quad . \qquad (4.1)$$

The energies of activation for viscous flow, ΔG^*, were calculated using the Eyring viscosity equation,[131]

$$\eta = \frac{hN}{V_m} e^{\Delta G^*/R'T} \qquad (4.2)$$

where h is the Planck's constant, N the Avogadro's number,

R' the universal gas constant and T the absolute temperature.

The energies of activation for viscous flow, ΔG^*, at the required temperatures are obtained using the relation,

$$\Delta G^* = \Delta H^* - T\Delta S^* \qquad (4.3)$$

for mixtures of several compositions. The terms ΔH^* and ΔS^* are the enthalpy and the entropy of viscous flow, respectively. Combining eqs. (4.2) and (4.3), linear plots have been obtained for

$$R\ln\left(\frac{\eta V_m}{hN}\right) \text{ Vs } \frac{1}{T} \text{ quantities}^{70}.$$

RESULTS AND DISCUSSION

For all the compositions of the binary mixtures and also for the two pure components, the plots indicate an almost parallel linear pattern. From the correlation procedure, ΔH^* values are obtained from the slopes of the curves, while ΔS^* values are obtained from the intercepts. For all the compositions, the plots indicate that ΔH^* values are almost constant in the investigated temperature range (Tables 4.3 and 4.4).

TABLE 4.1: FREE ENERGY OF ACTIVATION OF VISCOUS FLOW (kJ mol^{-1}) FOR BENZYL ALCOHOL + ISO-AMYL ALCOHOL SYSTEMS AS A FUNCTION OF TEMPERATURE.

SYSTEMS	A	B	C	D	E	F	G	H	I	L	M
T(K) / X⟶	0.000	0.105	0.208	0.310	0.412	0.513	0.612	0.710	0.810	0.904	1.00
298.15	19.827	20.140	20.213	20.305	20.420	20.621	20.738	20.894	21.069	21.321	21.45
303.15	19.799	20.064	20.139	20.245	20.358	20.496	20.679	20.829	21.011	21.251	21.40
308.15	19.699	19.986	20.068	20.170	20.297	20.436	20.633	20.773	20.948	21.192	21.36
313.15	19.615	19.910	19.993	20.105	20.234	20.374	20.562	20.713	20.887	21.139	21.29
318.15	19.528	19.843	19.933	20.057	20.194	20.334	20.525	20.681	20.853	21.105	21.25
323.15	19.381	19.792	19.890	20.012	20.152	20.304	20.496	20.649	20.833	21.070	21.23

X GIVES MOLE FRACTION OF BENZYL ALCOHOL.

The free energies of activation of viscous flow, ΔG^*, have been calculated for the binary systems, benzyl alcohol + iso-amyl alcohol and benzyl alcohol + iso-propyl alochol (Tables 4.1 and 4.2) using equation (4.2) and a computer program in fortran language (given in appendix).

On the basis of the fact that the plots of $R'\ell n(\frac{\eta V_m}{hN})$ Vs 1/T are linear (figs. 4.1 and 4.2) for all the binary systems of benzyl alcohol + iso-amyl alcohol and benzyl alcohol + iso-propyl alcohol, it may be suggested that the mechanism of viscous flow for these binary mixtures is a thermally activated process.

The values of ΔH^* are all positive and are almost constant. As regards ΔS^* values, these are all negative and decrease with increase in concentration of benzyl alcohol in both the systems. A brief examination of tables 4.3 and 4.4 reveals that there is very small difference in the values of ΔS^* in passing from one pure solvent to the other.

An attempt is made to explain the results using Eyring's hypothesis[131] of the flow mechanism which explains the flow process by the movement of dislocations or discontinuities in the fluid

TABLE 4.2: FREE ENERGY OF ACTIVATION OF VISCOUS FLOW (kJ mol^{-1}) FOR BENZYL ALCOHOL + ISO-PROPYL ALCOHOL SYSTEMS AS A FUNCTION OF TEMPERATURE.

SYSTEMS	A	B	C	D	E	F	G	H	I	L	M
T(K) / X ⟶	0.000	0.078	0.155	0.240	0.330	0.424	0.525	0.633	0.747	0.878	1.0
298.15	17.485	17.913	18.276	18.605	18.942	19.330	19.806	20.092	20.639	21.033	21.4
303.15	17.374	17.814	18.186	18.530	18.871	19.261	19.744	20.006	20.569	20.970	21.4
308.15	17.262	17.727	18.107	18.463	18.805	19.191	19.680	19.959	20.504	20.913	21.3
313.15	17.158	17.640	18.032	18.380	18.744	19.126	19.612	19.902	20.451	20.860	21.2
318.15	17.071	17.566	17.985	18.344	18.696	19.075	19.573	19.866	20.413	20.826	21.2
323.15	17.004	17.517	17.934	18.297	18.656	19.046	19.543	19.836	20.386	20.791	21.2

X GIVES MOLE FRACTION OF BENZYL ALCOHOL

layers. In a dynamic steady state and in an oversimplified picture, the movement of a dislocation by one layer position requires the cooperation of at least two moving elementary units: One is moving out of the standard position and requires energy, and the other is moving into this cavity and gives up energy. Therefore, the enthalpy of activation of viscous flow could be taken as a measure of the degree of cooperation between the species taking part in the flow process. In the liquid state, the opportunity of the formation of many discontinuities is warranted by statistical fluctuations of local density. In the low temperature range, as well as for highly structured components, a considerable degree of order is expected and the transport phenomena will take place cooperatively when the breaking in the ordered and polymerized fluid structure becomes very quick, by increasing the temperature or by adding a component that breaks a homopolymer hydrogen-bond network, the movement of the individual units becomes more disordered and the cooperation degree is reduced thus decreasing the overall molecular order in the system and the positive values of ΔS^* should thus be expected.[70]

TABLE 4.3: ENTHALPY (ΔH^*) AND ENTROPY (ΔS^*) OF ACTIVATION OF VISCOUS FLOW FOR BENZYL ALCOHOL + ISO-AMYL ALCOHOL SYSTEMS.

SYSTEMS	ΔH^* ($kJ\ mol^{-1}$)	ΔS^* ($J\ mol^{-1}\ K^{-1}$)
A	60.086	-57.243
B	60.086	-58.293
C	60.075	-58.640
D	59.789	-58.983
E	60.086	-59.235
F	59.853	-59.930
G	59.937	-60.303
H	60.086	-60.913
I	60.071	-61.423
L	60.086	-62.257
M	59.931	-62.876

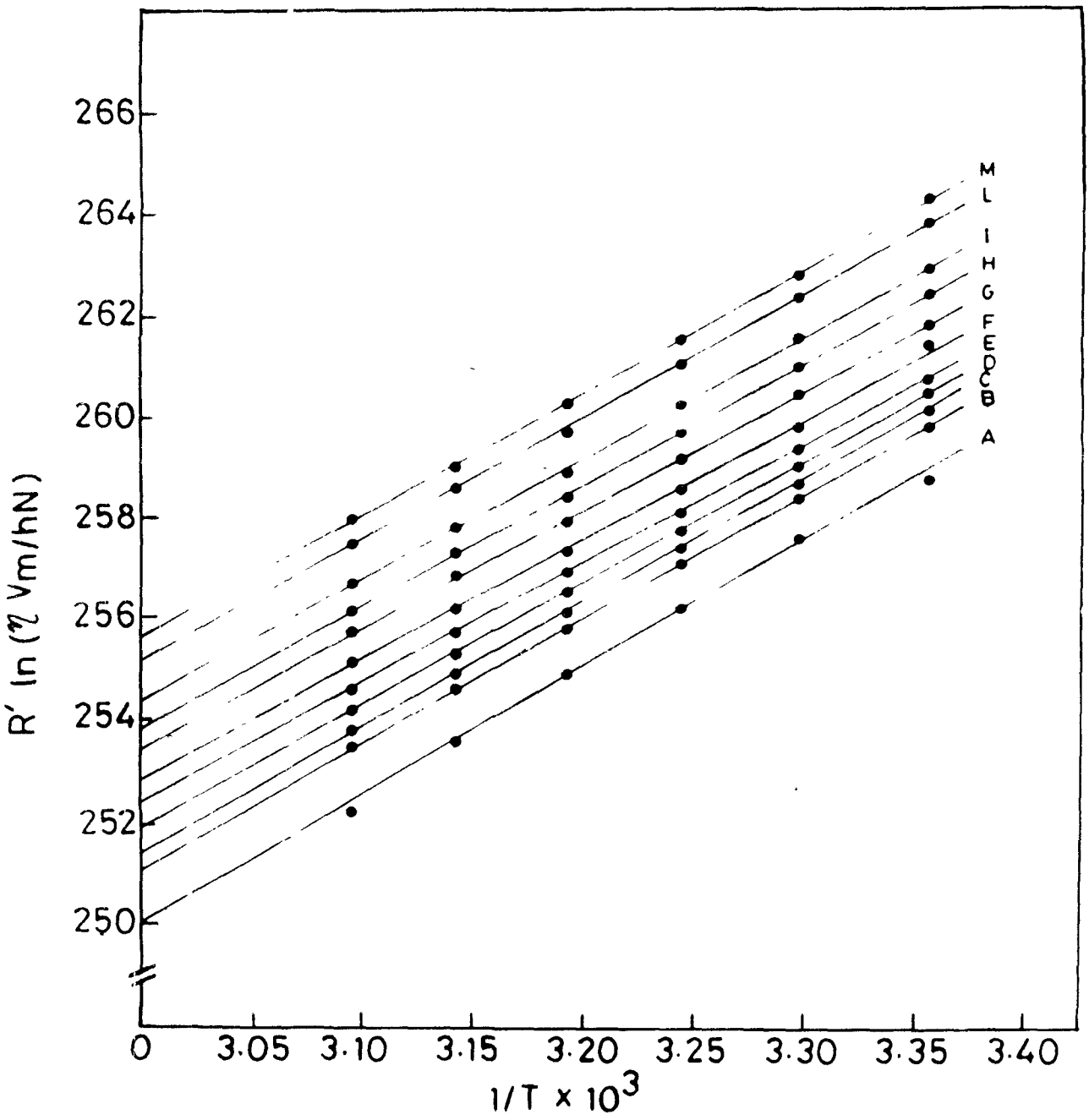

Fig. 4.1: Plots of $R' \ell n \left(\frac{\eta V_m}{hN}\right)$ versus $\frac{1}{T} \times 10^3$ for benzyl alcohol + iso-amyl alcohol systems.

TABLE 4.4: ENTHALPY (ΔH^*) AND ENTROPY (ΔS^*) OF ACTIVATION OF VISCOUS FLOW FOR BENZYL ALCOHOL + ISO-PROPYL ALCOHOL SYSTEMS.

SYSTEMS	ΔH^* (kJ mol^{-1})	ΔS^* (J mol^{-1} K^{-1})
A	28.674	-154.745
B	28.674	-156.182
C	26.795	-157.401
D	26.795	-158.502
E	26.795	-159.631
F	28.674	-160.934
G	26.795	-162.529
H	28.674	-163.491
I	26.795	-165.325
L	28.674	-166.647
M	28.674	-168.101

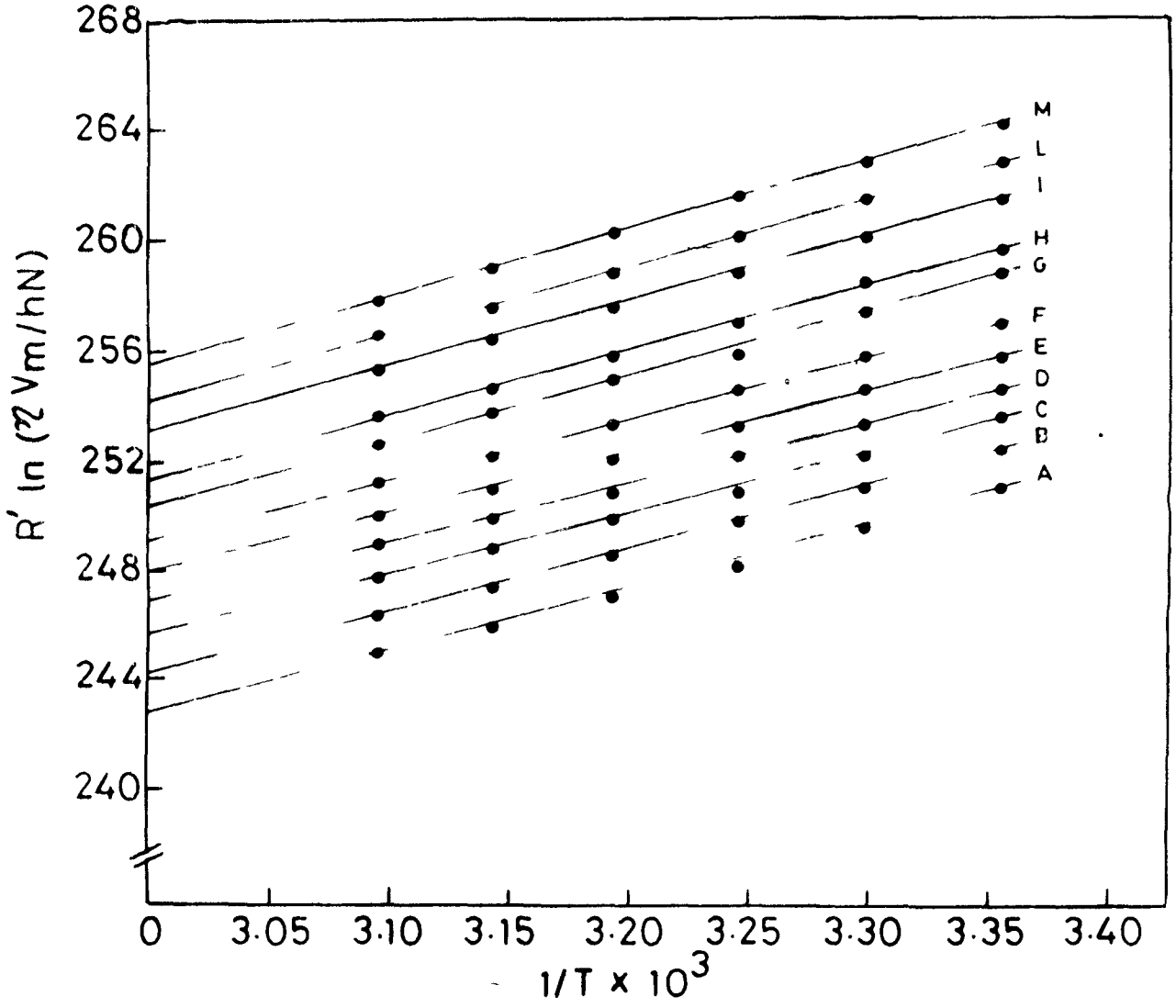

Fig. 4.2: Plots of $R'\ell n\left(\frac{\eta V_m}{hN}\right)$ versus $\frac{1}{T} \times 10^3$ for benzyl alcohol + iso-propyl alcohol systems.

In the systems under investigation, negative ΔS^* values are obtained, which can be explained on the basis of the formation of a stronger hydrogen-bond network on addition of second alcohol component to the first one which is expected to increase the cooperation degree thus causing more ordered movements of individual units and would give rise to negative ΔS^* values.

PART - III

CONSTRUCTION OF ENERGY-LEVEL DIAGRAMS FOR THE INTRA-CONFIGURATIONAL TRANSITIONS IN MIXED-LIGAND-TRANSITION METAL IONS

INTRODUCTION

Nickel tetrahalo tetrahedral complex ionic species have been selected for predicting the probable transitions in NiI_3Br^{2-}, $NiI_2Br_2^{2-}$, $NiIBr_3^{2-}$, $NiBr_3Cl^{2-}$, $NiBr_2Cl_2^{2-}$, $NiBrCl_3^{2-}$, NiI_3Cl^{2-}, $NiI_2Cl_2^{2-}$ and $NiICl_3^{2-}$ like those in NiI_4^{2-}, $NiBr_4^{2-}$ and $NiCl_4^{2-}$. The interionic interactions in each of these complex ionic species may vary in successive replacements of iodides by bromide ions, bromide by chloride ions, and also iodides by chloride ions. The measurements of density, viscosity, equivalent conductance, surface tension, molar refraction/refractive index of the systems having these ionic species as well as that of the ultrasonic velocity through them may throw some light on the variation of interionic/intermolecular interactions, provided changes in these properties/behaviour are perceptible for the latter. Out of these species, $NiCl_2Br_2^{2-}$, $NiCl_2I_2^{2-}$ and $NiBr_2I_2^{2-}$ have already been reported earlier[132] in which the agreement in the predicted energies of transitions and those of the experimental values has been excellent. This has,

therefore, led to compute the possible energies of transitions in all the possible types of mixed halide nickel complex ions. This was achieved by solving the Liehr-Ballhausen matrices using the ligand-field strength and the two electron-electron repulsion parameters in the proportion

$\left\{\frac{3}{4}[NiI_4]^{2-} + \frac{1}{4}[NiBr_4]^{2-}\right\}$, $\left\{\frac{1}{2}[NiI_4]^{2-} + \frac{1}{2}[NiBr_4]^{2-}\right\}$,

$\left\{\frac{1}{4}[NiI_4]^{2-} + \frac{3}{4}[NiBr_4]^{2-}\right\}$, $\left\{\frac{3}{4}[NiI_4]^{2-} + \frac{1}{4}[NiCl_4]^{2-}\right\}$,

$\left\{\frac{1}{2}[NiI_4]^{2-} + \frac{1}{2}[NiCl_4]^{2-}\right\}$, $\left\{\frac{1}{4}[NiI_4]^{2-} + \frac{3}{4}[NiCl_4]^{2-}\right\}$,

$\left\{\frac{3}{4}[NiBr_4]^{2-} + \frac{1}{4}[NiCl_4]^{2-}\right\}$, $\left\{\frac{1}{2}[NiBr_4]^{2-} + \frac{1}{2}[NiCl_4]^{-2}\right\}$,

$\left\{\frac{1}{4}[NiBr_4]^{2-} + \frac{3}{4}[NiCl_4]^{2-}\right\}$ for the NiI_3Br^{2-}, $NiI_2Br_2^{2-}$, $NiIBr_3^{2-}$ NiI_3Cl^{2-}, $NiI_2Cl_2^{2-}$, $NiICl_3^{2-}$, $NiBr_3Cl^{2-}$, $NiBr_2Cl_2^{2-}$ and $NiBrCl_3^{2-}$, respectively. The resulting twenty energy levels for some of these species have been tabulated (Tables 5.1 to 5.9 and few of these have also been shown in the diagrams (Figs. 5.1 to 5.6). The details of computation are given in the Appendix.

CONSTRUCTION OF ENERGY-LEVEL DIAGRAMS

The four-parameter model for $nd^{2,8}$ configuration has been derived by Liehr and Ballhausen[133]. It consists of five secular equations which yield eigen values and eigen-vectors of twenty electronic states as functions of the four ligand-field parameters, B, Gamma, Lambda and D_q. Here B is the Racah's B, 'Gamma' is the Racah's C/B, 'Lambda' is the spin-orbit coupling constant and D_q is the ligand-field strength parameter. The five Liehr-Ballhausen matrices are labelled as 'GAMMA ONE, GAMMA TWO, GAMMA THREE, GAMMA FOUR and GAMMA FIVE', respectively. Racah's parameters B and C are related to the parameters F_2 and F_4 used in the Liehr-Ballhausen secular equations through the expressions, $B = F_2 - 5F_4$ and $C = 35\ F_4$. Approximate values of these adjustable parameters, F_2 and F_4 are obtained by using the following relations[134] for the differences $^3P-^3F$ and $^1D-^3F$ from the experiment (for $^3T_1(P) \longleftarrow {}^3T_1(F)$ and $^1E(D) \longleftarrow {}^3T_1(F)$ transitions),

$$E(^3P-^3F) = 15\ F_2 - 75\ F_4$$

$$E(^1D-^3F) = 5\ F_2 + 45\ F_4$$

TABLE 5.1: CALCULATED ELECTRONIC ENERGY LEVELS OF $NiCl_4^{=}$ IONS [136]

		ENERGY (cm^{-1})			
		λ = - 275	B = 740.0	C/B = 3.97	
ORBITAL LEVELS		D_q = 0	D_q = 50	D_q = 100	D_q = 150
$^3T_1(F)$	1	0	0	0	0
	4	0	120	196	244
	3	0	237	433	585
	5	0	496	802	956
$^3T_2(F)$	4	1,119	1,399	1,701	2,074
	5	1,119	1,401	1,734	2,099
	3	1,119	1,532	1,931	2,345
	2	1,856	2,028	2,244	2,508
$^3A_2(F)$	5	1,856	2,384	3,085	3,878
$^1T_2(D)$	5	10,103	10,316	10,513	10,693
$^1E(D)$	3	10,103	10,490	10,313	11,082
$^3T_1(P)$	5	12,071	12,345	12,628	12,922
	3	12,071	12,409	12,730	13,036
	4	12,219	12,525	12,843	13,173
	1	12,423	12,728	13,045	13,374
$^1T_2(G)$	5	15,619	15,749	15,910	16,102
$^1T_1(G)$	4	15,619	16,032	16,430	16,844

$^1A_1(G)$	1	15,619	16,111	16,586	17,044
$^1E(G)$	3	15,619	16,000	16,487	17,069
$^1A_1(S)$	1	37,761	38,074	38,416	38,786
ORBITAL LEVELS		D_q = 200	D_q = 250	D_q = 300	D_q = 350
$^3T_1(F)$	1	0	0	0	0
	4	276	298	313	325
	3	699	783	845	892
	5	1,031	1,072	1,095	1,109
$^3T_2(F)$	4	2,485	2,910	3,342	3,778
	5	2,486	2,886	3,298	3,718
	3	2,764	3,188	3,617	4,050
	2	2,813	3,152	3,517	3,901
$^3A_2(F)$	5	4,721	5,591	6,481	7,382
$^1T_2(D)$	5	10,854	10,996	11,119	11,226
$^1E(D)$	3	11,298	11,468	11,597	11,692
$^3T_1(P)$	5	13,226	13,543	13,872	14,213
	3	13,335	13,639	13,954	14,283
	4	13,513	13,863	14,222	14,590
	1	13,713	14,061	14,418	14,783
$^1T_2(G)$	5	16,324	16,574	16,849	17,148
$^1T_1(G)$	4	17,263	17,687	18,116	18,549
$^1A_1(G)$	1	17,486	17,909	18,314	18,700
$^1E(G)$	3	17,732	18,457	19,229	20,038
$^1A_1(S)$	1	39,184	39,609	40,062	40,542

ORBITAL LEVELS		D_q = 400	D_q = 450	D_q = 500
$^3T_1(F)$	1	0	0	0
	4	334	341	346
	3	926	953	973
	5	1,118	1,123	1,125
$^3T_2(F)$	4	4,216	4,657	5,099
	5	4,144	4,576	5,013
	3	4,487	4,927	5,371
	2	4,300	4,711	5,131
$^3A_2(F)$	5	8,290	9,200	10,101
$^1T_2(D)$	5	11,319	11,404	11,493
$^1E(D)$	3	11,762	11,810	11,843
$^3T_1(F)$	5	14,567	14,929	15,303
	3	14,627	14,985	15,355
	4	14,965	15,347	15,736
	1	15,155	15,534	15,919
$^1T_2(G)$	5	17,466	17,806	18,160
$^1T_1(G)$	4	18,985	19,425	19,869
$^1T_1(G)$	1	19,069	19,419	19,751
$^1E(G)$	3	20,875	21,733	22,608
$^1A_1(S)$	1	41,049	41,581	42,138

TABLE 5.2: CALCULATED ELECTRONIC ENERGY-LEVELS OF $NiBr_3Cl^{2-}$ IONS

		ENERGY (cm^{-1})		
		λ = - 275, B = 695		C/B = 3.900
		F_2 = 1082.214,	F_4 = 77.443	
ORBITAL LEVELS	Γ	D_q = 338	D_q = 339	D_q = 340
$^3T_1(F)$	1	0	0	0
	4	322	322	323
	3	879	880	881
	5	1,104	1,104	1,104
$^3T_2(F)$	4	3,622	3,631	3,639
	5	3,672	3,681	3,689
	3	3,810	3,818	3,826
	2	3,952	3,961	3,970
$^3A_2(F)$	5	7,161	7,179	7,197
$^1T_2(D)$	5	10,519	10,521	10,523
$^1E(D)$	3	10,936	10,938	10,939
$^3T_1(P)$	5	13,461	13,468	13,475
	3	13,529	13,536	13,543
	4	13,839	13,846	13,854
	1	14,025	14,032	14,040

$^1T_2(G)$	5	16,124	16,130	16,137
$^1T_1(G)$	4	17,457	17,466	17,475
$^1A_1(G)$	1	17,584	17,591	17,599
$^1E(G)$	3	18,934	18,951	18,967
$^1A_1(S)$	1	37,896	37,906	37,916

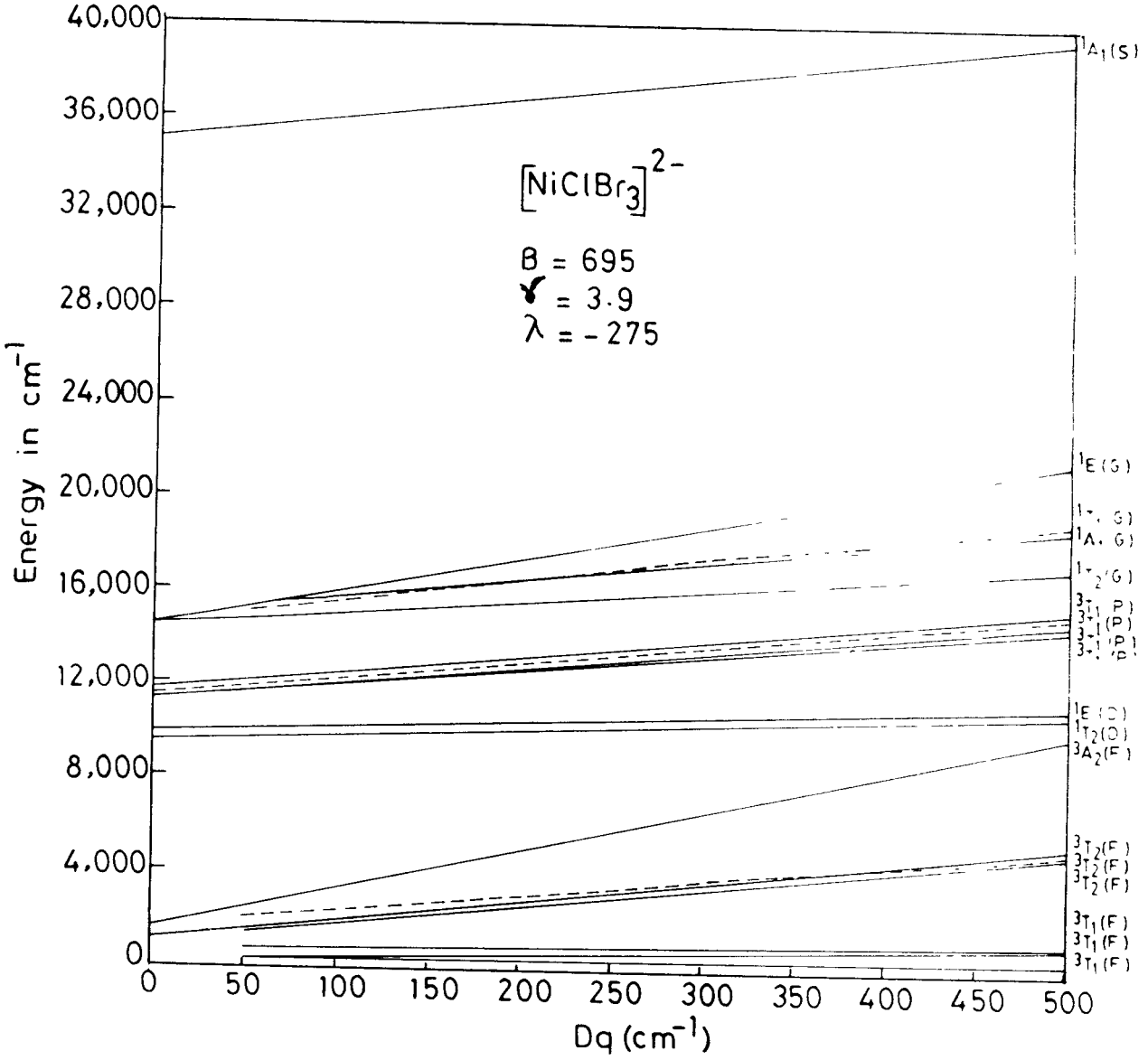

Fig. 5.1: Energy-level diagram for $[NiClBr_3]^{2-}$.

TABLE 5.3: CALCULATED ELECTRONIC ENERGY-LEVELS OF $NiBr_2Cl_2^{2-}$ IONS

ENERGY (cm^{-1})

λ = -275, B = 710, C/B = 3.930

F_2 = 1108.614, F_4 = 79.723

ORBITAL LEVELS	Γ	D_q = 344	D_q = 345	D_q = 346
$^3T_1(F)$	1	0	0	0
	4	323	324	324
	3	885	886	887
	5	1,106	1,106	1,107
$^3T_2(F)$	4	3,671	3,679	3,688
	5	3,725	3,733	3,742
	3	3,856	3,864	3,872
	2	4,002	4,011	4,020
$^3A_2(F)$	5	7,271	7,289	7,307
$^1T_2(D)$	5	10,766	10,768	10,770
$^1E(D)$	3	11,198	11,200	11,202
$^3T_1(P)$	5	13,726	13,733	13,740
	3	13,795	13,802	13,808
	4	14,104	14,111	14,119
	1	14,292	14,300	14,307

$^1T_2(G)$	5	16,486	16,492	16,498
$^1T_1(G)$	4	17,846	17,855	17,864
$^1A_1(G)$	1	17,980	17,987	17,995
$^1E(G)$	3	19,343	19,359	19,376
$^1A_1(S)$	1	38,825	38,835	38,845

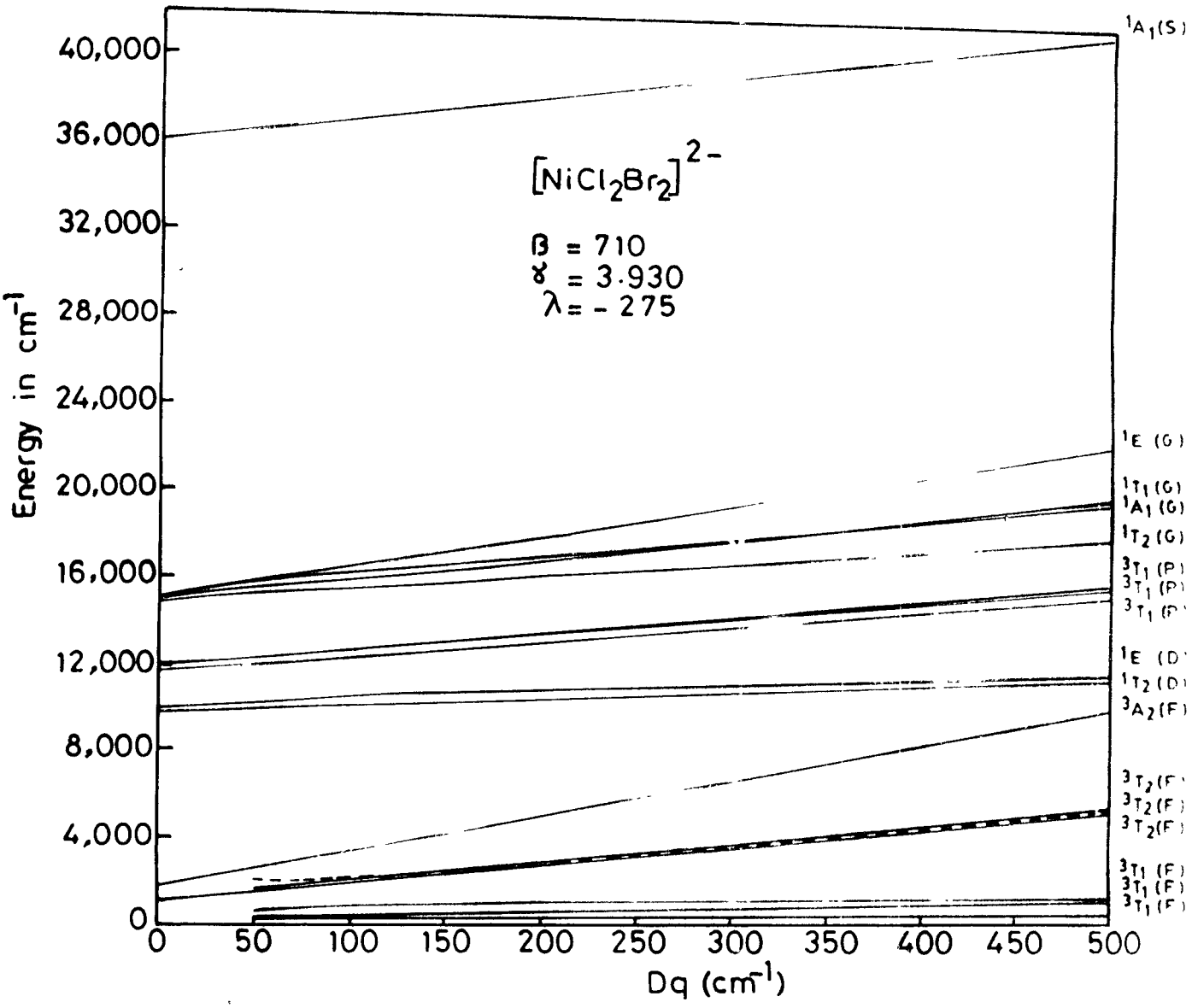

Fig. 5.2: Energy-level diagram for $[NiCl_2Br_2]^{2-}$.

TABLE 5.4: CALCULATED ELECTRONIC ENERGY-LEVELS OF $NiBrCl_3^{2-}$ IONS

ENERGY (cm^{-1})

λ = -275, B = 725, C/B = 3.950

F_2 = 1134.107, F_4 = 81.821

ORBITAL LEVELS	Γ'	D_q = 351	D_q = 352	D_q = 353
$^3T_1(F)$	1	0	0	0
	4	325	325	325
	3	891	892	893
	5	1,108	1,109	1,109
$^3T_2(F)$	4	3,728	3,736	3,745
	5	3,786	3,795	3,804
	3	3,910	3,918	3,926
	2	4,061	4,069	4,078
$^3A_2(F)$	5	7,399	7,417	7,435
$^1T_2(D)$	5	11,003	11,005	11,007
$^1E(D)$	3	11,451	11,452	11,454
$^3T_1(P)$	5	13,997	14,004	14,011
	3	14,066	14,073	14,079
	4	14,376	14,384	14,391
	1	14,567	14,574	14,582
$^1T_2(G)$	5	16,841	16,847	16,853

$^1T_1(G)$	4	18,231	18,240	18,249
$^1A_1(G)$	1	18,369	18,377	18,384
$^1E(G)$	3	19,756	19,772	19,789
$^1A_1(S)$	1	39,721	39,731	39,741

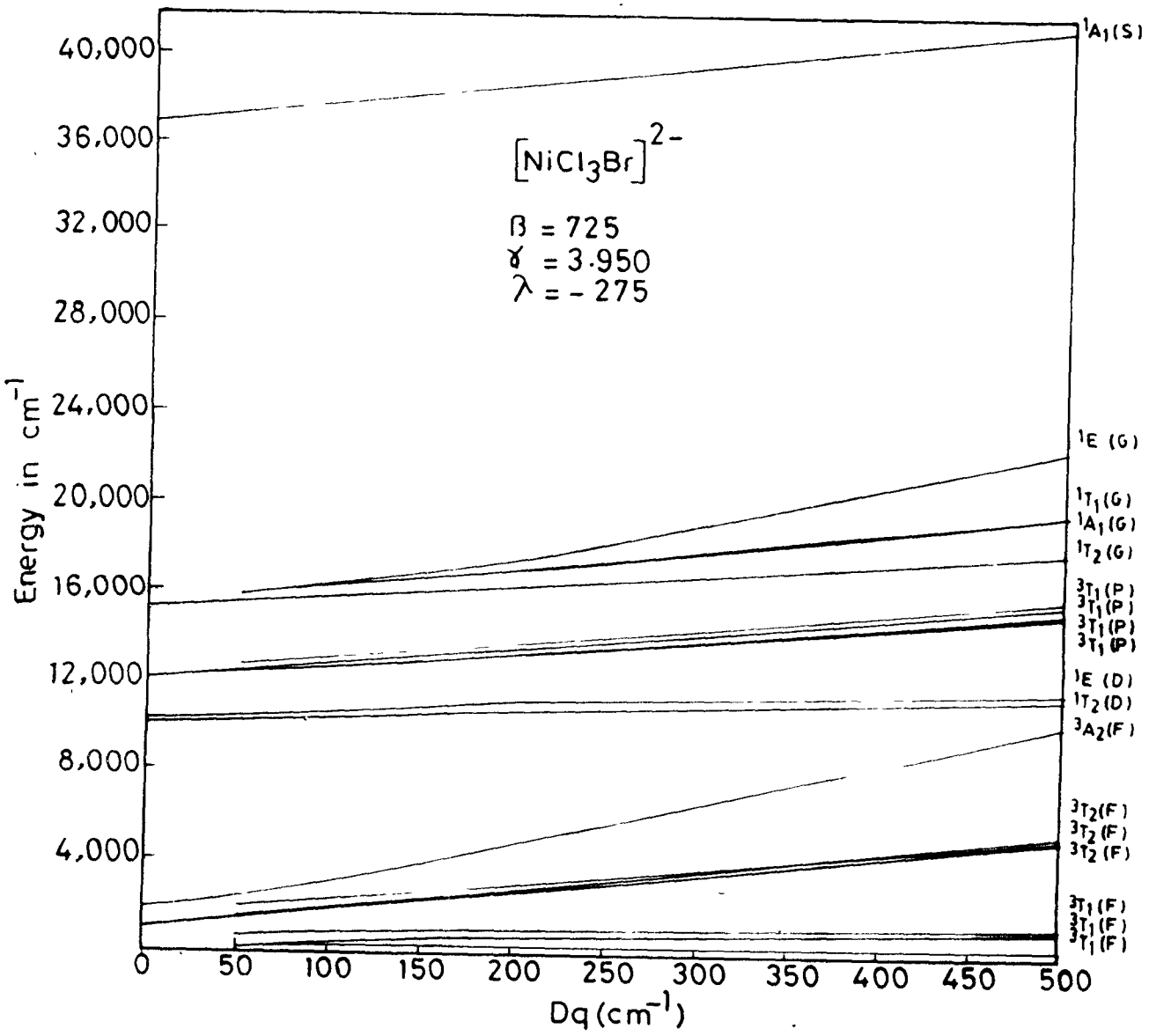

Fig. 5.3: Energy-level diagram for $[NiCl_3Br]^{2-}$.

TABLE 5.5: CALCULATED ELECTRONIC ENERGY LEVELS OF $NiBr_4^{=}$ IONS[136]

ORBITAL LEVELS		ENERGY (cm^{-1}) for $NiBr_4^{=}$			
		λ = - 275, B = 680.00 C/B = 3.88			
		D_q = 0	D_q = 50	D_q = 100	D_q = 150
$^3T_1(F)$	1	0	0	0	0
	4	00	120	196	244
	3	00	237	433	584
	5	00	495	802	956
$^3T_2(F)$	4	1,851	1,399	1,699	2,071
	5	00	1,403	1,736	2,102
	3	1,121	1,524	1,933	2,348
	2	1,121	2,021	2,239	2,504
$^3A_2(F)$	5	1,851	2,376	3,079	3,873
$^1T_2(D)$	5	9,215	9,429	9,626	9,805
$^1E(D)$	3	9,215	9,596	9,912	10,166
$^3T_1(P)$	5	11,175	11,148	11,730	12,024
	3	11,175	11,513	11,830	12,132
	4	11,321	11,627	11,947	12,279
	1	14,304	11,822	12,141	12,471
$^1T_2(G)$	5	14,304	14,435	14,601	14,800

$^1T_1(G)$	4	14,304	14,707	15,115	15,530
$^1A_1(G)$	1	11,516	14,794	15,267	15,720
^{1} (G)	3	14,304	14,690	15,190	15,794
$^1A_1(S)$	1	34,355	34,669	35,015	35,392
ORBITAL LEVELS		D_q = 200	D_q = 250	D_q = 300	D_q = 350
$^3T_1(F)$	1	0	0	0	0
	4	276	298	314	325
	3	698	782	843	889
	5	1,031	1,070	1,092	1,106
$^3T_2$	4	2,432	2,908	3,341	3,778
	5	2,490	2,892	3,305	3,727
	3	2,769	3,195	3,625	4,060
	2	2,811	3,152	3,519	3,906
$^3A_2(F)$	5	4,716	5,589	6,477	7,376
$^1T_2(D)$	5	9,963	10,101	10,220	10,324
$^1E(D)$	3	10,367	10,520	10,633	10,714
$^3T_1$	5	12,329	12,647	12,979	13,323
	3	12,429	12,734	13,053	13,388
	4	12,622	12,975	13,338	13,709
	1	12,812	13,163	13,523	13,891
$^1T_2(G)$	5	15,032	15,293	15,581	15,893
$^1T_1$ ( )	4	15,051	16,376	16,807	17,241

$^1A_1(G)$	1	16,155	16,569	16,963	17,337
$^1E(G)$	3	16,478	17,224	18,016	18,842
$^1A_1(S)$	1	35,800	36,237	36,705	37,202
ORBITAL LEVELS		D_q = 400	D_q = 450	D_q = 500	
$^3T_1(F)$	1	0	0	0	
	4	334	340	346	
	3	923	949	969	
	5	1,114	1,118	1,120	
$^3T_2(F)$	4	4,216	4,657	5,100	
	5	4,155	4,590	5,028	
	3	4,499	4,942	5,387	
	2	4,307	4,720	5,142	
$^3A_2(F)$	5	8,279	9,171	9,998	
$^1T_2(D)$	5	10,417	10,516	10,619	
$^1E(D)$	3	10,771	10,809	10,833	
$^3T_1(P)$	5	13,680	14,048	14,426	
	3	13,739	14,104	14,481	
	4	14,089	14,476	14,869	
	1	14,267	14,650	15,039	
$^1T_2(G)$	5	16,226	16,578	16,945	
$^1T_1(G)$	4	17,680	18,122	18,568	
$^1A_1(G)$	1	17,691	18,025	18,340	
$^1E(G)$	3	19,693	20,564	21,451	
$^1A_1(S)$	1	37,728	38,281	38,861	

Then these parameters are varied until they give energy levels reasonably close to those obtained experimentally.

The band assignments have been discussed using Bethe's symbols, Γ_i to give the spin-orbit representation and is followed by Mulliken's notation for the orbital representation and the free-ion term from which a state is derived is given in parentheses. Thus, the ground electronic state of nickel (II) in a tetrahedral field, Γ_d is denoted as $\Gamma_1 : {}^3T_1(F)$. Three transitions are spin-allowed, two of which are orbital transitions, $\Gamma_{2-5} : {}^3T_2(F) \longleftarrow \Gamma_1 : {}^3T_1(F)$, and $\Gamma_5 : {}^3A_2(F) \longleftarrow \Gamma_1 : {}^3T_1(F)$ and the third one is from the ground to the excited allowed electronic state, $\Gamma_5 : {}^3T_1(P) \longleftarrow \Gamma_1 : {}^3T_1(F)$. The first transition is not recorded although its position is established at $\sim$ 4000 cm^{-1}. The remaining two transitions have been reported by several authors and agree with those found in the present case at $\sim$ 7,500 and 14,280 cm^{-1}, respectively. In addition to the spin-allowed transitions, few extremely weak bands have also been reported, which are due to spin-forbidden transitions from the ground electronic state $\Gamma_1 : {}^3T_1(F)$ to the excited singlets.

TABLE 5.6: CALCULATED ELECTRONIC ENERGY LEVELS OF $NiI_4^{=}$ IONS [136]

		ENERGY (cm^{-1})			
		λ = - 275	B = 537	C/B = 5.51	
ORBITAL LEVELS		D_q = 0	D_q = 50	D_q = 100	D_q = 150
$^3T_1(F)$	1	0	0	0	0
	4	00	121	196	244
	3	00	238	433	585
	5	00	495	803	956
$^3T_2(F)$	4	1,123	1,405	1,739	2,108
	5	1,123	1,400	1,699	2,073
	3	1,123	1,526	1,937	2,356
	2	1,851	2,023	2,241	2,506
$^3A_2(F)$	5	1,851	2,377	3,081	3,879
$^1T_2(D)$	5	8,172	8,460	8,750	9,037
$^1E(D)$	3	8,172	8,490	8,801	9,104
$^3T_1(P)$	5	10,003	10,201	10,387	10,567
	3	10,003	10,391	10,678	10,889
	4	9,178	9,486	9,809	10,148
	1	9,377	9,685	10,008	10,344
$^1T_2(G)$	5	13,233	13,368	13,548	13,768
$^1T_1(G)$	4	13,233	13,635	14,045	14,464

$^1A_1(G)$	1	13,233	13,723	14,198	14,655
$^1E(G)$	3	13,233	13,634	14,178	14,837
$^1A_1(S)$	1	33,449	33,765	34,112	34,492

ORBITAL LEVELS		D_q = 200	D_q = 250	D_q = 300	D_q = 350
$^3T_1(F)$	1	0	0	0	0
	4	275	297	312	323
	3	698	781	841	885
	5	1,028	1,066	1,086	1,097
$^3T_2(F)$	4	2,499	2,907	3,325	3,752
	5	2,488	2,918	3,356	3,797
	3	2,780	3,211	3,647	4,087
	2	2,818	3,164	3,536	3,928
$^3A_2(F)$	5	4,726	5,602	6,496	7,400
$^1T_2(D)$	5	9,309	9,556	9,767	9,939
$^1E(D)$	3	9,391	9,653	9,876	10,050
$^3T_1(P)$	5	10,750	10,950	11,181	11,430
	3	11,058	11,222	11,407	11,633
	4	10,499	10,863	11,237	11,620
	1	10,694	11,055	11,426	11,806
$^1T_2(G)$	5	14,026	14,381	14,639	14,984
$^1T_1(G)$	4	14,889	15,319	15,754	16,195

$^1A_1(G)$	1	15,093	15,513	15,913	16,293
$^1E(G)$	3	15,580	16,380	17,218	18,085
$^1A_1(S)$	1	34,902	35,344	35,816	36,318

ORBITAL LEVELS		$D_q = 400$	$D_q = 450$	$D_q = 500$
$^3T_1(F)$	1	0	0	0
	4	332	338	342
	3	917	941	959
	5	1,103	1,105	1,105
$^3T_2(F)$	4	4,187	4,627	5,072
	5	4,242	4,668	5,136
	3	4,532	4,981	5,433
	2	4,335	4,755	5,183
$^3A_2(F)$	5	8,306	9,193	9,911
$^1T_2(D)$	5	10,079	10,214	10,500
$^1E(D)$	3	10,176	10,262	10,316
$^3T_1(P)$	5	11,757	12,097	12,462
	3	11,905	12,219	12,567
	4	12,012	12,412	12,819
	1	12,195	12,591	12,995
$^1T_2(G)$	5	15,350	15,733	16,130
$^1T_1(G)$	4	16,639	17,088	17,542

$^1A_1(G)$	1	16,653	16,994	17,316
$^1E(G)$	3	18,971	19,872	20,786
$^1A_1(S)$	1	36,848	37,406	37,991

TABLE 5.7: CALCULATED ELECTRONICS ENERGY-LEVELS OF NiI_3Cl^{2-} IONS

ENERGY (cm^{-1})

λ = - 275, B = 588, C/B = 5.030

F_2 = 1010.520, F_4 = 84.504

ORBITAL LEVELS	Γ	D_q = 337	D_q = 338	D_q = 339
$^3T_1(F)$	1	0	0	0
	4	321	321	321
	3	876	877	878
	5	1,098	1,098	1,098
$^3T_2(F)$	4	3,630	3,639	3,648
	5	3,676	3,685	3,693
	3	3,817	3,825	3,833
	2	3,961	3,970	3,979
$^3A_2(F)$	5	7,159	7,177	7,195
$^1T_2(D)$	5	10,271	10,274	10,277
$^1E(D)$	3	10,485	10,488	10,491
$^3T_1(P)$	5	12,029	12,035	12,042
	3	12,183	12,189	12,195
	4	12,263	12,271	12,278
	1	12,452	12,459	12,467

$^1T_2(G)$	5	15,436	15,443	15,450
$^1T_1(G)$	4	16,678	16,686	16,695
$^1A_1(G)$	1	16,808	16,815	16,823
$^1E(G)$	3	18,347	18,364	18,381
$^1A_1(S)$	1	37,272	37,282	37,292

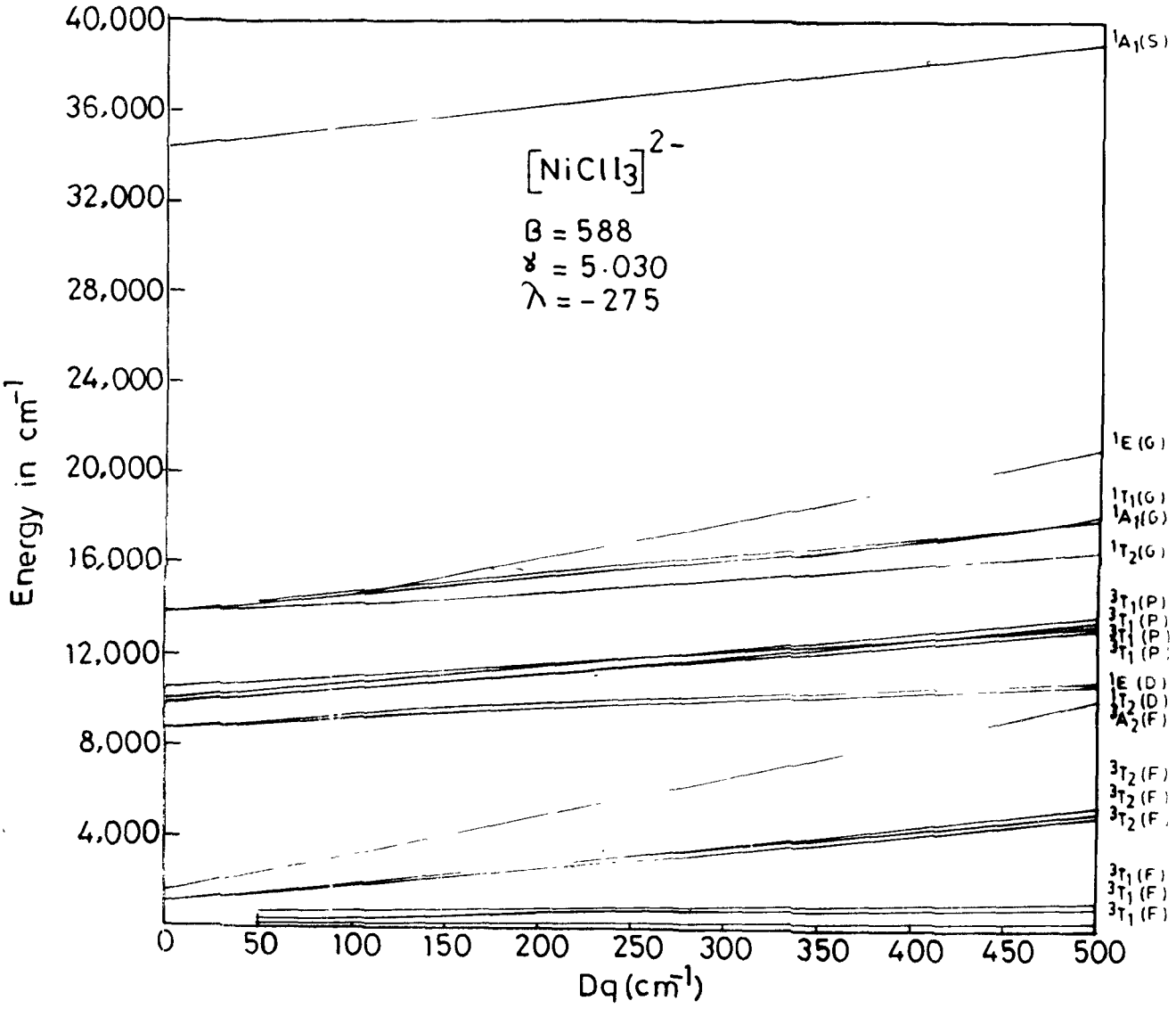

Fig. 5.4: Energy-level diagram for $[NiClI_3]^{2-}$.

TABLE 5.8: CALCULATED ELECTRONIC ENERGY-LEVELS OF $NiI_2Cl_2^{2-}$ IONS

ENERGY (cm^{-1})

λ = - 275, B = 639, C/B = 4.620

F_2 = 1060.740, F_4 = 84.348

ORBITAL LEVELS	Γ	D_q = 344	D_q = 345	D_q = 346
$^3T_1(F)$	1	0	0	0
	4	323	323	323
	3	884	884	885
	5	1,103	1,103	1,103
$^3T_2(F)$	4	3,681	3,690	3,698
	5	3,733	3,742	3,751
	3	3,865	3,873	3,881
	2	4,013	4,022	4,031
$^3A_2(F)$	5	7,281	7,299	7,318
$^1T_2(D)$	5	10,620	10,622	10,624
$^1E(D)$	3	10,929	10,930	10,932
$^3T_1(P)$	5	12,760	12,766	12,773
	3	12,876	12,882	12,888
	4	13,062	13,070	13,077
	1	13,252	13,260	13,267
$^1T_2(G)$	5	16,026	16,032	16,039

$^1T_1(G)$	4	17,330	17,339	17,348
$^1A_1(G)$	1	17,465	17,472	17,480
$^1E(G)$	3	18,956	18,973	18,990
$^1A_1(S)$	1	38,403	38,413	38,423

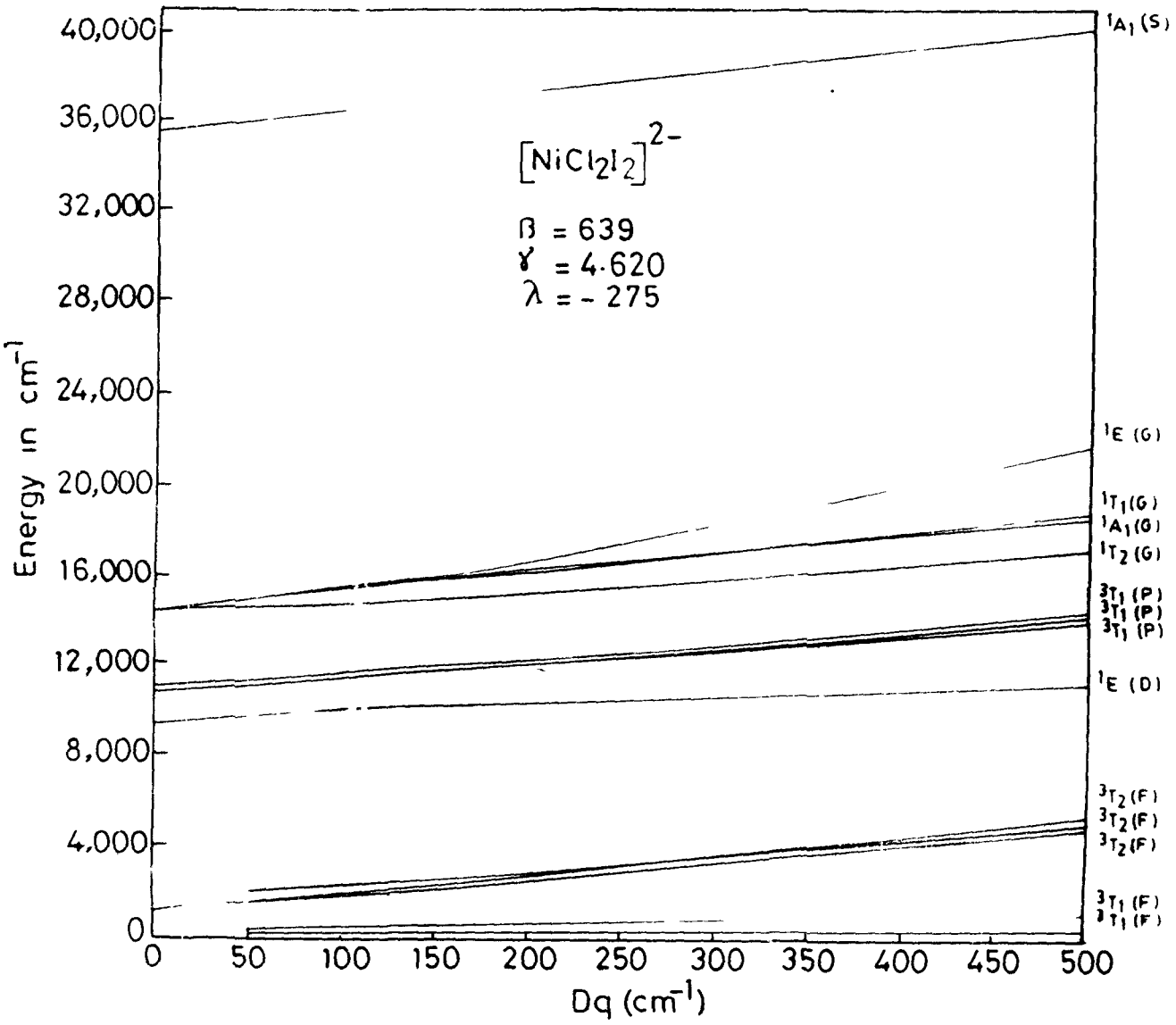

Fig. 5.5: Energy-level diagram for $[NiCl_2I_2]^{2-}$.

TABLE 5.9 : CALCULATED ELECTRONIC ENERGY-LEVELS FOR $NiICl_3^{2-}$ IONS

ENERGY (cm^{-1})

λ = - 275, B = 689, C/B = 4.270

F_2 = 1109.290, F_4 = 84.058

ORBITAL LEVELS	T	D_q = 350	D_q = 351	D_q = 352
$^3T_1(F)$	1	0	0	0
	4	324	325	325
	2	890	891	891
	3	1,107	1,107	1,107
$^3T_2(F)$	4	3,725	3,733	3,742
	5	3,781	3,790	3,799
	3	3,907	3,914	3,922
	2	4,058	4,066	4,075
$^3A_2(F)$	5	7,386	7,404	7,422
$^1T_2(D)$	5	10,928	10,930	10,932
$^1E(D)$	3	11,318	11,320	11,321
$^3T_1(P)$	5	13,493	13,499	13,506
	3	13,581	13,587	13,594
	4	13,840	13,848	13,855
	1	14,031	14,039	14,046
$^1T_2(P)$	5	16,592	16,599	16,605

$^1T_1(G)$	4	17,953	17,962	17,971
$^1A_1(G)$	1	18,092	18,100	18,107
$^1E(G)$	3	19,533	19,550	19,567
$^1A_2(S)$	1	39,471	39,481	39,491

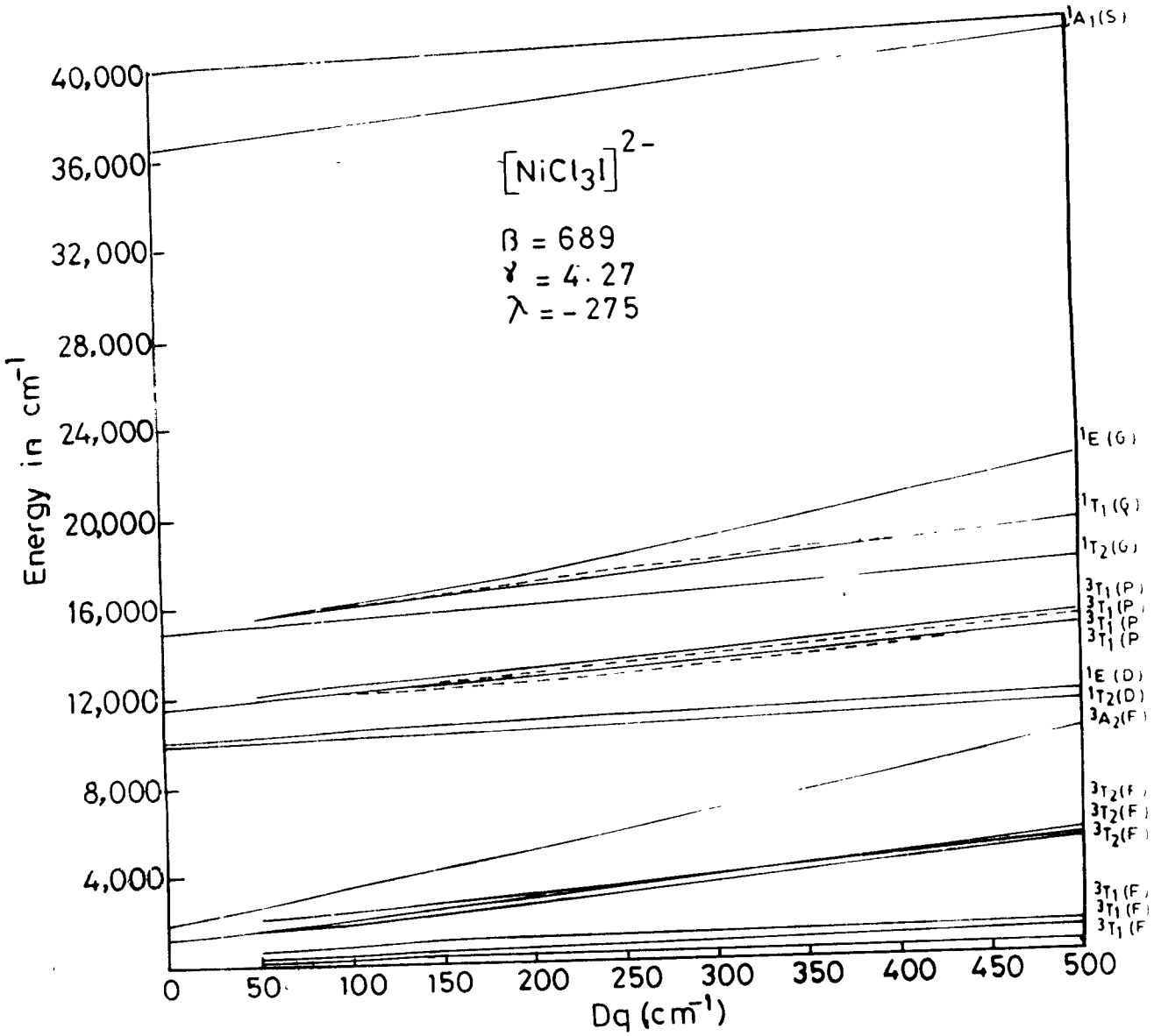

Fig. 5.6: Energy-level diagram for $[NiCl_3I]^{2-}$.

These are $\Gamma_5 : {}^1T_2(D) \leftarrow \Gamma_1 : {}^3T_1(F)$, $\Gamma_3 : {}^1E(D) \leftarrow \Gamma_1 : {}^3T_1(F)$, $\Gamma_5 : {}^1T_2(G) \leftarrow \Gamma_1 : {}^3T_1(F)$, $\Gamma_4 : {}^1T_1(G) \leftarrow \Gamma_1 : {}^3T_1(F)$, $\Gamma_1 : {}^1A_1(G) \leftarrow \Gamma_1 : {}^3T_1(F)$, and $\Gamma_3 : {}^1E(G) \leftarrow \Gamma_1 : {}^3T_1(F)$ transitions respectively. The transitions to the ^1D states are expected at $\sim$ 11,200 and $\sim$ 11,700 cm^{-1}, respectively. On the other hand, for the transitions to the ^1G states, it has been found difficult to assign the experimental data to the specific transitions predicted theoretically.

Energy level diagrams shown in Figs. 5.1 to 5.6 have been constructed by computing the energy levels using Liehr-Ballhausen secular equations on a VAX-1178 computer by a standard matrix-diagonalization procedure.

REFERENCES

1. M.C.S. Rao, Ind. J. Pure and Appl. Phys., 9, 169 (1971).
2. K. Seshagiri and K.C. Reddy, Acustica, 29, 59 (1973).
3. K. Ramamurthy and P.S. Varadachari, Ind. J. Pure and Appl. Phys., 11, 238 (1973).
4. M.V. Kaulgud and K.J. Patil, Ind. J. Pure and Appl. Phys., 13, 322 (1975).
5. J.D. Pandey, R.L. Mishra and T. Bhatt, Acustica, 38, 83 (1977).
6. V. Tiwari and J.D. Pandey, Ind. J. Pure and Appl. Phys., 18, 51 (1980).
7. S. Gnanamba and B.R. Rao, Ind. J. Pure and Appl. Phys., 7, 468 (1969).
8. B. Krishnamurthy, C.H.V.K.S. Sastry and G.L.N. Sastry, Ind. J. Pure Appl. Phys., 5, 453 (1967).
9. R.J. Fort and W.R. Moore, Trans. Farad. Soc., 61, 2102 (1975).
10. I. Prigogine, A. Bellemans and A. Erglerichowles, J. Chem. Phys., 24, 518 (1956).
11. V.A. Tabhane, V.B. Badhe and B.A. Patki, Ind. J. Pure and Appl. Phys., 20, 159 (1982).

12. O. Nomoto, J. Phys. Soc. Jpn., 13, 1528 (1968).

13. K.C. Reddy, S.V. Subramanyam and J. Bhimsenachar, Trans. Farad. Soc., 58, 2352 (1962).

14. W. Van Dael and E. Vangeel, Proc. Ist Int. Conf. Cal. Therm. Warsaw, P. 555 (1969).

15. B. Jacobson, Acta. Chem. Scand., 6, 1485 (1952); J. Chem. Phys., 20, 927 (1952).

16. K.C. Reddy and K. Seshadri. Acustica, 29, 59 (1973).

17. M.V. Kaulgud, Acustica, 10, 316 (1960).

18. M.V. Kaulgud, Ind. J. Phys., 36, 577 (1962).

19. K. Seshadri and K.C. Reddy, J. Acoust. Soc. Ind., 4, 1951 (1973).

20. K.R. Prasad and K.C. Reddy, Proc. Ind. Acad. Sci., 82A, 217 (1975).

21. R. Nutch-Kuhnkies, Acustica, 15, 383 (1965).

22. G. Maheshwari, Ph.D. Thesis, Maulana Azad Library, A.M.U., Aligarh (1985).

23. A.P. Srivastava, Acoust. Lett., 9, 181 (1986).

24. W. Schaarfs, Z. Phys.,114, 110 (1939); 115, 69 (1940).

25. J.D. Pandey, Electrochimica Acta, 27, 1097 (1982).

26. J.D. Pandey, R.K. Upadhyay and U. Gupta, Acoust. Lett., 5, 120 (1982).

27. J.D. Pandey and U. Gupta, Eelectrochimica Acta, 28, 1047 (1983).

28. R.K. Dewan, J. Kaur and S.K. Mehta, Acoust. Lett., 9, 13 (1985).

29. J.D. Pandey, V.N. Srivastava, V. Vyas and N. Panta, Ind. J. Pure and Appl. Phys., 25, 467 (1987).

30. H. Eyring, V.G. Gerrard, T. Ree and W. Lu. J. Chem. Phys., 49, 797 (1968).

31. Naseem, Ph.D. Thesis, Maulana Azad Library, A.M.U., Aligarh (1992).

32. O. Nomoto and H. Endo, Bull. Chem. Soc. Jpn, 44, 16 (1971).

33. H. Uedaira and Y. Suzuki, Bull. Chem. Soc. Jpn., 52 (10), 2787 (1979).

34. F. Hirata and K. Arakawa, Bull. Chem. Soc. Jpn., 45, 2715 (1972).

35. K. Patil and G. Mehta, J. Chem. Soc. Farad Trans. I, 84 (7), 2297 (1988).

36. R.H. Stokes and R. Mills. Viscosity of Electrolytes and Related Properties. Pergamon Press, New York (1971).

37. S. Glasstone, K.J. Laidler and H. Eyring, 'The Theory of Rate Processes', Mc Graw-Hill, New York, N.Y., Chapter 9 (1941).

38. A.K. Doolittle, J. Appl. Phys., 22, 1471 (1951); 23, 236 (1952).

39. M.L. Williams, R.F. Landel and J.D. Ferry, J. Am. Chem. Soc., 77, 3701 (1955).

40. M.H. Cohen and D. Turnbull, J. Chem. Phys., 31, 1164 (1959).

41. P.B. Macedo and T.A. Litovitz, Ibid, 42, 245 (1965).

42. V.A. Bloomfield and R.K. Dewan, J. Phys. Chem. 75, 3113 (1971).

43. J.D. Pandey and U. Gupta, Electrochimica Acta, 29, 403 (1984).

44. B.R. Chaturvedi and J.D. Pandey, Chemica Scripta, 18, 227 (1981).

45. P.J. Flory, J. Am. Chem. Soc., 87, 1833 (1965).

46. A. Abe and P.J. Flory, J. Am. Chem. Soc., 87, 1838 (1965).

47. J.D. Pandey, B.R. Chaturvedi and N. Pant, Chemica Scripta, 18, 221 (1981).

48. V.A. Bloomfield and R.K. Dewan, J. Phys. Chem. 79, 1975 (1970).

49. B.K. Sharma, H.L. Bhatnagar, Ind. J. Pure and Appl. Phys., 15, 640 (1977).

50. R.D. Dunlop and R.L. Scott, J. Phys. Chem. 66, 631 (1962).

51. L.A.K. Stavely, K.R. Hart and W.J. Tupman, Trans. Farad. Soc. Dissc. 15, 130 (1953).

52. J.D. Pandey, N. Pant and B.R. Chaturvedi, Chemica Scripta, 18, 224 (1981).

53. S. Ganesan et al., Can. J. Phys., 40, 91 (1962).

54. D.N. Batchelder et al., J. Phys., Chem. 41, 2327 (1964).

55. L. Knopoff and J.N. Shapiro, Phys. Rev. B1, 3893 (1970).

56. S.K. Kor, U.S. Tandon and B.K. Singh, Phys. Lett., 38A, 187 (1972).

57. E.A. Guggenheim, 'Mixtures', Clarendon Press, Oxford (1952).

58. N.K. Board, A.R. Palmer and E. Heymann, Trans. Farad. Soc., 51, 277 (1955).

59. G. Bertozzi and G. Sternheim, J. Phys. Chem., 68, 2908 (1964).

60. G. Bertozzi, J. Phys. Chem., 69, 2606 (1965).

61. D.A. Nissen and B.H.V. Domelen, J. Phys. Chem., 79, 2003 (1975).

62. D.A. Nissen, J. Phys. Chem., 82, 429 (1978).

63. B.B. Owen and T.E. Cooke, J. Am. Chem. Soc., 59, 2273 (1937).

64. R.M. Rush and J.S. Johnson, J. Phys. Chem., 72, 767 (1968).

65. G. Scatchard, J. Am. Chem. Soc., 83, 2636 (1961).

66. H.L. Friedman, J. Chem. Phys., 32, 1134 (1960).

67. R.H. Wood and H.L. Anderson, Ibid, 71, 1871 (1967).

68. W.Y. Wen, K. Miyajima and A. Otsuka, J. Phys. Chem., 75, 2148 (1971).

69. R. Palepu, J. Oliver and D. Campbell, J. Chem. Eng. Data, 30, 355 (1985).

70. F. Cooradini, L. Marcheselli, A. Marchetti, M. Tagliazuchhi, L. Tassi and G. Tossi, Bull. Chem. Soc. Jpn., 65, 503 (1992).

71. O. Samoilov, Zh. Fiz. Khim., 20, 1411 (1916).

72. M.D. Danford and H.A. Levy, J. Am. Chem. Soc., 84, 3965 (1962).

73. A.I. Vogel, 'Text Book of Practical Organic Chemistry', 3rd Edition, Longman Green and Co., London, pp. 170, 173, 564, 711 (1924).

74. C.T. Moynihan, J. Phys. Chem., 70, 3399 (1966).

75. N. Islam, M.R. Islam and R. Ahmad, Ind. J. Chem., 17A, 285 (1979).

76. C. Tanford, 'Physical Chemistry of Macromolecules', John Wiley and Sons, Inc., New York, N.Y. P. 329 (1961).

77. E.W. Washburn, 'International Critical Table of Numerical Data of Physics , Chemistry and Technology', (Mc Graw Hill Book Co., Inc. New York). Vol. III, PP. 27-29, 33 (1928) and Vol. VII, P. 220 (1930).

78. J. Nath and G. Singh, J. Chem. Eng. Data, 31, 327 (1986).

79. V.A. Tabhane and B.A. Patki, Ind. J. Pure and Appl. Phys., 21, 155 (1983).

80. V.K. Rattan, B.P.S. Sethi and K.S.N. Raju, Aust. J. Chem, 42, 1077 (1989).

81. K.J. Patil, Ind. J. Pure and Appl. Phys., 16, 608 (1978).

82. J.D. Pandey, A. Shukla R.D. Rai and K. Mishra, J. Chem. Eng. Data, 34, 29 (1989).

83. R.L. Mishra and J.D. Pandey, Acustica, 40, 355 (1978).

84. R.L. Mishra and J.D. Pandey, J. Acoust. Soc. Ind., 11, 145 (1979).

85. S.N. Jajoo, V.S. Deogaonkar and C.S. Adgaonkar, Ind. J. Pure and Appl. Phys., 21, 61 (1983).

86. R.L. Mishra and J.D. Pandey, Ind. J. Pure and Appl. Phys., 15, 505 (1977).

87. J.D. Pandey, P. Dubey and M.C. Saxena, Acustica, 48, 277 (1981).

88. J.D. Pandey and S.N. Srivastava, Acustica, 51, 66 (1982).

89. K.J. Patil and D.N. Raut, Ind. J. Pure and Appl. Phys., 18, 499 (1980).

90. C.G. Balachandran, J.Ind. Inst. Sci., 37, 27 (1955).

91. G.M. Marks, J. Acoust. Soc. Am., 31, 936 (1959).

92. S.V. Subramanyam and T. Bhimsenachar, J. Phys. Soc. Jpn., 17, 1447 (1961).

93. S. Rajgopalan, Ind. J. Pure and Appl. Phys., 7, 206 (1969); 21, 67 (1983).

94. N. Auerbach, Experienti , 4, 473 (1948).

95. L. Hall, Phys. Rev., 73, 775 (1948).

96. M.J. Hey, D.W. Shield, J.M. Speight and M.C. Wills, J. Chem. Soc. Farad. Trans. I, 77, 123 (1981).

97. R.P. Rastogi, J. Nath and J. Mishra, J. Phys. Chem., 71, 1277 (1967).

98. N. Berkowitz and S.C. Srivastava, Can. J. Chem., 41, 1787 (1963).

99. D.R. Rossensky, J. Phys. Chem., 81, 1578 (1977).

100. C.V. Suryanarayan, J. Acoust. Soc. Ind., 4, 111 (1977).

101. F.C. Colline, W.W. Brandit and M.H. Navidi, J. Chem. Phys., 25, 581 (1958).

102. R.J. Buchler, R.H. Wentroff, J.O. Hirschfelder and C.F. Curtiss, J. Chem. Phys., 19, 61 (1951).

103. R.P. Pandey and B.R. Chaturvedi, Chemica Scripta, 18, 65 (1981).

104. R.A. Aziz, C.C. Lim and D.H. Bowman, Can. J. Phys., 50, 646 (1972).

105. N.F. Carnahan and K.E. Starling, J. Chem. Phys., 51, 635 (1969).

106. E.J. Thiele, J. Chem. Phys., 39, 474 (1963).

107. L.V. Woodcock, J. Chem. Soc. Farad. Trans. II, 72, 731 (1976); 74, 11 (1978).

108. R.J. Speedy, J. Chem. Soc. Farad. Trans. II, 714 (1977).

109. J.L. Lebowitz, H.L. Fisch and E. Helfand, J. Chem. Phys., 34, 1037 (1961).

110. W.G. Hoover and F.H. Ree, J. Chem. Phys., 49, 3609 (1968).

111. D. Henderson and J.A. Barker, Mol. Phys., 21, 187 (1971).

112. D. Henderson, Mol. Phys., 30, 971 (1975).

113. W.W. Wood, J. Chem. Phys., 52, 729 (1970).

114. C.V. Chaturvedi and S. Pratap, Acustica, 42, 260 (1979).

115. J.D. Pandey and K. Mishra, Acoust. Lett., 6, 148 (1983).

116. L.A.K. Stavely, K.R. Hart and W.J. Tupman, Trans. Farad. Soc., 51, 323 (1955).

117. H. Hoker and P.J. Flory, Trans. Farad. Soc., 65, 1188 (1968).

118. R.K. Nigam and P.P. Singh, Trans. Farad. Soc., 65, 950 (1969)

119. D.V.S. Jain, V.K. Gupta and B.S. Lark, Ind. J. Chem., 8, 815 (1970).

120. G. Delmas and S. Turrell, J. Chem. Soc. Farad. I, 70, 572 (1974).

121. V.H. Khan and S.V. Subramanyam, Trans. Farad. Soc., 67, 2282 (1971).

122. J.K. Holz-hauer and W.T. Zeigler, J. Phys. Chem., 79, 590 (1975).

123. V.H. Khan, K. Malakondaiah and S.V. Subramanyam, J. Acoust. Soc. Ind., 5, 95 (1977).

124. J.D. Pandey, B.R. Chaturvedi and R.P. Pandey, J. Phys. Chem., 85, 1750 (1981).

125. J.D. Pandey and U. Gupta, J. Phys. Chem., 86, 5234 (1982).

126. H. Eyring and J.O. Hirschfelder, J. Phys. Chem., 41, 249 (1937).

127. J.O. Hirschfelder, D. Stevenson and H. Eyring, J. Chem. Phys., 5, 896 (1937).

128. G.N. Swamy, G. Dharmaraju and G.K. Raman, Can. J. Chem., 58, 229 (1980).

129. J.S. Rowlinson, "Liquids and Liquid Mixtures", 2nd ed., Butterworth and Co. Ltd., London (1969), P. 159.

130. S.K. Quardi, Ph.D. Thesis, Maulana Azad Library, A.M.U., Aligarh (1984).

131. H. Eyring and M.S. John, "Significant Liquid Structure", John Wiley and Sons, New York (1969).

132. N. Islam, M.R. Islam, S. Ahmad and B. Waris, J. Am. Chem. Soc., 97, 3026 (1975).

133. A.D. Liehr and C.J. Ballhausen, Ann. Phys., (New York), 6, 134 (1959).

134. C.J. Ballhausen, 'An Introduction to Liq d-Field Theory', P. 23, Mc Graw-Hill Book Co., Inc. New York, (1962).

135. G.P. Smith, C.H. Liu and T.R. Griffiths, J. Am. Chem. Soc., 86, 4796 (1964).

136. S. Ahmad, Ph.D. thesis, Maulana Azad Library, A.M.U., Aligarh (1974).

APPENDIX-I

APPENDIX

```
PROGRAM THRY (INPUT, OUTPUT);
CONST
   K = 1.3806E-16;
   R = 8.3143E07;
M1 = 84.99
M2 = 101.10
NA = 6.023E23;
VAR
   I,N: INTEGER;
   L,AL1,AL2,B1,B2,A1,A2,T,V1,V2,VC1,VC2,VR1,VR2,TR1,TR2,TC1,TC2,
   PC1,PC2,Y1,Y2,BT1,BT2:REAL;
VRO,V,X1,X2,S1,S2,Q1,Q2,VOR,TR,VRE,VRC,VRE2,VE,VR,AL3,A3,PAI,B3,
NS,TS,VC:REAL;
VEC,VEE,X12,PC,TC,DGM,LNMIX,SR,SC,ST,UT,SO,U,D,XVE,STVE,STVEC,
STVEE,E1,E2,FX,LNMIXNE2,NE2,MNE,STNE2,STNE,FQ,E12,QX,NE3:REAL;
XVRE,STVRE,STVRE2,MST,STST,STSO,E,F,G,H,D1,D2,N1,N2,N3,T1,T2,T3,
D3,NE,NT,MN,STNS,STNT:REAL;
VO1,VO2,ST1,ST2,TCT1,TCT2,DA1,DA2,YO1,YO2,BS1,BS2,BS,Z1,Z2,Z,
R1,R2,RQ,RX,UTH1,BSM,BSM,BW1,BW2,B,UTH22,UT2,MUT,STUT2,STUTH22,
STUTH1,
VO3,ST3,TCT3,DA3,YO3,BT3,Y3,PC3,PI1,PI2,PI3,SHR1,SHR2,SHR3,GP1,
GP2,GP3:REAL;
BT1X,BT1Y,BT1Z,BT11,BT2X,BT3X,BT2y,BT3y,BT2Z,BT3Z,BT22,BT33,
TRM:REAL;
```

```
BEGIN
     READLN (N,A1,B1,V1,A2,B2,V2,A3,B3,V,X1,X2);
     T: = 303.15;
   PAI: = 22/7;
FOR  I: = 1 TO N DO
     BEGIN
     READLN(U,T1,T2,TS,N3,D3,T3,U1,U2);
     T: = T+5.0;
WRITELN('    TEMPERATURE ==' T,'     X1 ==',X1);
     AL1: = (B1*0.0001)/(B1*0.0001*T+A1);
WRITELN('     AL1 = ' AL1);
AL2: = (B2*0.0001)/(B2*0.0001*T+A2);
WRITELN('    AL2 = ' AL2);
AL3: = (B3*0.0001)'/(B3*0.0001*T+A3);
WRITELN('       AL3 = ',AL3);
  D: = A3 - (B3*0.0001*T);
D1: = A1 - (B1*0.0001*T);
D2: = A2 - (B2*0.0001*T);
WRITELN('     D1 = 'D1,    D2 = ',D2,'    D = ',D);
N1: = (D1*T1)/(D3*T3))*N3;
N2: = ((D2*T2)/(D3*T3))*N3;
  NS: = ((D*TS)/(D3*T3))*N3;
NE: = NS - ((X1*N1)+(X2*N2));
  VR1: = ((AL1*T/(3+(3*AL1*T)))+1)**3;
WRITELN('      VR1 = '   VR1);
```

```
VR2: = ((AL2*T/(3+(3*AL2*T)))+1)**3;
WRITELN('     VR2 = =', VR2);
VC1: = (V1/D1)/VR1;
VC2: = (V2/D2)/VR2;
VC: = (X1*VC1)+(X2*VC2);
WRITELN('    VC =', VC);
E1: = V1/D1;
E2: = V2/D2;
E12: = V/D;
  WRITELN('      E1 = ',E1,'  E2 = ',E2,'    E12 = ',E12);
TR1: = (VR1**(1/3)-1)/(VR1**(4/3));
WRITELN('      TR1 = ', TR1);
TR2: = (VR2**(1/3)-1)/(VR2**(4/3));
WRITELN('       TR2 = ',TR2);
TC1: = T/TR1;
TC2: = T/TR2;
VO1: = V1/A1;
VO2: = V2/A2;
  VO3 : = V/A3;
ST1: = 6,3*(10,0**(-4))*D1*(U1**(3/2));
ST2: = 6,3*(10.0**(-4))*D2*(U2**(3/2));
ST3: = 6,3*(10.0**(-4))*D*(U**(3/2));
WRITELN('   ST1 = 'ST1,   ST2 = ' ST2,'    ST3 = ' ST3);
WRITELN('   VO1 = ', VO1,'  VO2 = ', VO2,'  VO3 = 'VO3);
TCT1: = T/(1-((VO1/(V1/D1))**(10/3)));
```

```
TCT2: = T/(1-((VO2/(V2/D2))**(10/3)));
TCT3: = T/(1-((VO3/(V/D))**(10/3)));
WRITELN('   TCT1 = '  TCT1, '   TCT2 = ' TCT2,'  TCT3 = ',TST3);
DA1: = (((V1/D1)/(7.2*(10.0**19)))*((ST1/TCT1)**(1/4)))**(2/5);
DA2: = (((V2/D2)/(7.2*(10.0**19)))*((ST2/TCT2)**(1/4)))**(2/5);
DA3: = (((V/D)/(7.2*(10.0**19)))*((ST3/TCT3)**(1/4)))**(2/5);
WRITELN('   DA1 = ',DA1,'    DA2 = '  DA2,  DA3 = ',DA3);
YO1: = (PAI*(DA1**3)*NA)/(6*(V1/D1));
YO2: = (PAI*(DA2**3)*NA)/(6*(V2/D2));
YO3: = (PAI*(DA3**3)*NA)/(6*(V/D));
WRITELN('    YO1 = 'YO1,'   YO2 = ',YO2',  YO3 = ',YO3);
BT11: = (V1/D1)/(R*T)*(((1-YO1)**3)/(1+YO1));
BT22: = (V2/D2)/(R*T)*(((1-YO2)**3)/(1/YO2));
BT33: = (V/D)/(R*T)*(((1-YO3)**3)/(1+YO3));
BT1X: = (E1/(R*T))*(((1-YO1)**4)/((1+(2*YO1))**2));
BT2X: = (E2/(R*T))*(((1-YO2)**4/((1+(2*YO2))**2));
BT3X: = (E12/(R*T))*(((1-YO3)**4)/((1+(2*YO3))**2));
BT1: = (E1/(R*T))*(((1-YO1)**3)/(1+(5*YO1)+(9*(YO1**2))-
       (3*(YO1**3))));
BT2: = (E2/(R*T))*(((1-YO2)**3)/(1+(5*YO2)+(9*(YO2**2))-
       (3*(YO2**3))));
BT3: = (E12/(R*T))*(((1-YO3)**3)/(1+(5*YO3)+(9*(YO3**2))-
       (3*(YO3**3))));
BT1Y: = (E1/(R*T))*(((1-YO1)**4)/(1+(4YO1)+(4*(YO1**2))-
        (4*(YO1**3))+(YO1**4)));
```

```
BT2Y: = (E2/(R*T)))*(((1-YO2)**4)/(1+(4*YO2)+(4*(YO2**2))-
        (4*(YO2**3))+(YO2**4)));
BT3Y: = (E12/(R*T))*(((1-YO3)**4)/(1+(4*YO3)+(4*(YO3**2))-
        (4*(YO3**3))+(YO3**4)));
BT1Z: = (E1/(R*T))*(((1-YO1)**3)/(1+3*YO1));
BT2Z: = (E2/(R*T))*(((1-YO2)**3)/(1+3*YO2));
BT3Z: = (E12/(R*T))*(((1-YO3)**3)/(1+3*YO3));
WRITELN('  ISOTHRMAL COMPRESSIBILITIES--BT1X=',BT1X,'BT2X=',BT2X,'
      BT3X=',BT3X);
WRITELN('   BT1 = ',BT1,'    BT2 = ',BT2,'   BT3 = ' BT3);
WRITELN('  BT1Y = ',BT1Y,' BT2Y = ',BT2Y,  BT3Y = ',BT3Y);
WRITELN('  BT1Z = ',BT1Z,  BT2Z = ',BT2Z,   BT3Z = ',BT3Z);
WRITELN('  BT11 = ',BT11,   BT22 = ',BT22,'     BT33 = ',BT33);
PI1: = ((2**(1/6))*R*T)/(((2**'1/6))*E1)-(DA1*(NA**(1/3))*
       (E1**(2/3))));
PI2: = ((2**(1/6))*R*T)/(((2**(1/6))*E2)-(DA2*(NA**(1/3))*
       (E2**(2/3))));
PI3: = ((2**(1/6))*R*T)/(((2**(1/6))*E12)-(DA3*(NA**(1/3))*
       (E12**(2/3))));
WRITELN('  INTERNAL PRESSURE   PI1 = ', PI1,  PI2 = ',PI2,
                                      PI3);
Y1: = AL1/BT1;
Y2: = AL2/BT2,
Y3: = AL3/BT3;
PC1: = Y1*T*(VR1**2);
PC2: = Y2*T*(VR2**2);
```

```
VR: = ((AL3*T/(3+AL3*T)))+1)**3;
PC3: = Y3*T*(VR**2);
VRO: = (V/D)/((X1*VC1)+(X2*VC2));
S2: = X2/((X2+X1)*(VC1/VC2));
S1: = 1-S2;
Q2: = S2/((S2+S1)*((VC1/VC2)**(-1/3)));
Q1: = 1-Q2;
VOR: = (S1*VR1)+(S2*VR2);
TOR: = ((VOR**(1/3))-1)/(VOR**(4/3));
TR: = (VRO**(1/3)-1)/(VRO**(4/3));
VRE: = (VOR**(7/3))*((4/3)-(VOR**(1/3)))**(-1)*(TR-TOR);
VRC: = VOR-VRE;
VRE2: = VRO-VOR;
VE: = VRE2*((X1*VC1)+(X2*VC2));
VEC: = ((X1*VC1)+(X2*VC2))*(VR-(S1*E1+S2+E2));
VEE: = E12-(X1*E1+X2*E2);
X12: = PC1*((1-(VC2/VC1)**(-1/6))*((PC2/PC1)**(1/2)))**2);
PC: = (S1*PC1)+(S2*PC2)-(S1*Q2*X12);
TC: = ((((S1*PC1)/TC1)+((S2*PC2)/TC2))**)-1))*((S1*PC1)+
      (S2*PC2,-(S1*Q2*X12));
TRM: = ((S1*PC1*TR1)+(S2*PC2*TR2))/(((S1*PC1)+(S2*PC2))-
       (S1*Q2*X12));
WRITELN ('          TR = ', TR',   TRM = ',TRM);
E: = (1/VR1)-(1/VR);
F: = 3*TR1*LN(((VR1**(1/3))-1)/((VR**(1/3))-1));
G: = (1/VR2)-(1/VR);
H: = 3*TR2*LN(((VR2**'1/3))-1)/((VR**(1/3))-1));
```

```
DGM: = (X1*PC1*VC1*(E+F))+(X2*PC2*VC2*(G+H))+(X1*VC1*Q2*X12* 12);
LNMIX: = -(DGM/(R*T))+(1/(VR-1))-(X1/(VR1-1))-(X2/(VR2-1)+
          (X1*LN(N1))+(X2*LN(N2));
 NT: = EXP(LNMIX);
LNMIXNE2: = - (DGM/(R*T))+(1/VR-1))-(X1/(VR1-1))-(X2/VR2-1);
NE2: = EXP(LNMOXNE2);
NE3: = LNMIX-((X1*LN(N1))+(X2*LN(N2)));
MNE: = (NE2+NE)/2;
BS1: = (1/((U1*100)**2))*(1/D1);
BS2: = (1/((U2*100)**2))*(1/D2);
BS: = (1/((U*100)**2))*(1/D);
Z1: = D1*U*100;
Z2: = D2*U2*100;
Z: = D*U*100;
R1: = E1*((U1*100)**(1/3));
R2: = E2*((U2*100)**(1/3));
RQ: = E12*((U*100)**(1/3));
RX: = (X1*R1)+(X2*R2);
UTH1: = (RX/E12)**3;
BSE: = BS-(X1*BS1+X2*BS2);
BSM: = (X1*BS1)+(X2*BS2);
BW1: = E1*(BS1**(-1/7));
BW2: = E2*(BS2**(-1/7));
B: = E12*(BS**(-1/7));
UTH22: = (1/((X1/(M1*SQR(U1)))+(X2/(M2*SQR(U2)))*((M1*X1)+
          (M2*X2))))**(1/2);
```

```
WRITELN('   STNE2 = ', STNE2,'     STNE = ',STNE);
FX: = (X1/(M1*(U1**2)))+(X2/(M2(U2**2)));
FQ: = FX*((X1*M1)+(X2*M2));
QK: = 1/FQ;
UT2: = QK**0.5;
MUT: = (UTH22+(UTH1+UT2)/3;
STUT2: = SQRT(((UT2-MUT)**2)/2);
STUTH22: = SQRT(((UTH22-MUT)**2)/2);
STUTH1: = SQRT(((UTH1-MUT)**2/2);
WRITELN('   ADIABATIC COMPRESSIBILITY BS1=',BS1,' BS2=',BS2,'
       BS = ',BS);
SHR1: = BT1/BS1;
SHR2: = BT2/BS2;
SHR3: = BT3/BS;
GP1: = (SHR1-1)/(T*AL1);
GP2: = (SHR2-1)/(T*AL2);
GP3: = (SHR3-1)/(T*AL3);
WRITELN('   SPECIFIC HEAT RATIO--SHR1=', SHR2=',SHR2,'SHR3='SHR3);
WRITELN('  GRIENSEN PARAMETER--GP1=',GP1,GP2=',GP2','GP3=',GP3);
WRITELN('  SPECIFIC ACOUSTIC IMPEDENCE Z1=',Z1,' Z2=',Z2, Z=',Z);
WRITELN('  RX = ', RX,' UTH1 = ', UTH1);
WRITELN('  BSE=',BSE,'  BSM=',BSM);
SR: = ((0.33*(VR**(-5/3)))-(((VR**(1/3))-1)/(VR**2))*LN
     (((VR**(1/3))-0.5)/((VR**(1/3))-1)))/VR;
SC: = (K**(1/3))*(PC**(2/3))*(TC**(1/3));
```

```
ST: = SC*SR*VR;
UT: = (ST/(6.3*(10.0**(-4))*D))**(2/3);
SO: = (U**(3/2))*6.3*(10.0**(-4))*D;
XVRE:= (VRE+VRE2)/2;
WRITELN('   WADA CONSTANT  BW1=',BW1,' BW2=',BW2,' B=',B);
WRITELN('   UTH22 = ',UTH22,'   UT2 = ',UT2);
WRITELN('  STUT2 =', STUT2, ' STUTH1 = ', STUTH1);
WRITELN('  STUTH22 = ', STUTH22);
MST: = (ST+SO)/2;
MN: = (NS+NT)/2;
WRITELN('   A1 = ', A1,  A2 = ', A2);
WRITELN('   VC1 = ',VC1, ' VC2 = ', VC2, 'V1 = ',V1,' V2=',V2);
WRITELN('   TR1=',TR1, TR2 = ', TR2, TC1 = ', TC1,' TC2 = ',TC2);
WRITELN('  PC1 = ', PC1', PC2 = ', PC2,  PC3 = ', PC3);
WRITELN('  THERMAL PRESSURE COEFFICIENT  Y1 = ',Y1,' Y2 = ',Y2',
        Y3 = ',Y3);
WRITELN('   VRO = ', VRO,'  S1 = ',S1', S2 = ',S2);
WRITELN('  Q1 = ',Q1,'  Q2 = ',Q2, VOR = ', VOR);
WRITELN('  TOR = ', TOR, ' TR = ', TR,'   VRE = ',VRE);
WRITELN('  VE =', VE,  VEC = ', VEC,'  VEE =', VEE);
WRITELN('  ********    X12 = ', X12);
WRITELN('   PC = ', PC,'   TC = ', TC);
WRITELN('  DGM = ',DGM,'  LNMIX = ', LNMIX);
WRITELN('   SR = ;SR,   SC = ',SC,'   ST = ',ST);
WRITELN('  SURFACE TENSION   SO= ', SO,'    ST =',ST);
```

```
WRITELN('  UT = ',UT,'  D = ',D,'  D1 = ',D1, D2 = ',D2);
WRITELN('  STVE = ', STVE,'  STVEC = ',.STVEC,' STVEE = ',STVEE);
WRITELN('  STVRE=',STVRE,'  STVRE2=',STVRE2);
WRITELN('  STST=',STST,'    STSO=',STSO);
WRITELN('  VISCOSITY    N1 =',N1,'   N2=',N2);
WRITELN('  NS=',NS,'   NT=',NT);
WRITELN('  STNS=',STNS,'   STNT=',STNT);
WRITELN('  EXCESS VISCOSITY  NE=',NE,'  NE2=',NE2,' NE3=',NE3);
WRITELN('-------------------------------------------------
END;
END.
```

APPENDIX-II

APPENDIX

```
Program to calculate free energy
real     t(6), x, a,b,eta (6), r(6), vm (6), ml,m2
real     gas-const, h,n,z,delta-g
character    fil-in*13,fil-out*13
data     t/298.15, 303.15,308.15,313,15,318.15,323.15/
gas-const = 8.314
h = 6.626e - 34
n = 6.022e + 23

type 5
format ('spl, enter the data file name')
accept 10,fil-in
type 7
format ('spl, enterthe result file name ')
accept 10, fil-out
format (a)

open(unit = 1, file = fil-in, type = 'old' read only)
open(unit = 2, file = fil-out, type = 'new')
read (1,12) ml,m2
format (2f10.3)
read (1,20, end = 100) x,a,b,(eta(i), i = 1,6)
format (9f8.3)
```

Contd....

```
doi = 1,6
          r(i) = a+b*t(i)
          vm(i) = (x*m1+(1-x)*m2)/r(i)
          write (2,25)i,r(i),i,vm(i)
          format (1h  , R (',I1',) = 'F10.4,5x,'VM(',I1,')=',F10.4)
end do
doi = 1,6
   vm(1) = vm(i)*1.0e-06
   z = gas - const* log(eta(i)*vm(i))
   delta - g = gas - const*t(i)*log((eta(i)*vm(i))/(h*n))
   write (2,30) delta-g,t(i),z
   format (1h, DELTA-G = ',F10.4,' ON TEMP. ',F8.2,
1  'AND VALUE OF Z = ',F10.4)
end do
goto 15
continue
close (1)
close (2)
stop
end
```

APPENDIX-III

APPENDIX

```
PROGRAM PEDRO III
MATRIX DIAGONALIZATION
IMPLICIT REAL *8 (A-F, O-Z)
REAL LAMBDA
DIMENSION ADQ (100), (30,30) ROOTS (20,100), EMOD (20,100)
WRITE (*,*) 'PL. ENTER NOJOBS IN 13 FORMAT
READ (*,100) NOJOBS
FORMAT (13)
DO 99 JOB = 1, NOJOBS
WRITE (*,*) 'PL. ENTER B, GAMMA, LAMBDA IN F9.2 FORMAT'
READ (*, 101) B, GAMMA, LAMBDA
FORMAT (3F 9.2)
F4 = B+5. *F4
WRITE (*,*) 'PL, ENTER NODQ, ADQ(I) IN 13 AND F6.1 FORMAT'
READ (*, 102) NODQ (ADQ(I), I=1, NODQ)
FORMAT (13/(F6.1))
WRITE (*,110)B, GAMMA, LAMBDA, F2,F4
FORMAT (26H1D) (2-8) CUBIC STRONG FIELD/3X, 5H B = F9.3,3X,9H
                                                    GAMMA
1 = F9.3, 3X, 10H LAMBDA = F9.3,3X/6H F2 = F9.3,3X,6H F4=F9.3)
FIRST MATRIX
MATRIX OF GAMMA ONE
DC 10 IDQ, NODQ
DQ = ADQ (IDQ)
```

```
H(1,1) = 8.*F2+51.*F4+12.*DQ
H(1,2) = -2.ODO*DSQRT (3.ODO)*LAMBDA
H(1,3) = 0.ODO
H(1,4) = DSQRT (6.ODO)*(2.*F2+25.*F4)
H(2,2) = 4.*F2-69.*F4+2*DQ-LAMBDA
H(2,3) = -6.*F2+30.*F4+2.*LAMBDA
H(2,4) = -2.*DSQRT (2.ODO)*LAMBDA
H(3,3) = -5.*F2-24.*F4-8.*DQ+2.*LAMBDA
H(3,4) = 2.*DSQRT (2.ODO)*LAMBDA
H(4,4) = 10.*F2+76.*F4-8.*DQ
WRITE (*,103)DQ
FORMAT (13H1FIRST MATRIX, 6H DQ = F8.1)
CALL DANDW (H,4)
DO 8 J = 1,4
ROOTS (J,IDQ) = H(J,J)
CONTINUE
CONTINUE
SECOND MATRIX
MATRIX OF GAMMA TWC
DO 20 IDQ, NODQ
DQ = ADQ( IDQ)
H(1,1) = -8.*F2-9.*F4+2.*DQ-LAMBDA
WRITE (*,104)DQ
FORMAT (14H1SECOND MATRIX, 6H DQ = F8.1)
CALL DANDW (H,1)
```

```
ROOTS (5,IDQ) = H(1,1)
CONTINUE
THIRD MATRIX
MATRIX OF GAMMA THREE
DO 30 IDQ = 1,NODQ
DQ = ADQ(IDQ)
H(1,1) = 21.*F4+12.*DQ
H(1,2) = DSQRT (6.0DO)*LAMBDA
H(1,3) = DSQRT (6.0DO)*LAMBDA
H(1,4) = 0.0DO
H(1,5) = 2.*DSQRT (3.0DO)*(F2-5.*F4)
H(2,2) = -8.0DO*F2-9.0DO*F4+2.0DO*DQ+0.5DO*LAMBDA
H(2,3) = -1.5*DQ*LAMBDA
H(2,4) = -3.*LAMBDA
H(2,5) = 0.0DO
H(3,3) = 4.0DO*F2-69.0DO*F4+2.0DO+DC 0.5DO*LAMBDA
H(3,4) = -6.*F2+30.*F4-LAMBDA
H(3,5) = -2,*DSQRT (2.0DO)*LAMBDA
H(4,4) = -5.*F2-24.*F4-LAMBDA-8.*DQ
H(4,5) = -DSQRT (2.0DO)*LAMBDA
H(5,5) = F2+16.*F4-8.*DQ
WRITE (*,105)DQ
FORMAT (13H1THIRD MATRIX, 6H DQ = F8.1)
CALL DANDW (H,5)
DO 28 J = 1,5
```

```
ROOTS (J+5,IDQ) = H(J,J)
CONTINUE
CONTINUE
FOURTH MATRIX
MATRIX OF GAMMA FOUR
DO 40 IDQ = 1,NODQ
DQ = ADQ (IDQ)
H(1,1) = -8.0DO*F2-9.0DO*F4+2.0DO*DQ+0.5DO*LAMBDA
H(1,2) = 0.5DO*DSQRT (3.0DO)*LAMBDA
H(1,3) = DSQRT (3.0DO)*LAMBDA
H(1,4) = 0.5DO*DSQRT (6.0DO)*LAMBDA
H(2,2) = 4.0DO*F2-69.0DO*F4+2.0DO*DQ-0.5DO*LAMBDA
H(2,3) = -6.*F2+30.*F4+LAMBDA
H(2,4) = 0.5DO+DSQRT (2.0DO)*LAMBDA
H(3,3) = -5.*F2-24.*F4-8.*DQ+LAMBDA
H(3,4) = DSQRT (2.0DO)*LAMBDA
H(4,4) = 4.*F2+F4+2.*DQ
WRITE (*,106)DQ
FORMAT (14H1FOURTH MATRIX, 6H DQ = F8.1)
CALL DANDW(H,4)
DO 38 J = 1,4
ROOTS (J+10, IDQ) = H(J,J)
CONTINUE
CONTINUE
FIFTH MATRIX
```

```
MATRIX OF GAMMA FIVE
DO 50 IDQ = 1, NODQ
DQ = ADQ (IDQ)
H(1,1) = -8.*F2-9.*F4+12.*DQ
H(1,2) = 2.*DSQRT (2.ODO)*LAMBDA
H(1,3) = O.ODO
H(1,4) = 2.*LAMBDA
H(1,5) = O.ODO
H(1,6) = O.ODO
H(2,2) = -8.ODO*F2-9.ODO*F4+2.ODO*DQ-O.5DO*LAMBI
H(2,3) = O.5DO*DSQRT (3.ODO)*LAMBDA
H(2,4) = -O.5DO*DSQRT (2.ODO)*LAMBDA
H(2,5) = -DSQRT (3.ODO)*LAMBDA
H(2,6) = DSQRT (6.ODO)*LAMBDA
H(3,3) = 4.DO*F2-69.DO*F4+2.ODO*DQ+O.5DO*LAMBDA
H(3,4) = -O.5DO*DSQRT (6.ODO)*LAMBDA
H(3,5) = 6.*F2-30.*F4+LAMBDA
H(3,6) = DSQRT (2.ODO)*LAMBDA
H(4,4) = 21.*F4+2.*DQ
H(4,5) = -DSQRT (6.ODO)*LAMBDA
H(4,6) = 2.*DSQRT (3.ODO)*(F2-5.*F4)
H(5,5) = -5.*F2-24.*F4-8.*DQ-LAMBDA
H(5,6) = DSQRT (2.ODO)*LAMBDA
H(6,6) = F2+16.*F4-8.*DQ
WRITE (*.107)DO
```

```
FORMAT (13H1FIFTH MATRIX, 6H DQ = F8.1)
CALL DANDW (H,6)
DO 48 J = 1,6
ROOTS (J+14, IDQ) = H(J,J)
CONTINUE
CONTINUE
DO 60 IDQ = 1, NODQ
DQ = ADQ (IDQ)
EMIN = ROOTS (1,IDQ)
DO 65 I = 2,20
IF (EMIN -ROOTs (I,IDQ) 65,65,64
EMIN = ROOTS (I,IDQ)
CONTINUE
DO 67 I = 1, 20
EMOD (I, IDQ) = ROOTS (I,IDQ)-EMIN
WRITE (*,153)DQ
FORMAT (20H1DIFFERENCE MATRICES, 6H DQ = F8.1)
WRITE (*,154)EMIN
FORMAT(16HO(LOWEST ROOT = E20.11, 1H))
WRITE (*,203)
FORMAT (17HOGAMMA ONE MATRIX)
WRITE (*,151)(EMOD (I,IDQ), I = 1,4)
FORMAT (E20.11)
WRITE (*,204)
FORMAT (17HOGAMMA TWO MATRIX)
```

```
WRITE (*,151) EMOD (5,IDQ)
WRITE (*,205)
FORMAT (19HOGAMMA THREE MATRIX)
WRITE (*,151)(EMOD (I,IDQ), I = 6,10)
WRITE (*,206)
FORMAT (18HOGAMMA FOUR MATRIX)
WRITE(*,151) (EMOD (I,IDQ), I = 11, 14)
WRITE(*,207)
FORMAT (18HOGAMMA FIVE MATRIX)
WRITE(*,151)(EMOD (I,IDQ), I = 15,20)
CONTINUE
CONTINUE
STOP
END

SUBROUTINE DANDW (H,N)
IMPLICIT REAL*8(A-H,O-Z)
DIMENSION H(30,30),U(30,30)
CALL HDIAG (H,N,O,U,NR)
WRITE (*,203)
FORMAT (23HOROOTS AND COEFFICIENTS)
DO 240 J = 1,N
WRITE (*,204)J,H(J,J)
FORMAT (1X,I3,8H ROOT = F20.11)
DO 240 I = 1, N
WRITE (*,205)I,J,U(I,J)
```

```
FORMAT (1X,I3,I3,15H COEFFICIENT = E20.11)
CONTINUE
RETURN
END

SUBROUTINE HDIAG (H,N,IEGEN,U,NR)
IMPLICIT REAL*8 (A-H, O-Z)
DIAGONALIZES REAL SYMMETRIC MATRIX BY JACOBI METHOD.
CALL HDIAG (H,N, IEGEN, U, NR)
H IS ARRAY TO BE DIGONALIZED.

N IS ORDER OF MATRIX H,
IEGEN SET TO ZERO IF EIGENVALUES AND EIGENVECTORS ARE
TO BE COMP
UTED
IEGEN SET UNEQUAL TO ZERO IF ONLY EIGENVALUES ARE DESIRED.
U IS THE UNITARY MATRIX USED FOR FORMATION OF EIGENVECTORS.
NR IS THE NUMBER OF ROTATIONS.
INSERT A DIMENSION STATEMENT IN MAIN PROGRAMO
DIMENSION H(30,30), U(30,30)
DIMENSION X(30), IQ(30), U(30,30), H(30,30)
SUBROUTINE OPERATES ONLY ON ELEMENTS OF H THAT ARE TO RIGHT OF
DIAGONAL, SO ONLY TRIANGULAR SECTION NEED BE STORED IN ARRAY H.
IF (IEGEN) 15,10,15
DO 14 I = 1,N
DO 14 J = 1,N
IF (I-J) 12.11,12
U (I,J) = 1.0DO
```

```
      GO TO 14
      U (I,J) = 0.0D0
      CONTINUE
      NR = 0
      IF (N-1) 1000, 1000, 17
C     SCAN FOR LARGEST OFF-DIAGONAL ELEMENT IN EACH ROW.
C     X(I) CONTAINS LARGEST ELEMENT IN ITH ROW.
C     IX(I) HOLDS SUBSCRIPT DEFINING POSITION OF ELEMENT
      NMI1 = N-1
      DO 30 I = 1, NMI1
      X(I) = 0.0D0
      IPL1 = I+1
      DO 30 J = IPL1,N
      IF (X(I) - DABS (H(I,J))) 20,20,30
      X(I) = DABS (H(I,J))
      IQ(I) = J
      CONTINUE
C     DOUBLE PRECISION VERSION.
C     SET INDICATOR FOR SHUT-OFF. RAP = 2**-27, NR = NO.OF ROTATION.
      RAP = 5.960464D-8
      HDTEST = 1.0D30
C     FIND MAXIMUM OF X(I) FOR PIVOT ELEMENT AND TEST FOR ENF OF
C     PROB
      ILEM
      DO 70 I = 1, NMI1
      IF (I-1) 60,60,45
```

```
IF (XMAX - X(I)) 60,70,70

XMAX = X(I)

IPIV = I

JPIV = IQ(I)

CONTINUE

IF MAX, X(I) EQUAL TO ZERO, IF LESS THAN HDTEST, REV AND SE
HOTEST.

IF (XMAX) 1000,1000,80

IF( HDTEST) 90,90,85

IF (XMAX - HDTEST) 90,90,148

HDIMIN = DABS(H1,1))

DO 110 I = 2,N

IF (HDIMIN - DABS (H(I,I)))110,110,100

HDIMIN = DABS (H(I,I))

CONTINUE

HDTEST = HDIMIN*RAP

RETURN IF MAX. H(I,J) LESS THAN (I**-27)ABSF(H(K,K)-MIN)

IF (HDTEST - XMAX) 148,1000,1000

NR = NR + 1

COMPUTE TANGENT, SINE, AND COSINE, H(I,I), H(J,J)

TANG = DESIGN (2.0DO, (H(IPIV,IPIV)-H(JPIV,JPIV)))*H(IPIV,JPIV)

/(DABS (H(IPIV,IPIV)-H (JPIV,JPIV))+DSQRT((H(IPIV,IPIV)-H(JP
 IV,JPIV))**2 + 4.0DO*H(IPIV,JPIV)**2))

COSINE = 1.0/DSQRT (1.0DO + TANG**2)

SINE = TANG*COSINE

HII = H(IPIV,IPIV)
```

```
H(IPIV,IPIV) = COSINE**2*(HII + TANG*(2.*H(IPIV,JPIV)+TANG*H(J
PIV,JPIV)))

H(JPIV,JPIV) = COSINE**2*(H(JPIV,JPIV) - TANG*(2.*H(IPIV,JPIV)-
TANG*HII))

H(IPIV,JPIV) = 0.0D0

PSEUDO RANK THE EIGENVALUES

ADJUST SINE AND COS FOR COMPUTATION OF H(IK) AND U(IK)

IF (H(IPIV,IPIV) - H(JPIV-JPIV)) 152,153,153

HTEMP = H(IPIV,IPIV)

H(IPIV,IPIV) = H(JPIV,JPIV)

H(JPIV,JPIV) = HTEMP

RECOMPUTE SINE AND COS

HTEMP = DESIGN (1.0D0,-SINE)*COSINE

COSINE = DABS (SINE)

SINE = HTEMP

CONTINUE

INSPECT THE IQS BETWEEN I+1 AND N-1 TO DETERMINE WHETHER
A NEW MAXIMUM VALUE SHOULD BE COMPUTED, SINCE THE PRESENT
MAXIMUM IS IN THE I OR J ROW.

DO 350 I = 1, NM11

IF(I=IPIV) 210,350,200

IF(I-JPIV) 210,350,210

IF(IQ(I) - IPIV) 230,240,230

IF(IQ(I) - JPIV) 350,240,350

K = IQ(I)

HTEMP = H(I,K)

H(I,K) = 0.0D0
```

```
IPL1 = I+1
X(I) = 0.0D0
SEARCH IN DEPLETED ROW NEW MAXIMUM
DO 320 J = IPL1,N
IF (X(I) - DABS (H(I,J))) 300,300,320
X(I) = DABS (H(I,J))
IQ(I) = J
CONTINUE
H(I,K) = HTEMP
CONTINUE
X(IPIV) = 0.0D0
X(JPIV) = 0.0D0
CHANGE ORDER OF ELEMENTS OF H
DO 530 I = 1, N
IF (I-IPIV) 370,530,420
HTEMP = H(I,IPIV)
H(I,IPIV) = COSINE*HTEMP + SINE*H(I,JPIV)
IF (X(I) - DABS (H(I,IPIV))) 380,390,390
X(I) = DABS (H(I,IPIV))
IQ(I) = IPIV
H(I,JPIV) = -SINE*HTEMP + COSINE*H(I,JPIV)
IF(X(I) - DABS (H(I,JPIV))) 400,530,530
X(I) = DABS (H(I,JPIV))
IQ(I) = JPIV
GO TO 530
```

```
      IF (I-JPIV) 430,530,480
      HTEMP = H(IPIV,I)
      H(IPIV,I) = COSINE*HTEMP + SINE*H(I,JPIV)
      IF (X(IPIV) - DABS (H(IPIV,I))) 440,450,450
      X(IPIV) = DABS (H(IPIV,I))
      IQ(IPIV) = I
      H(I,JPIV) = -SINE*HTEMP + COSINE*H(I,JPIV)
      IF X(I) - DABS(H(I,JPIV))) 400,530,530
      HTEMP = H(IPIV,I)
      H(IPIV,I) = COSINE*HTEMP + SINE*H(JPIV,I)
      IF (X(IPIV)-DABS (H(IPIV,I))) 490,500,500
      X(IPIV) = DABS (H(IPIV,I))
      IQ(IPIV) = I
      H(JPIV,I) = -SINE*HTEMP + COSINE*H(JPIV,I)
      IF (X(JPIV) - DABS (H(JPIV,I))) 510,530,530
      X(JPIV) = DABS (H(JPIV,I))
      IQ(JPIV) = I
      CONTINUE
      TEST FOR COMPUTATION OF EIGENVECTORS
      IF (IEGEN) 40,540,40
      DO 550 I = 1, N
      HTEMP = U(I,IPIV)
      U(I,IPIV) = COSINE*HTEMP + SINE*U(I,JPIV)
      U(I,JPIV) = -SINE*HTEMP + COSINE*U(I,JPIV)
      GO TO 40
      RETURN
      END
```